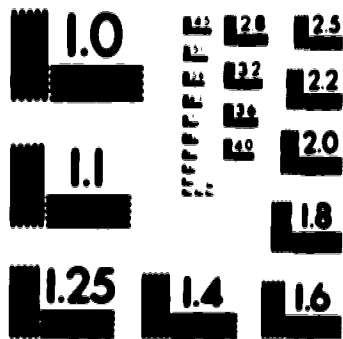


1

PM-1 3 1/2" x 4" PHOTOGRAPHIC MICROCOPY TARGET
NBS 1910a ANSI/ISO #2 EQUIVALENT



PRECISION™ RESOLUTION TARGETS



National Library
of Canada

Acquisitions and
Bibliographic Services Branch

385 Wellington Street
Ottawa, Ontario
K1A 0N4

Bibliothèque nationale
du Canada

Direction des acquisitions et
des services bibliographiques

385, rue Wellington
Ottawa (Ontario)
K1A 0N4

Number of copies

Library of Congress

NOTICE

The quality of this microform is heavily dependent upon the quality of the original thesis submitted for microfilming. Every effort has been made to ensure the highest quality of reproduction possible.

If pages are missing, contact the university which granted the degree.

Some pages may have indistinct print especially if the original pages were typed with a poor typewriter ribbon or if the university sent us an inferior photocopy.

Reproduction in full or in part of this microform is governed by the Canadian Copyright Act, R.S.C. 1970, c. C-30, and subsequent amendments.

AVIS

La qualité de cette microforme dépend grandement de la qualité de la thèse soumise au microfilmage. Nous avons tout fait pour assurer une qualité supérieure de reproduction.

S'il manque des pages, veuillez communiquer avec l'université qui a conféré le grade.

La qualité d'impression de certaines pages peut laisser à désirer, surtout si les pages originales ont été dactylographiées à l'aide d'un ruban usé ou si l'université nous a fait parvenir une photocopie de qualité inférieure.

La reproduction, même partielle, de cette microforme est soumise à la Loi canadienne sur le droit d'auteur, SRC 1970, c. C-30, et ses amendements subséquents.

UNIVERSITY OF ALBERTA

**NEW METABOLITES OF *PELLINUS TREMULAE*:
2-CARBOMETHOXYOXEPIN AND
TREMULANE SESQUITERPENES**

BY



ELIZABETE RANGEL CRUZ

**A thesis submitted to the Faculty of Graduate Studies and Research in partial fulfillment of
the requirements for the degree of DOCTOR OF PHILOSOPHY.**

DEPARTMENT OF CHEMISTRY

EDMONTON, ALBERTA

SPRING 1994



National Library
of Canada

Acquisitions and
Bibliographic Services Branch

305 Wellington Street
Ottawa, Ontario
K1A 0N4

Bibliothèque nationale
du Canada

Direction des acquisitions et
des services bibliographiques

305 rue Wellington
Ottawa (Ontario)
K1A 0N4

0-612-11183-0

0-612-11183-0

The author has granted an irrevocable non-exclusive licence allowing the National Library of Canada to reproduce, loan, distribute or sell copies of his/her thesis by any means and in any form or format, making this thesis available to interested persons.

L'auteur a accordé une licence irrévocable et non exclusive permettant à la Bibliothèque nationale du Canada de reproduire, prêter, distribuer ou vendre des copies de sa thèse de quelque manière et sous quelque forme que ce soit pour mettre des exemplaires de cette thèse à la disposition des personnes intéressées.

The author retains ownership of the copyright in his/her thesis. Neither the thesis nor substantial extracts from it may be printed or otherwise reproduced without his/her permission.

L'auteur conserve la propriété du droit d'auteur qui protège sa thèse. Ni la thèse ni des extraits substantiels de celle-ci ne doivent être imprimés ou autrement reproduits sans son autorisation.

ISBN 0-612-11183-0

Canada

UNIVERSITY OF ALBERTA

RELEASE FORM

NAME OF AUTHOR ELIZABETE RANGEL CRUZ

TITLE OF THESIS NEW METABOLITES OF *PELLINUS TREMULAE*
2-CARBOMETHOXYOXEPIN AND TREMULANE
SESQUITERPENES.

DEGREE FOR WHICH THESIS WAS PRESENTED DOCTOR OF PHILOSOPHY

YEAR THIS DEGREE GRANTED 1994

Permission is hereby granted to the University of Alberta Library to reproduce single copies of the thesis and to lend or sell such copies for private, scholarly or scientific research purposes only.

The author reserves all other publication and other rights in association with the copyright in the thesis, and except as hereinbefore provided neither the thesis nor any substantial portion thereof may be printed or otherwise reproduced in any material form whatever without the author's prior written permission.

Elizabeth Rangel Cruz.....

Permanent address:

Rua Carlos Ronchete, 19 - C. Grande

23087-480 - Rio de Janeiro - RJ

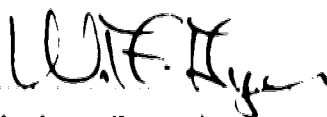
Brazil

Date: *Feb 4/94*.....

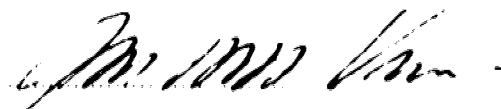
UNIVERSITY OF ALBERTA

FACULTY OF GRADUATE STUDIES AND RESEARCH

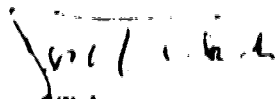
The undersigned certify that they have read, and recommend to the Faculty of Graduate Studies and Research for acceptance, a thesis entitled *NEW METABOLITES OF PHELLINUS TREMULAE: 2-CARBOMETHOXYOXEPIN AND TREMULANE* SESQUITERPENES submitted by ELIZABETE RANGEL CRUZ in partial fulfillment of the requirements for the degree of DOCTOR OF PHILOSOPHY in CHEMISTRY



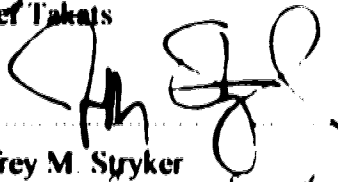
W. A. Ayer, Supervisor



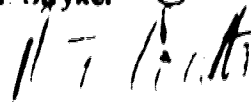
John C. Vederas



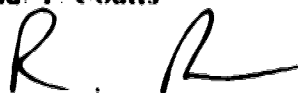
Josef Takats



Jeffrey M. Stryker



Ronald T. Coutts



Raymond Andersen, External Examiner

Date: Feb. 1/94

"Lunar is the same thing
to your system, you still all that you require,
to your surroundings."

Proverbs 10: 25

"Lunas as amandas corque la luna.
A luna para a sua vida de sabedoria e mudi' alma..."

- Sol

"A luna foi a sua vida de sabedoria
e a sua vida de sabedoria e a sua vida de sabedoria..."

- Sol

*As meu Deus, e minha família
e a base que sustentam*

ABSTRACT

The annual harvest of trembling aspen (*Populus tremuloides*) has increased dramatically over the past decade, especially in Alberta. However, the commercial use of aspen has been limited because of its susceptibility to decay and staining organisms. The most important cause of decay in live aspen is *Phellinus tremulae* which is responsible for about 39% of the trunk decay volume in aspen. This pathogen is antagonistic to a large number of aspen occurring fungi and this antagonism may be associated with defense metabolites generated by this fungus. The metabolites produced by *P. tremulae* were examined. The isolation for the first time of 2-carbomethoxyoxepin, the postulated arene oxide intermediate in the biosynthesis of methyl salicylate, and the isolation of seven sesquiterpenes, the tremulanes, possessing a previously unreported substituted perhydroazulene carbon skeleton are described. The structures were determined by NMR techniques and other physical methods including, in the case of tremulenolide A, X-ray crystallography. Chemical correlations were also used to verify structural assignments. Biosynthetic studies indicate that 2-carbomethoxyoxepin is derived from benzoic acid through methyl benzoate. The oxidase activity of *P. tremulae* towards a different aromatic substrate was examined. Feeding experiments using *o*-toluic acid reveal that a reductive process takes place leading to the formation of *o*-tolualdehyde in addition to methyl *o*-toluate. The tremulane biosynthesis was also investigated using singly and doubly labelled acetate. The incorporation pattern indicates that one of the isoprene units undergoes rearrangement during formation of the tremulane skeleton. Two possible mechanisms are proposed. One *via* cyclization-rearrangement of humulene and another *via* condensation-cyclization-rearrangement of geranyl pyrophosphate and dimethylallyl pyrophosphate. The stereochemical course of both biosyntheses is discussed. The presence of the tremulanes in rotted aspen and in the *P. tremulae* fruiting body (conk) was not detected.

ACKNOWLEDGEMENTS

It was a privilege to conduct my research under the supervision of Prof. William A. Ayer, whose wisdom and thoughtful guidance gave me the freedom of working at my own pace. I am grateful for his encouragement and support during these years as a graduate student in which I developed a profound admiration for the great scientist and the grand man he is.

I would also like to thank Dr. José Daniel Figueroa Villar who was my inspiration to pursue this degree. His motivation and confidence were crucial to keep me going, especially in the first two years of the program. Without his help and support I would not have come to Canada.

My initial steps in natural product bench-work as well as in the operation of NMR spectrometer were very well guided by Dr. Peter A. Crow to whom I express my deepest gratitude.

I wish to thank all colleagues in the group with especial mention to Heiena Orszanska and Luis Diego Jimenez for their help and friendship. My thanks to Dr. Lois Browne for her companionship.

The technical staff of this department greatly assisted in the completion of this work. Dr. Tom T. Nakashima, Tom Brisbane, Glen Bigan, G. Aarts, and L. Kong in the NMR Spectroscopy Laboratory, John Olekszyk, L. Harrower, D. Morgan, A. Jodhan, and Dr. A. M. Hogg in the Mass Spectrometry Laboratory, Diane Formanski, Bob Swindlehurst, and Jim Hoyle in the Spectral Services and Microanalytical Laboratories, and all the personnel in the Electronics, Glass Blowing, and Machine Shops. My gratitude to the administrative staff as well.

I especially thank Tom Brisbane for the extra time he spent teaching me how to run 1D and 2D experiments in the 400-NMR and Drs. Tom T. Nakashima and Gabrielle Pausler for the lessons in the 500-NMR.

I am grateful for the financial support from: Conselho Nacional de Desenvolvimento Científico e Tecnológico (CNPq - Brazil), Department of Chemistry (U. of A.), and the Natural Sciences and Engineering Research Council of Canada.

The regular meetings of the multidisciplinary aspen group including Y. Hiratsuka and colleagues, Northern Forestry Centre, and L. Sigler, University of Alberta Microfungus Collection, provided an useful opportunity for presentation and discussion of my results.

I am pleased to have met Luis Jimenez, Floria Roa, and Marcia Vasquez, which have proved to be truly friends during the most difficult times.

I wish to thank some friends from Brazil for their help and encouragement: Ismênia Guimaraes, Luis F. Vieira, Karen Hayes, Leopold Hartman, Libia Ariza, Francis Sanches, Anibal Reis, Paulo Fragas and colleagues from IME. My return to academe was possible due to the help of Dr. Armando C. Fabriani to start my master degree.

The love and strength received from my mother, my sisters, my nephews and nieces made it more tolerable to be by myself overseas. My mother Zezilda and my sisters Jozilda and Joseni were particularly present during all this time. I am proud of the way they handled everything for me and I am happy to realize how much each of them have grown up during these three years, with especial mention to Joseni and Jozenilda for their degrees. All my love to these six great women - my family.

Toda gratidão à minha mãe por ter se esforçado para me dar os primeiros oito anos de educação escolar e por ter me incentivado a prosseguir meus estudos conquistando meus próprios recursos.

TABLE OF CONTENTS

I. INTRODUCTION	1
II. RESULTS AND DISCUSSION	9
2.1. Isolation of the Metabolites	9
2.2. Aromatic and Heterocyclic Compounds	11
2.2.1. Characterization	11
2.2.2. Biosynthesis	14
2.3. Sesquiterpenes	20
2.3.1. Characterization	20
Tremulenolide A (23)	20
Tremulenolide B (24)	34
Tremulenedial (25)	38
Tremulenediols A (26) and B (27)	46
Tremulenediol A (26)	47
Tremulenediol B (27)	56
Tremulenediol C (28) and tremuladienol (29)	66
2.3.2. Absolute Stereochemistry	72
2.3.3. Chemical conversions	76
2.3.3.1. Oxidation of tremulenediol A (26) to tremulenolide A (23)	76
2.3.3.2. Reduction of tremulenedial (25) to tremulenediol B (27)	77
2.3.4. Biosynthesis	80
2.4. Additional Studies	94
2.4.1. Bioactivity	94
2.4.2. Oxidase activity	96
2.4.3. Rotted aspen and conk study	99

III CONCLUSIONS	102
IV EXPERIMENTAL	105
4.1 Growth of <i>Phellinus tremulae</i>	107
4.2 Isolation of the metabolites	108
Methyl salicylate (7)	109
Methyl benzoate (5)	109
2-Carbomethoxyoxepin (22)	109
Tremulenolide A (23)	110
Ozonolysis of tremulenolide A	111
Tremulenolide B (24)	112
Tremulenedial dibenzyl acetal (25)	112
Tremulenediol A (26)	113
Tremulenediol B (27)	114
<p><i>p</i>-Bromobenzoylation of 26 and 27</p>	115
di- <i>p</i> -Bromobenzoyl derivative of 26 (26a)	115
di- <i>p</i> -Bromobenzoyl derivative of 27 (27a)	116
Tremulenediol C (28)	117
Tremuladienol (29)	117
Oxidation of tremulenediol A (26): preparation of tremulenolide A (23)	118
Reduction of tremulenedial (25): preparation of tremulenediol B (27)	118
4.3. Labelling experiments	119
4.3.1. Administration of benzoic acid- α - ^{13}C	119
Labelled methyl salicylate (7)	119
Labelled methyl benzoate (5)	119
Labelled 2-carbomethoxyoxepin (22)	119
4.3.2. Administration of labelled acetate	120
[1,2- $^{13}\text{C}_2$] acetate labelled metabolites	120
[1- ^{13}C] acetate labelled metabolites	121
[2- ^{13}C] acetate labelled metabolites	121

4 4	Oxidase activity	122
4 4 1	Preparation of methyl <i>o</i> -toluate	122
4 4 2	Administration of <i>o</i> -toluic acid directly into the medium (exp-1)	122
4 4 3	Citrate-phosphate buffer pH 4 assay (exp-2)	123
4 4 4	Extraction of rotted aspen and <i>Phellinus</i> conks	124
V	BIBLIOGRAPHY	125

LIST OF TABLES

Table		page
1	Growth of <i>P. tremulae</i> in the presence and absence of HP 20 resin	9
2	Calculated UV absorption for the oxepin tautomer of 22	13
3	Incorporation of benzoic acid- α - ^{13}C by <i>Phellinus tremulae</i>	16
4	^{13}C NMR chemical shift data (CDCl_3) for tremulanes 23 to 29	22
5	^1H NMR data (CDCl_3) for tremulanes 23 to 29	23
6	^1H and ^{13}C NMR data for ozonolysis product 23a	33
7	Correlations observed in the NOESY spectrum of diol 26	50
8	Comparison of ^1H NMR chemical shifts between 26 and 26a	62
9	Comparison of ^1H NMR chemical shifts between 27 and 27a	65
10	^{13}C NMR data of doubly labelled tremulenediols A (26a) and B (27a)	84
11	Bioactivity of compounds produced by <i>P. tremulae</i> against aspen occurring fungi	95
12	Oxidase activity of <i>P. tremulae</i> using <i>o</i> -toluic acid	98

LIST OF FIGURES

Figure	page
1 A portion of lignin macromolecule and the fungal degradation products	4
2 Hepatic metabolism of benzene oxide	7
3 Sequence of elution of metabolites of <i>Phellinus tremulae</i> on silica gel flash chromatography	10
4 ¹ H NMR and ¹ H- ¹ H COSY spectra of 2-carbomethoxyoxepin (22) in CDCl ₃	12
5 HMQC spectrum and ¹ H and ¹³ C NMR shifts for 2-carbomethoxyoxepin (22) in CDCl ₃	12
6 ¹³ C NMR spectra of methyl salicylate, 2-carbomethoxyoxepin, and methyl benzoate after incorporation of benzoic acid- α - ¹³ C by <i>P. tremulae</i>	17
7 ¹ H NMR, ¹ H- ¹ H COSY spectra (CDCl ₃) and chemical shift assignment of 23	24
8 ¹³ C chemical shift of <i>gem</i> -dimethyl groups in five-, six-, and seven-membered rings	25
9 HMQC spectrum of tremulenolide A (23)	27
10 Significant HMBC correlations of tremulenolide A (23)	27
11 A computer generated drawing of the final X-ray model of tremulenolide A (23)	28
12 Shielding of H-12 β and homoallylic coupling between H-3 and H-10 α in 23	29
13 Carbonyl cone effect and axial-axial zig-zag coupling in compound 23	30
14 NOE enhancements observed in tremulenolide A (23)	30
15 ¹ H spectrum (400 MHz, CDCl ₃) and chemical shift assignment of tremulenolide B (24)	35
16 HMQC spectrum and ¹³ C shift assignment for tremulenolide B (24)	37
17 ¹ H NMR spectrum (400 MHz, CDCl ₃) and chemical shift assignment of 25a	40

18	Proposed configuration of 25a , NOE enhancements, and NOESY spectrum of 25a	42
19	HMQC spectrum (expanded regions) and ^{13}C NMR assignment of 25a	43
20	Significant HMBC correlations of tremulenedial dibenzyl acetal (25a)	44
21	^1H NMR spectrum (400 MHz, CDCl_3) and chemical shift assignment of 26	48
22	Absorption IR spectra of diol 26 in CH_2Cl_2 at different concentrations indicating the presence of intramolecular hydrogen bonding	49
23	Representation of the W- and homoallylic couplings observed in compound 26	51
24	NOESY spectrum of tremulenediol A (26)	51
25	HMQC spectrum and ^{13}C NMR chemical shift assignment of 26	53
26	HMBC spectrum of tremulenediol A (26) with expansion of the ^1H field area	54
27	Significant HMBC correlations of tremulenediol A (26)	55
28	^1H NMR spectrum (400 MHz, CDCl_3) and chemical shift assignment of 27	56
29	Absorption IR spectrum of diol 27 in dichloromethane indicating the presence of intramolecular hydrogen bonding	57
30	^{13}C NMR chemical shift assignment of tremulenediol B (27)	59
31	^1H - ^1H COSY spectra of di- <i>p</i> -bromobenzoate 26a	60
32	^1H NMR spectrum (400 MHz, CDCl_3) and chemical shift assignment of 26a	61
33	HMQC spectrum, ^{13}C NMR assignment of compound 26a , and chemical shift differences in relation to 26 (negative values indicate deshielding and positive values indicate shielding relative to 26)	63
34	^1H and ^{13}C assignments for tremulenediol A dibenzoate (5a)	64
35	^{13}C NMR assignment of compound 27a and chemical shift differences in relation to 27 (negative values indicate deshielding and positive values indicate shielding relative to 27)	65
36	^1H NMR spectrum and chemical shift assignment for tremulenediol C (28)	66

37	HMQC spectrum of tremulenediol C (28)	68
38	Significant HMBC correlations of tremulenediol C (28)	68
39	¹ H NMR spectrum and chemical shift assignment for tremuladienol (29)	70
40	¹³ C NMR chemical shift assignment for tremuladienol (29)	71
41	Relationship between chirality and the Cotton effect sign in allylic alcohol	72
42	The olefin octant rule: (a) intersecting symmetry planes, (b) front octants viewed along the Z-axis, (c) rear octants viewed along the Z-axis, (d) rear octants viewed along the Y-axis, (e) front octants viewed along the Y-axis	73
43	Conformation of tremulenediol A (26) and the intersecting symmetry planes for the octant projection	73
44	Olefin octant rule projection for tremulenediol A (26): (a) front octants viewed along Z-axis from C-1 to C-2; (b) rear octants viewed along Z-axis from C-1 to C-2; (c) front octants viewed along Y-axis	74
45	Comparison of the partial ¹ H NMR spectrum of tremulenediol B di- <i>p</i> -bromobenzoate (27a) with that of the dideuteride 33a	79
46	¹³ C NMR spectrum (125 MHz) of the doubly labelled tremulenediol A di- <i>p</i> -bromobenzoate (26a)	83
47	INADEQUATE spectrum of the doubly labelled tremulenediol A di- <i>p</i> -bromobenzoate (26a)	86
48	¹³ C NMR spectra of 26a: natural abundance (bottom), [1- ¹³ C] labelled (center), and [2- ¹³ C] labelled (top)	88
49	Summary of incorporation of singly and doubly labelled acetate administered to cultures of <i>P. tremulae</i> in tremulane sesquiterpenes	87
50	GC of rotted aspen and liquid culture extract of <i>P. tremulae</i>	100
51	GC-MS analysis of rotted aspen extract	101

LIST OF SCHEMES

Scheme		page
1	Salicylic acid biosynthesis and metabolism in plants	14
2	Rearrangement of 2-carbomethoxyoxepin (22) to methyl salicylate via NIH shift	15
3	Biosynthesis of methyl salicylate from benzoic acid in <i>Phellinus tremulae</i>	18
4	Ozonolysis of tremulenolide A (23)	31
5	Base peak formation in the mass spectrum of 23a	31
6	Mass spectral fragmentation of 23a to form the fragment m/z 139	32
7	Benzylation of the dialdehyde tremulenedial (25)	38
8	Cross peaks observed in the NOESY spectrum of 25a	41
9	Possible mechanism of formation of the dibenzyl acetal 25a	45
10	Fragmentation of tremulenediol A (26) to form the base peak at m/z 189	46
11	Conversion of tremulenediol A into the di- <i>p</i> -bromobenzoate 26a	59
12	Conversion of tremulenediol C (28) into tremuladienol (29)	69
13	Conversion of tremulenediol A (26) into tremulenolide A (23)	76
14	Possible intermediates involved in the oxidation of diol 26 with MnO_2	77
15	Reduction of tremulenedial (25) with $NaBH_4$ and $NaBD_4$	78
16	Stereochemical course of the tremulane biosynthesis from FPP via humulene, exemplified for tremulenediol A (26)	90
17	Labelling pattern expected for tremulane following humulene pathway (tremulane is numbered according to humulene)	91
18	GPP-DMAPP-mechanism in the tremulane biosynthesis: generation of the acyclic intermediate 39	92
19	Stereochemical course of the tremulane biosynthesis in the GPP-DMAPP- mechanism of tremulane biosynthesis	93

LIST OF ABBREVIATIONS

[α]	specific rotation
APT	attached proton test
b	broad (spectral)
Bn	benzyl
Bz	benzoyl
CD	circular dichroism
CI	chemical ionization
CIMS	chemical ionization mass spectrometry
COSY	correlated spectroscopy
δ	chemical shift in parts per million downfield from tetramethylsilane
d	doublet (spectral)
DMAPP	dimethylallyl pyrophosphate
DNA	Deoxyribonucleic acid
FPP	farnesyl pyrophosphate
FTIR	Fourier transform infrared
g	gram(s)
GC	gas chromatography
GC-IR	gas chromatography-infrared
GC-MS	gas chromatography-mass spectrometry
gPP	geranyl pyrophosphate
HMBC	heteronuclear multiple bond coherence
HMQC	heteronuclear multiple quantum coherence
HREIMS	high resolution electron impact mass spectrometry
Hz	hertz
INADEQUATE	incredible natural abundance double quantum transfer experiment
INAPT	insensitive nuclei assigned by polarization transfer
IPP	isopentenyl pyrophosphate
IR	infrared
J	coupling constant (in NMR)
L	liter(s)

m	multiplet (spectral), milli
M	mol
Me	methyl
MVA	mevalonic acid, mevalonate
<i>m/z</i>	mass to charge ratio (in mass spectrometry)
NIH	National Institutes of Health
NOF	Northern Forest Research Centre
NMR	nuclear magnetic resonance
NOE	nuclear Overhauser enhancement
NOESY	nuclear Overhauser enhancement and exchange spectroscopy
p	pentet (spectral)
Ph	phenyl
PAL	phenylalanine ammonia lyase
PTLC	preparative thin layer chromatography
py	pyridine
q	quartet (spectral)
<i>R_f</i>	retention factor (in chromatography)
RNA	ribonucleic acid
rt	room temperature
s	singlet (spectral)
SAM	S-adenosylmethionine
SAR	systemic acquired resistance
θ	molar ellipticity
t	triplet (spectral)
TFA	trifluoroacetic acid
TLC	thin layer chromatography
<i>t_R</i>	retention time (in chromatography)
UAMH	University of Alberta Microfungus Herbarium
UV	ultraviolet
=>	affects the signal at (in NMR)
<=>	correlates to (in NMR)

I. INTRODUCTION

The demand for forestry products has increased substantially over the years, making necessary the search for alternative wood sources to supplant the commercially valuable, but increasingly scarce, softwood timber. In Canada, attention has been directed to two hardwood species, trembling or quaking aspen (*Populus tremuloides* Michx.) and balsam poplar (*Populus balsamifera* L.). These *Populus* species are the most commonly occurring standing crop in the prairie provinces, with aspen being the most dominant¹. Aspen was once regarded as a weed species that hindered efficient harvesting of the more valuable softwoods. However, this attitude towards the commercial usefulness of aspen has changed in the past decade due to the recognition of some of its unique anatomical, chemical, physical, and mechanical properties, and to the development of new technologies to use this resource more efficiently¹. In Canada, aspen represents 54% of the net merchantable hardwood timber and 11% of the entire Canadian timber resource². In Alberta, it makes up 85% of the growing stock of hardwood species, which represents 40% of the total forest resources³.

Aspen is used in the production of oriented strand board and more recently has found use in the pulp and paper industry. Secondary forest products such as pallets, cartons, corrugated boxes, firewood, chopsticks, popsicle sticks, and cattle pellets are also produced from aspen¹. However, the commercial use of aspen has been limited because of its susceptibility to decay and staining organisms. Heartwood decay by fungi is the most common type of rot. Among the fungi identified as causing decay of live aspen, *Phellinus tremulae* (Bond.) Bond. & Borisov is by far the most important. In Alberta, *P. tremulae* is responsible for about 39% of the trunk decay volume in aspen². This delignifying decay is characterized by a prominent black line surrounding the rotted heartwood, which becomes spongy and exudes a peculiar wintergreen odor. Hoof-shaped conks are characteristic external indicators of the presence of *P. tremulae*³. This perennial fruiting body can

measure up to 20 cm across. The upper surface is greyish black, rough, often cracked, and the margin is fawn during active growth^{4,5}. In culture, *P. tremulae* grows slowly, 5-25 mm in 2 weeks on 2% malt extract agar, and produces the strong and sweet aroma of wintergreen (*Gaultheria procumbens*). The colonies are yellow ocher to buckthorn brown, finally umber brown to antique brown. The agar shows distinct pigmentation, copper to coffee brown, outside the mycelium. It gives a positive test for extracellular oxidase. This pathogen was formerly known as *Fomes igniarius* var. *populinus*⁵.

P. tremulae is undoubtedly one of the most serious parasites of the North American and European trembling aspen and one of the most serious polyporous pathogens of hardwoods in the northern temperate and boreal zones. According to the most popular theory, the species penetrates into the heartwood along dead branches, which provide canals through the bark and resistant sapwood⁵. This theory is supported by observations that spore germination occurs more readily on aged wood extract medium than on fresh sapwood medium. In addition, old wounds have a more favorable pH, about 4.6, than fresh sapwood, 6.0 to 6.3. Apparently *P. tremulae* is a late-comer in the pathogen succession of aspen wood, being preceded in the heartwood by bacteria and other nondecaying fungi⁵. Once it establishes itself in a tree no other fungus invades. An exception to this is the decay organism *Peniophora polygonia* (Pers.:Fr.) Boud. which is found in decayed and discolored wood³. These two fungi are mutually antagonistic and they are seldom found in the same tree. When they coexist in a tree, there are clear demarcation lines between the areas infected by each organism. This antagonism is also observed *in vitro* when the fungi are grown in paired culture on artificial media and on wood². There is evidence that *P. tremulae* occurs less frequently in aspen inflicted with black galls (stem deformities) than in non-gall trees³. One of the reasons for this may be that the causal organisms of black gall formation produce metabolites that protect the tree from infection by decay organisms. Based on this assumption, over 100 species of fungi were isolated from black galls and tested against *P. tremulae*⁶. Among the isolated

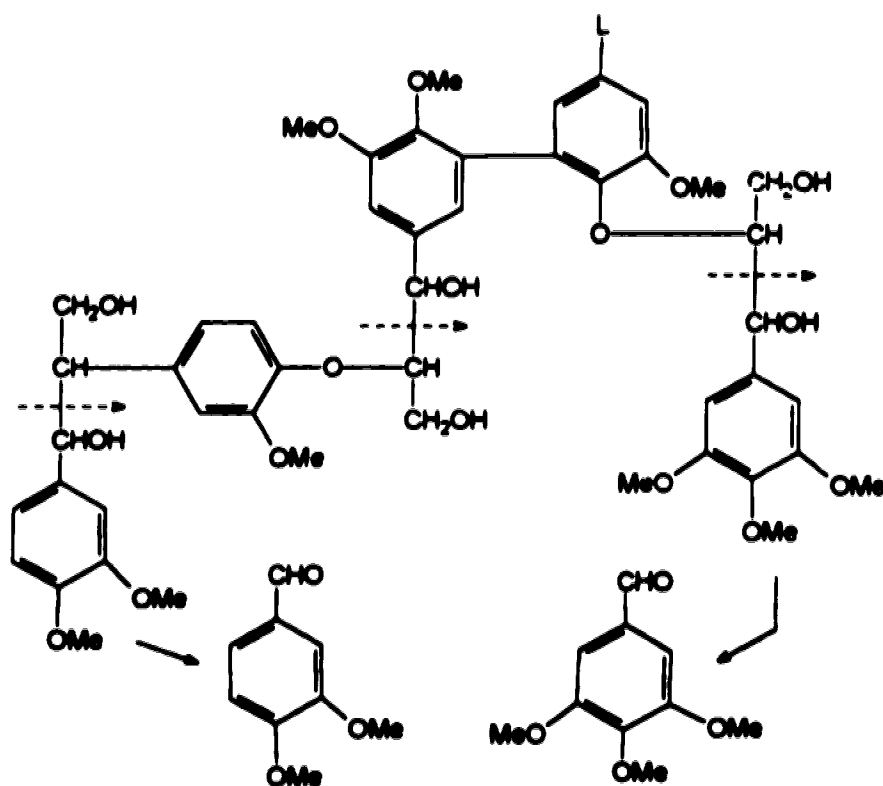
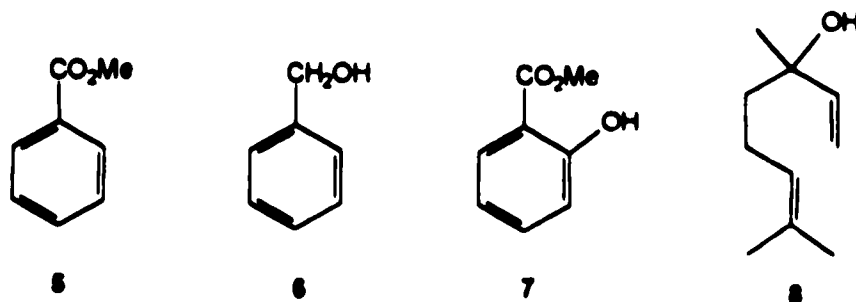
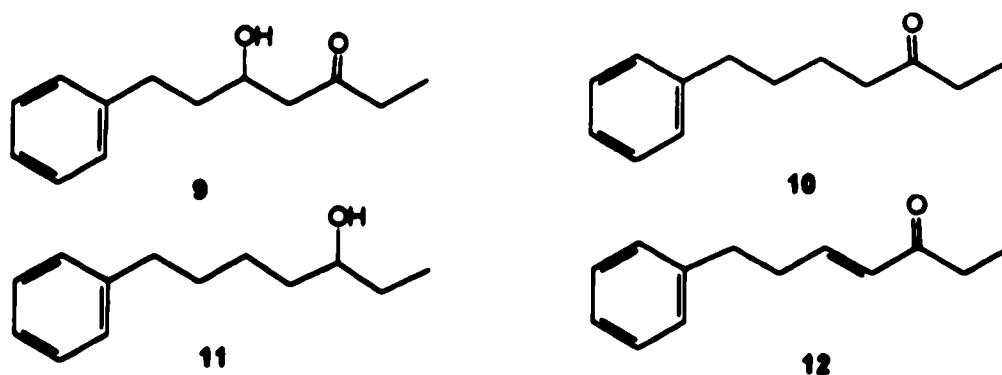


Figure 1 - A portion of lignin macromolecule and the fungal degradation products.

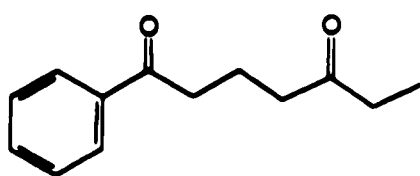
The antagonism exhibited by *P. tremulae* against a variety of fungi associated with aspen shows that it is indeed a very resistant fungus⁶. This resistance may be associated with defense metabolites produced by this organism. Consequently, *P. tremulae* is expected to generate compounds of biological interest. Previous studies on the chemistry of this pathogen have been reported. The first one describes the analysis of the odorous constituents produced by *P. tremulae* when it is grown on 2% diamalt liquid medium¹³. After 10 days, the broth was steam-distilled at atmospheric pressure and the distillate was extracted with ether. The volatile compounds were resolved by gas chromatography and characterized by infrared spectroscopy. The major constituents identified in the extract were: methyl benzoate (5, 48.1%), benzyl alcohol (6, 11.1%), methyl salicylate (7, 10.2%), and linalool (8, 8.5%). This was the first time that compounds 5 to 7 were isolated from a fungal source.



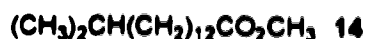
Another study describes the isolation of novel 7-phenyl-3-heptanones directly from the decayed aspen infected by *P. tremulae*¹⁴. The decayed wood was extracted with acetone and partitioned between water and hexanes. The hexanes residue was distilled under reduced pressure using short-path distillation. The distillate exhibited antibiotic activity on certain saprophytic fungi usually found in aspen. Four compounds (9-12) were identified by GC-MS. The identity was confirmed by comparison with the mass spectra and GC retention times of authentic compounds prepared by synthesis. These compounds could not be found in healthy wood, but they were produced in sterilized wood inoculated with *P. tremulae*. The authors did not report whether or not any of the individual heptanones were active. Compound 12 may be an artifact produced from 9



More recently, a new metabolite, 1-phenyl-1,5-heptanedione (13), was isolated directly from conks of *P. tremulae*¹⁵. The conks were extracted with methanol, partitioned between water and hexanes, and the hexanes extract was submitted to silica gel chromatography to afford methyl esters of long-chain fatty acids (14-21), the previously reported phenylheptanone 10, and the new phenylheptanedione 13.



13



15 n=14	18 n=19	21 n=22
16 n=16	19 n=20	
17 n=18	20 n=21	

The isolation of methyl esters among metabolites produced by *P. tremulae* is consistent with the results described by Harper *et al.*^{16,17} which shows the ability of *Phellinus* species to convert aliphatic and aromatic carboxylic acids into their esters using chloromethane as methylating agent. Particularly, they have demonstrated that CD₃-labelled methyl benzoate is formed when *Phellinus pomaceus* is incubated in the presence of benzoic acid and deuterated chloromethane. Chloromethane is a gaseous natural product released as a secondary metabolite by many wood-rotting fungi and labelling experiments reveal that it is derived from methionine^{16,18}. It has been suggested that ester formation in the genus *Phellinus* is biochemically linked with chloromethane biosynthesis, since methyl benzoate occurrence is confined to CH₃Cl-producing species^{16,19}. Although it seems unusual that the fungus utilizes this peculiar methyl donor in certain metabolic processes in preference to the conventional biological methylating agent *S*-adenosyl-methionine (SAM), experimental data strongly support this hypothesis^{16,17}. The experiments were carried out with several monocarboxylic acids using washed mycelium of *P. pomaceus* in citrate buffer (pH 4) incubated with CD₃Cl. The methyl ester formation was analysed by GC-MS. The percentage of incorporation ranged from 38 to 83% in the different substrates. Production of labelled methyl salicylate was also observed when benzoic acid was the substrate but not when salicylic acid was the substrate. This suggests that methyl salicylate is formed by *o*-hydroxylation of methyl benzoate rather than by direct esterification of salicylic acid^{16,17}.

The process of *o*-hydroxylation of aromatic compounds is believed to proceed via arene oxides produced by oxidation of aromatic substrates by monooxygenase enzymes²⁰.

This postulate was initially proposed in 1950 to explain the formation of *trans*-dihydrodiols and glutathione conjugates from polycyclic aromatic substrates in mammals²⁰ and was experimentally verified in 1968 with the isolation of naphthalene 1,2-oxide as a metabolite of naphthalene²¹. The metabolic conversion of aromatic compounds to phenols in mammals has long been considered a means of detoxification and excretion of a variety of foreign substances from the organism²⁰. This concept has changed since the observations that the highly reactive intermediate arene oxide is involved in this reaction. The arene oxide exists in tautomeric equilibrium with the oxepin²², but it is assumed that under physiological conditions the equilibrium is shifted towards the oxide, the reactive species. The hepatic metabolism of benzene oxide is illustrated in Figure 2. Thus, arene oxides can undergo isomerization to phenols, hydration to diols, and conjugation with glutathione²⁰. These three mechanisms contribute to the detoxification of arene oxides in the organism. However, the facile reaction of arene oxides with nucleophiles indicates that they can equally well bind to DNA, RNA, and protein. This binding has been directly associated with the toxic, carcinogenic, and mutagenic effects of aromatic compounds in mammals²⁰.

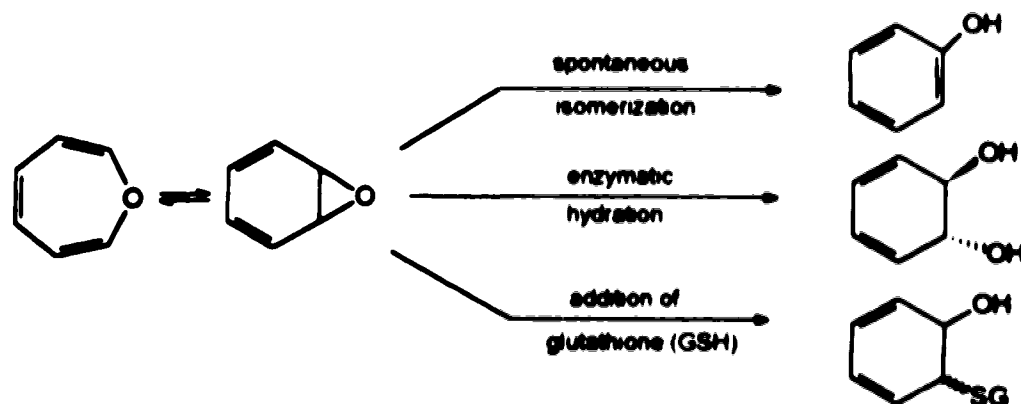


Figure 2 - Hepatic metabolism of benzene oxide

This understanding of the metabolism of arene oxides in animals may help us to understand their roles in plants and microorganisms.

In spite of the number of metabolites already isolated from *P. tremulae*, it is still unclear why this pathogen is so resistant to other fungi. Therefore, more information about the chemistry of this fungus seemed desirable. The present study forms part of a larger study being carried out by our research group in collaboration with Dr. Y. Hiratsuka and his group at the Northern Forest Centre, Forestry Canada, Edmonton, which is directed towards developing methods for controlling fungal decay and staining in aspen. The objectives were: (1) to isolate and characterize the metabolites produced by *P. tremulae* when it is grown in liquid culture, (2) to investigate the biosynthetic origin of the metabolites, (3) to see if the same metabolites are present in the diseased tree and conk, (4) to investigate whether *P. tremulae* is capable of oxidizing another aromatic compound in addition to benzoic acid.

The strain of *P. tremulae* used in this work was isolated from basidiomes associated with *Populus tremuloides* collected from Alberta forests.

There is still controversy over the role of secondary metabolites in nature. It has been suggested^{1,2,3} that they are just waste products with no particular use, or nature's way of ridding the organism of unnecessary primary metabolites. This has been advanced as the reason for the greater production of secondary metabolites in plants and microorganisms than in animals. However, since much more is known about animal metabolism than about plant and microorganism metabolism, many people now feel that this view is premature and that as we learn more about the metabolism of these species we will find that many of the secondary metabolites serve important functions in the organism. The first step in understanding the role of these compounds is their isolation and structure determination. Once the structures are known it is important to determine how they are biosynthesized. The aim of this work is to provide some of this background information about the secondary metabolites of the fungus *Phellinus tremulae*.

II. RESULTS AND DISCUSSION

2.1. Isolation of the Metabolites

Phellinus tremulae was cultivated in shake culture on 2% malt extract broth for 16 days. The liquid culture developed the wintergreen smell which is characteristic of this fungus. It was found that the odorous components of this culture were lost during concentration of the broth under reduced pressure. This was circumvented by introducing an additional extraction prior to concentration. Although this procedure led to the isolation of the volatile compounds, the yields were low. Improvement of the yield was achieved by growing *P. tremulae* in the presence of DIAION HP 20^{24a}, which is a nonionic highly porous resin capable of absorbing organic metabolites from aqueous media^{24b,24c}. The net result of the use of this resin is an increase in metabolite production, presumably because it prevents the fungus from being exposed to its own active metabolites at high concentrations^{24b}. This ability of the resin to absorb metabolites was clear after comparison of the yields obtained for the cultures grown in the presence and in the absence of the resin, as outlined in Table 1. The recovery of metabolites remaining in the broth was negligible.

Table 1 - Growth of *P. tremulae* in the presence and absence of HP 20 resin

CH ₂ Cl ₂ extract	With resin (mg/L)	Without resin (mg/L)
Resin extract	500	-
Non-concentrated broth	6	77
Concentrated broth	4	20

The additional advantage of the use of this resin is the simplification of the workup. The optimized conditions involve vacuum filtration of the liquid culture followed by extraction of the resin and wet mycelium with dichloromethane. TLC analysis indicates that the mycelium is not simultaneously extracted in this procedure.

Flash chromatography of the crude extract using gradient elution with MeOH-CH₂Cl₂ gave methyl salicylate, methyl benzoate, and 2-carbomethoxyoxepin (22), followed by seven sesquiterpenes, the tremulanes 23 to 29. The separation and the yields of metabolites are summarized in Figure 3. Methyl salicylate and methyl benzoate have been reported previously as metabolites of *P. tremulae*¹³. The other metabolites are new natural products.

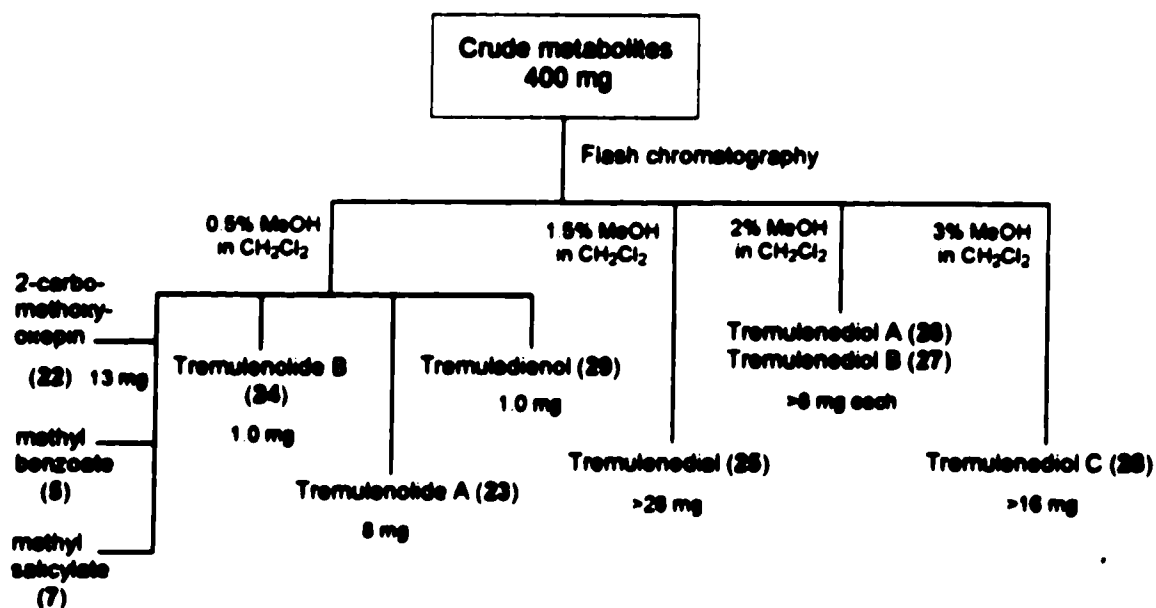


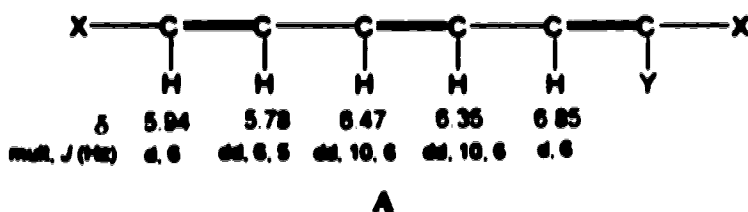
Figure 3 - Sequence of elution of metabolites of *Phellinus tremulae* on silica gel flash chromatography.

2.2. Aromatic and Heterocyclic Compounds

2.2.1. Characterization

The first two compounds eluted from the flash chromatographic column were identified as methyl salicylate and methyl benzoate by comparison of their NMR and GC-MS data with that of authentic samples.

The next metabolite eluted was a yellow oil which showed a molecular ion at m/z 152 in the HREIMS corresponding to a molecular formula $C_8H_8O_3$. The UV absorption at 313 nm is indicative of an extended chromophore. In the IR spectrum a carbonyl absorption at 1728 cm^{-1} is consistent with a conjugated ester. The ^1H NMR spectrum shows five olefinic protons, belonging to the same spin system, and a methoxy signal at δ 3.82. The results obtained from the homonuclear selective decoupling and ^1H - ^1H COSY^{25a} experiments (Figure 4) suggest the connectivity displayed in partial structure A. The lower field doublet (δ 6.85) was assigned to a proton *vicinal* to the carbomethoxy group based on the deshielding effect of the carbonyl. This partial structure A and the ester functionality account for four of the five unsaturation equivalents indicating that compound 22 is monocyclic. The ^{13}C NMR spectrum (APT)^{25b} shows 8 signals: 5 protonated olefinic carbons, 1 quaternary olefinic carbon, a carbonyl carbon, and a methoxy carbon. These data are consistent with structure 22. The ^{13}C NMR assignment shown in Figure 5 is based on HMQC^{25c} experiments complementing the previously assigned ^1H NMR. INAPT^{25d} experiments correlate the H-3 proton (δ 6.85) with the carbonyl carbon and the C-2 carbon, and the H-7 proton (δ 5.94) with C-2 as well as C-4 and C-5. The ^1H NMR and IR spectra are identical with those of authentic 2-carbomethoxyoxepin prepared synthetically²⁵.



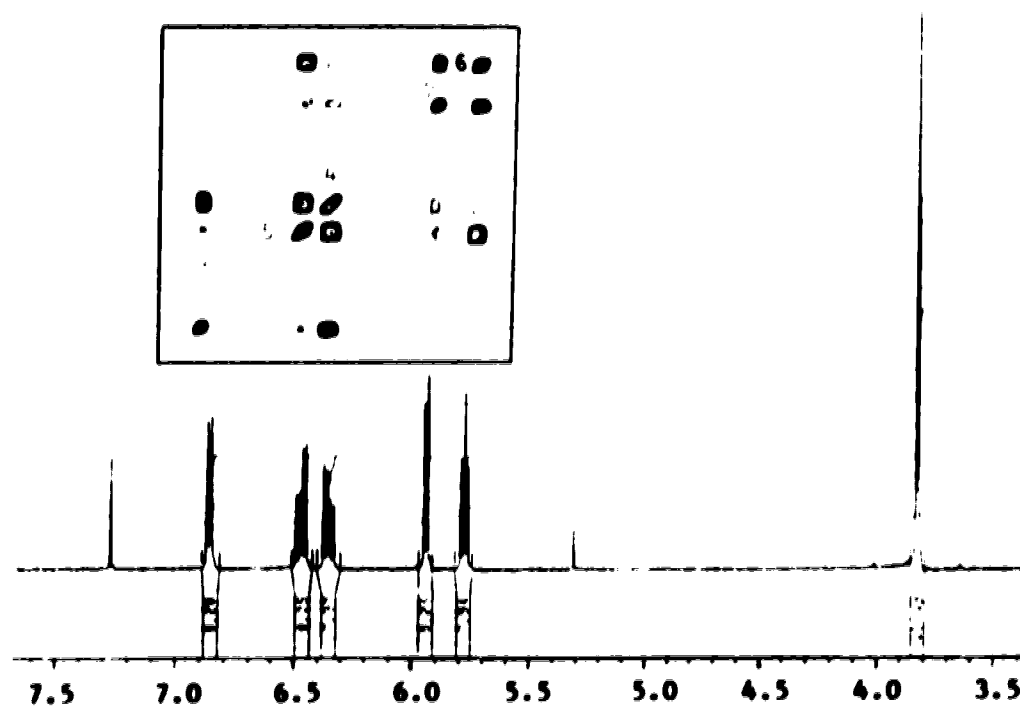


Figure 4 - ^1H NMR and ^1H - ^1H COSY spectra of 2-carbomethoxyoxepin (22) in CDCl_3 .

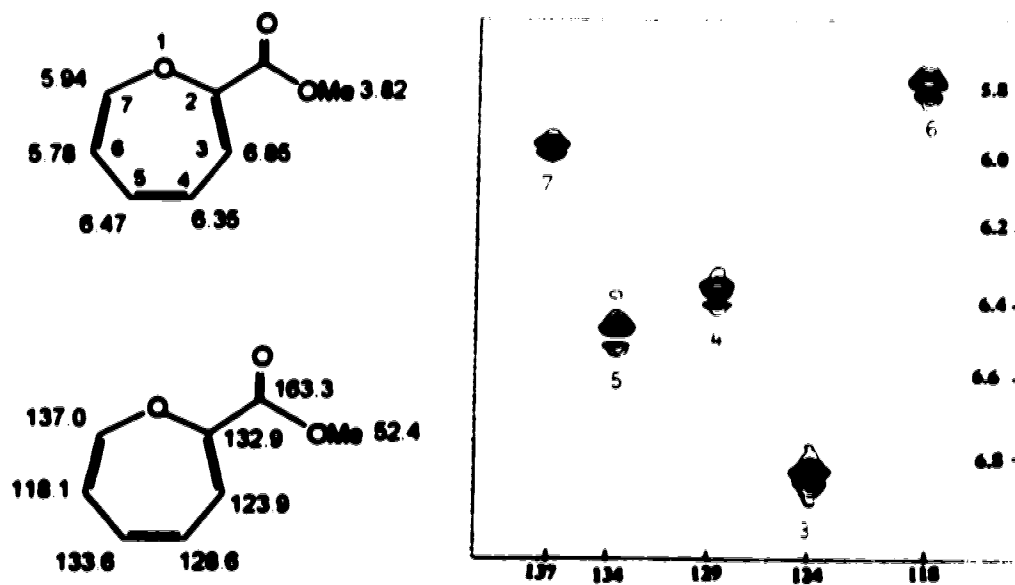


Figure 5 - HMQC spectrum and ^1H and ^{13}C NMR shifts for 2-carbomethoxyoxepin (22) in CDCl_3 .

Oxepin is believed to exist in equilibrium with its valence tautomer benzene oxide²². The position of this equilibrium is dependent upon the nature and location of substituents. In the case of 2-substitution, especially by conjugative electron-withdrawing groups, it favors the oxepin²⁶. ¹³C NMR studies carried out at low temperatures indicated that the ¹³C signals for the oxepin tautomer are at δ 141.8 (C-2, C-7), 117.6 (C-3, C-6), and 130.8 (C-4, C-5), and for the benzene oxide tautomer are at δ 56.6 (C-1, C-2) and 128.7 for the other carbons²⁷. Since the signal for C-7 in 22 (δ 137.0) is little shifted from the corresponding signal in oxepin, it appears that the arene oxide tautomer makes a very small contribution in CDCl₃ at room temperature. This is consistent with the UV absorption at 313 nm²² (calc²⁸ 317 nm, Table 2) and is explained in terms of the resonance stabilization of the oxepin tautomeric form^{26b}:

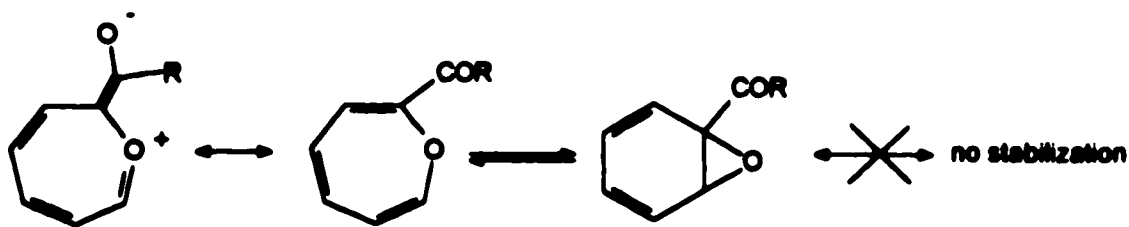


Table 2 - Calculated UV absorption for the oxepin tautomer of 22.^a

	oxepin tautomer
α,β disubstituted unsaturated ester	217
endocyclic α,β double bond in seven-membered ring	+ 5
double bond extending conjugation (2)	+ 60
oxygen at α position	+ 35
Total:	317

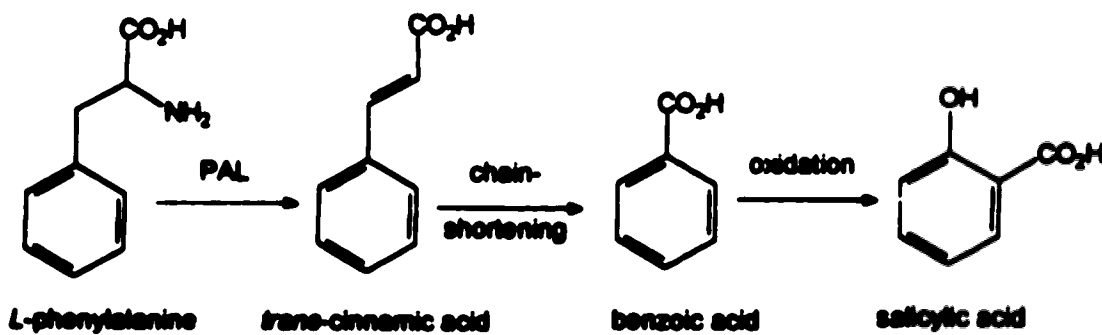
^a experimental value for benzene oxide is 270 nm²².

Addition of a drop of trifluoroacetic acid to a solution of **22** in CDCl_3 in a NMR tube, at room temperature, led to complete rearrangement to methyl salicylate within one hour, in accord with the previous observation²⁹. This transformation has been shown to proceed *via* an NIH shift and will be discussed later.

The isolation of 2-carbomethoxyoxepin from a natural source provided the opportunity to investigate whether this heterocyclic compound is actually involved in the biogenesis of phenolic secondary metabolites, as postulated in the literature²⁹.

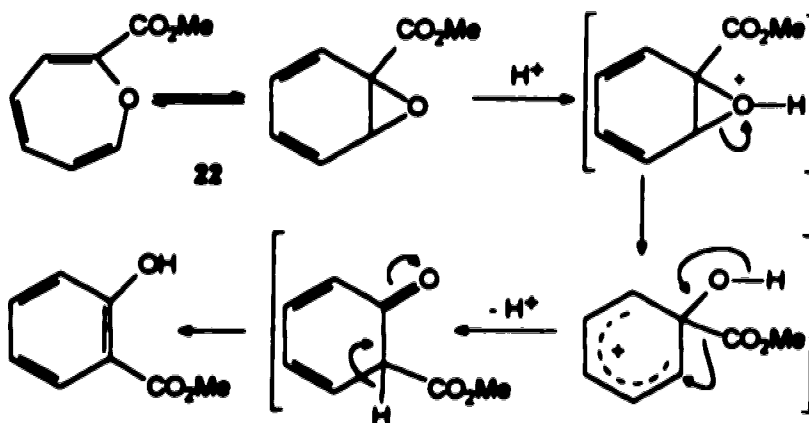
2.2.2 Biosynthesis

The biosynthesis of salicylic acid and, by analogy, methyl salicylate is generally regarded as deriving *via* the shikimic acid pathway^{30,31}, though different intermediates seem to be involved as far as bacteria³⁰ and plants³¹ are concerned. In bacteria, chorismic and isochorismic acids are the only intermediates involved³⁰. In plants, it is believed that salicylic acid is derived from the phenylpropanoid pathway, in which *L*-phenylalanine is converted to *trans*-cinnamic acid by phenylalanine ammonia lyase (PAL) catalysis. Chain-shortening degradation leads to benzoic acid, which is oxidized to salicylic acid (Scheme 1)³¹. The involvement of benzoic acid is supported by the results of the administration of [¹⁴C]benzoic acid to plants with subsequent isolation of labelled salicylic acid³¹, presumably through the 1,2-oxide of benzoic acid³².



Scheme 1 - Salicylic acid biosynthesis and metabolism in plants.

As mentioned in the Introduction, the monooxygenase-catalyzed formation of phenolic secondary metabolites from aromatic substrates has been postulated to proceed *via* arene oxides. This postulate is based on observations of substituent migration using labelled or strategically substituted aromatic compounds³¹, as well as on the isolation of some arene oxides from natural sources^{21,33}. The other evidence for arene oxide intermediacy was shown in an elegant study by Boyd and Berchtold²⁹, where they prepared a number of 1-carboxy- and 1-carbomethoxybenzene oxides and showed that these undergo facile acid-catalyzed rearrangement to the corresponding phenols. In particular, they showed that 1-carbomethoxybenzene 1,2-oxide (22) is readily transformed to methyl salicylate *via* an NIH shift involving migration of the carbomethoxyl group²⁹ (Scheme 2).



Scheme 2 - Rearrangement of 2-carbomethoxyoxepin (22) to methyl salicylate *via* NIH shift

Investigations by Harper *et al.* demonstrated that *Phellinus* species have the ability to convert benzoic acid into methyl benzoate using chloromethane as methyl donor^{16,17}. They also suggested that methyl salicylate is biosynthesized from methyl benzoate^{16,17}. Based on this evidence and in order to test the *in vivo* participation of arene oxides as intermediates in the methyl salicylate biosynthesis²⁹, benzoic acid- α -¹³C was administered to *P. tremulas*. The culture was prepared as described previously (with resin) and was

periodically supplemented with injections of a sterile solution of sodium benzoate- α - ^{13}C . After 16 days of growth, the culture was harvested and the crude extract was chromatographed as before. The incorporation of labelled benzoic acid was determined by ^{13}C NMR spectroscopy of the isolated methyl benzoate, methyl salicylate, and 2-carbomethoxyoxepin (22). The enrichment (Table 3) was calculated based on the intensity of the quaternary carbons indicated in Figure 6. In the natural abundance spectra these quaternary carbons have the same intensity as the ester carbonyl.

Table 3 - Incorporation of benzoic acid- α - ^{13}C by *Phellinus tremulae*.

Compound	δ	Atom % enrichment ^a
Methyl benzoate (5)	167.0	37
Methyl salicylate (7)	170.6	38
2-Carbomethoxyoxepin (22)	163.2	94

$$^a \text{Atom \% enrichment} = \frac{\text{sodium benzoate labelled intensity}}{\text{natural abundance intensity}} - 1.1$$

The level of incorporation of labelled benzoic acid in these three esters shows that methyl salicylate is biosynthesized from benzoic acid *via* its arene oxide in *P. tremulae*. In the study by Harper *et al.* on the methylation of benzoic acid by chloromethane in *P. pomaceus*, it was found that ester biosynthesis was maximal at 0.5 mM of benzoic acid but was practically inhibited when benzoic acid concentration in the medium exceeded 3 mM¹⁶. They noticed that the decrease in the methyl benzoate pool was followed by a secondary peak in the chromatogram, which was not methyl salicylate. They proposed that the fungus was directing benzoic acid into alternative metabolic pathways at certain stages of growth. Analyzing this hypothesis on the basis of our results, it is possible that the increasing concentration of benzoic acid in the medium was stimulating the mono-oxygenase to catalyze the oxidation of methyl benzoate to 2-carbomethoxyoxepin (22).

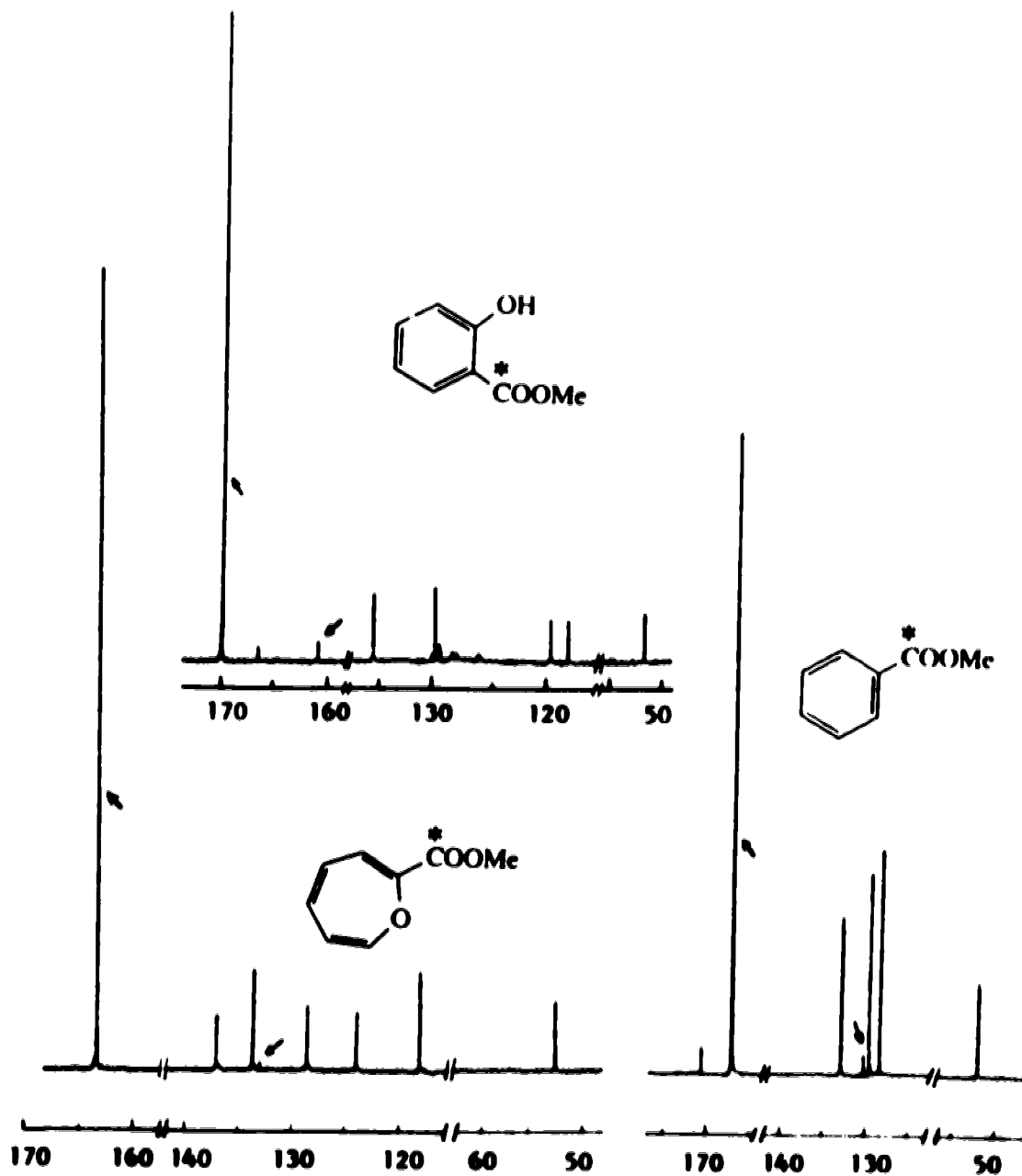
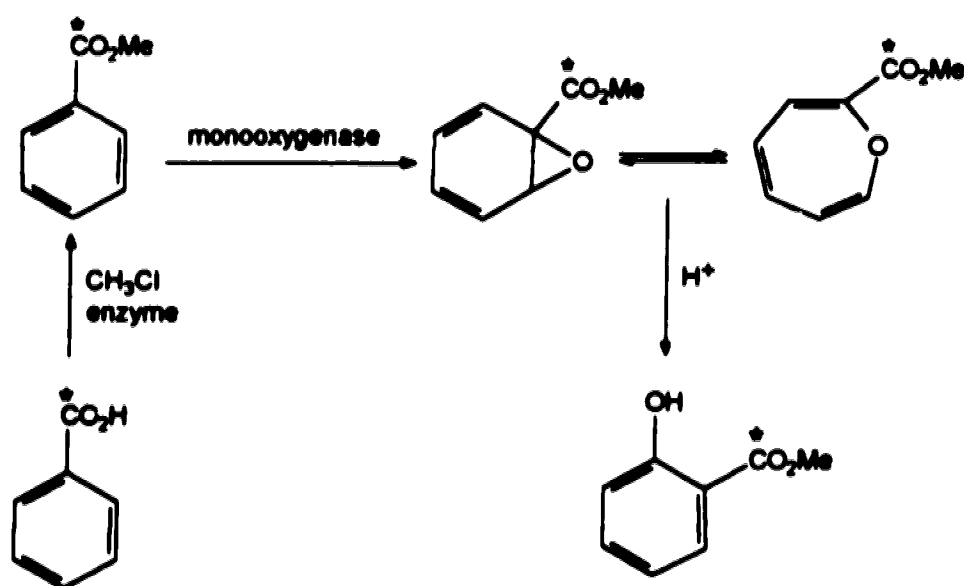


Figure 6 - ^{13}C NMR spectra of methyl salicylate, 2-carbomethoxyoxepin, and methyl benzoate after incorporation of benzoic acid- α - ^{13}C by *P. tremulae*.

Therefore, the biosynthesis of methyl salicylate in *P. tremulae* follows the pathway proposed by Harper *et al.*^{16,17} and mimics the salicylic acid biosynthesis in plants³¹. The initial step is the esterification of benzoic acid followed by 1,2-epoxidation of the methyl benzoate formed. The presence of the electron-withdrawing carbomethoxy group favors rearrangement to 2-carbomethoxyoxepin and finally acid catalyzed or spontaneous isomerization affords methyl salicylate (Scheme 3).



Scheme 3 - Biosynthesis of methyl salicylate from benzoic acid in *Phellinus tremulae*.

These results serve to highlight several points. First, it shows that *P. tremulae* metabolizes benzoic acid to produce methyl salicylate, through a process involving the initial methylation of benzoic acid to methyl benzoate with subsequent oxidation of the latter to its arene oxide. Second, it is a direct evidence of the intermediacy of an arene oxide in the formation of this type of phenolic metabolite. Third, the esterification of benzoic acid may be viewed as a strategy used by *P. tremulae* to block the production of salicylic acid by the tree. Salicylic acid is now recognized as a systemic signal in induced plant disease resistance. Some plants produce salicylic acid in response to pathogen

infection as a means of activating induced defenses³¹. In this process, host cells in the vicinity of the pathogen penetration 'commit coordinated suicide', at the same time killing the pathogen or restricting its spread³¹. Since salicylic acid in plants is believed to be derived from benzoic acid, its formation can be suppressed by utilizing benzoic acid for the production of a compound that does not act as an inducer of resistance. It is thus possible that the esterification of benzoic acid is the way that *P. tremulae* attempts to shut down a defense mechanism of the tree^{34a}. Furthermore, preliminary results of an ongoing project in our laboratories indicate that black gall bearing trees produce benzoic acid in greater amounts than do "clean" trees. Since, as mentioned in the Introduction, black gall trees are less susceptible to *P. tremulae* infection, it is possible that black galls protect the tree by increasing the production of benzoic acid as a precursor of salicylic acid which is then part of the defense system.

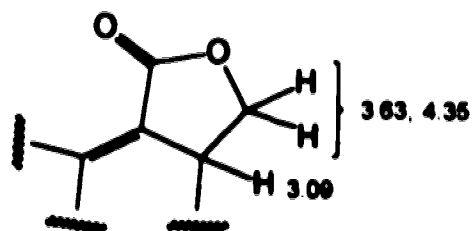
2.3. Sesquiterpenes

2.3.1. Characterization

A series of sesquiterpenes was eluted from the flash chromatography (Figure 3) after 2-carbomethoxyoxepin (22). These sesquiterpenes belong to a new group of sesquiterpenes for which we have coined the name "tremulanes".

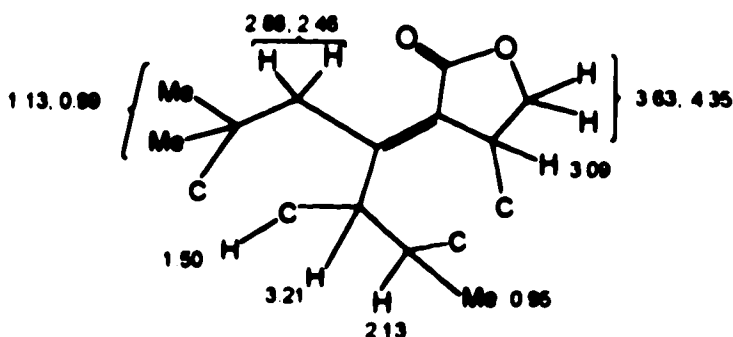
Tremulenolide A (23)

Tremulenolide A (23) was eluted as a colorless oil and crystallized from hexanes to give colorless needles having a melting point 110-112°C. The HREIMS and CIMS indicated a molecular formula $C_{15}H_{22}O_2$ (m/z 234). The base peak at m/z 219 reflects the loss of a methyl radical. The presence of an α,β -unsaturated γ -lactone is apparent from UV absorption at 236 nm and an intense carbonyl absorption at 1753 cm^{-1} in the FTIR spectrum. This is supported by ^{13}C NMR (Table 4) signals at δ 171.5 (C-11), δ 161.5 (C-1), and δ 120.7 (C-2). Since these carbon signals are singlets and there is evidence of coupling between the oxygenated methylene protons (δ 4.35 and 3.63) and the allylic proton at δ 3.09 in the ^1H NMR spectrum (Table 5), it is clear that the double bond in the α,β -unsaturated γ -lactone is fully substituted and exocyclic to the lactone ring. The calculated UV absorption maximum for such a system is 235 nm²⁸.



The allylic methylene pair at δ 2.88 and 2.46 ($J_{gem} = 19\text{ Hz}$) was assigned *vicinal* to a fully substituted carbon, since they do not show coupling to neighboring hydrogens. The

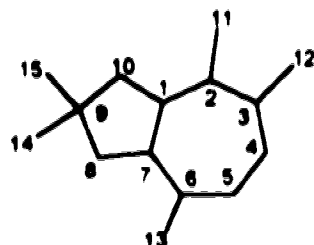
remaining allylic position was assigned to the methine at δ 3.21 which shows further coupling to the protons at δ 2.13 and 1.50. Three methyl groups are present in the ^1H NMR spectrum (Figure 7). These are a secondary methyl at δ 0.95 which is coupled to the signal at δ 2.13 by 7.5 Hz and two tertiary methyls at δ 1.13 and 0.99. An NOE^{34b} enhancement of 8.7% is observed on the allylic proton at δ 2.46 upon saturation of the methyl at δ 1.13. Since all the remaining carbons in the ^{13}C NMR spectrum carry hydrogen, these tertiary methyl groups must be attached to the quaternary carbon *vicinal* to the allylic methylene group.



The α,β -unsaturated γ -lactone accounts for three of the five units of unsaturation, indicating that tremulenolide A is tricyclic. The connectivities established in the previous partial structure leave only two possibilities of ring combination, either to form a 6,6 or a 5,7 fused AB-ring system. Considering that the *gem*-dimethyl groups are located in one of these rings, their carbon chemical shifts can be used as a starting point to establish the ring size. Thus, examples of five-, six-, and seven-membered rings having *gem*-dimethyl substituents were obtained from the literature^{35,38} (Figure 8) and examined in terms of the chemical shift difference between the carbon resonances of the methyl groups. It was noted that the chemical shift difference between *gem*-dimethyl groups on six-membered rings is usually >10 ppm^{36,37} whereas in five- and seven-membered rings it is ~ 3 ppm^{35,36,38}. The chemical shifts of the *geminal* methyl groups in tremulenolide A (23) are at δ 27.3 and 29.0, therefore $\Delta\delta$ is less than 3 ppm. This tentatively excludes the

presence of a six-membered ring, but it does not allow differentiation between five- and seven-membered rings

Table 4 - ^{13}C NMR chemical shift data (CDCl_3) for tremulanes 23 to 29



Atom	23	24	25a	26	26a	27	27a	28	29
C-1	161.5	137.0	139.5	145.6	150.3	145.6	144.2	140.1	142.8
C-2	120.7	45.8	49.2	132.3	126.5	47.4	42.4	134.5	147.4
C-3	41.0	38.7	47.9	45.4	41.3	48.2	44.7	50.4	50.5
C-4	28.1	28.8	27.5	22.5	21.2	29.5	29.7	20.8	26.6
C-5	32.9	28.4	29.6	32.6	31.7	30.8	30.4	32.0	32.2
C-6	32.7	33.0	34.0	31.6	31.4	35.7	35.7	32.4	33.6
C-7	45.5	48.0	48.4	46.0	46.6	48.5	48.2	43.7	50.4
C-8	44.9	42.2	43.2	45.5	45.3	42.8	42.7	41.2	45.0
C-9	37.2	42.6	42.1	37.0	37.2	41.6	41.6	40.7	42.9
C-10	48.4	143.5	142.0	48.0	48.3	138.6	139.9	83.5	139.5
C-11	171.5	177.0	107.5	65.6	69.0	60.8	63.4	22.8	112.6
C-12	70.9	71.9	107.9	63.2	63.2	66.7	68.1	62.8	63.7
C-13	17.7	19.3	18.5	11.6	11.7	19.4	19.6	12.4	12.0
C-14	29.0	29.4	29.3	28.5	28.4	29.4	29.2	26.5	29.1
C-15	27.3	27.1	27.9	26.9	26.8	26.8	26.4	21.0	27.2

Table 5 - ^1H NMR data (CDCl_3) for tremulanes 23 to 29

Proton	δ , multiplicity, J in Hz						
	23	24	25a	26	27	28	29
H-2	-	3.63, d, 9.5	3.52, dd, 8, 5.2	-	2.85, ddd, 8.5, 5, 4	-	-
H-3	3.09, m	2.71, m	2.48, m	2.53, m	1.70, m	2.24, m	2.63, m
H-4 α	1.84, m	1.92, m	1.52, m	1.80, bd, 11.5	1.60, m	1.78, dm, 11	1.78, m
H-4 β	1.73, dddd 13.6, 5.2, 5.1, 5	1.50, m	1.84, m	1.59, dd, 11.5, 3.5	1.52, m	1.58, m	1.62, m
H-5 α	2.05, m	1.43, m	1.44, m	1.83, m	1.34, m	1.78, dm, 11	1.78, m
H-5 β	1.46, m	1.43, m	1.44, m	1.61, dd, 12, 3	1.34, m	1.54, m	1.62, m
H-6	2.13, pd, 7.5, 2	1.81, m	1.83, m	1.76, m	1.88, ddq, 10, 7.5, 7.5	1.69, m	1.80, m
H-7	3.21, tm, 10	3.16, m	2.93, m	3.10, tm, 9	2.94, dddd 11.5, 10.6, 5.2, 5	2.97, m	3.13, ddt, 10, 7.5, 2.5
H-8 α	1.50, d, 10	1.37, dd, 12.5, 10	1.37, dd, 13, 9	1.38, dd, 12.5, 12	1.32, dd, 11.5, 11.5	1.22, dd, 12, 12	1.50, dd, 12, 10
H-8 β		1.72, dd, 12.5, 7.5	1.73, dd, 13, 7.5	1.52, ddd, 12.5, 8, 2.5	1.61, dd, 11.5, 6.5	1.46, dd, 12, 8.5	1.71, dd, 12, 7.5
H-10 α	2.46, ddd, 19, 4.5, 3.5	-	-	1.93, bd, 15.5	-	-	-
H-10 β	2.88, dd, 19, 2.5	5.50, d, 2.2	5.47, d, 2.2	2.29, dd, 15.5, 2.5	5.32, d, 2.5	4.03, dd, 2, 2	5.71, d, 2.8
H-11 α	-	-	-	4.24, d, 11	3.90, dd, 11, 8.5	1.94, dd, 2, 2	5.22, d, 2.5
H-11 β	-	-	5.20, d, 5.2	3.83, bd, 11	3.64, dd, 11, 5	-	4.80, d, 2.5
H-12 α	4.35, dd, 8.5, 8.5	4.36, dd, 9.5, 7	-	3.61, dd, 9, 5	3.62, dd, 11, 4	3.79, dd, 10, 8	3.76, dd, 10.5, 9.5
H-12 β	3.63, dd, 10.5, 8.5	4.09, dd, 9.5, 3.2	4.98, d, 1.5	4.01, dd, 10, 9	3.58, dd, 11, 6.5	3.64, dd, 10, 7	3.61, dd, 10.5, 6
13-Me	0.95, d, 7.5	0.85, d, 7	0.83, d, 7	0.82, d, 7	0.84, d, 7.5	0.78, d, 7	0.79, d, 7.2
14-Me	1.13, s	1.10, s	1.09, s	1.07, s	1.04, s	1.02, s	1.09, s
15-Me	0.99, s	1.06, s	1.02, s	0.87, s	0.98, s	0.82, s	1.03, s

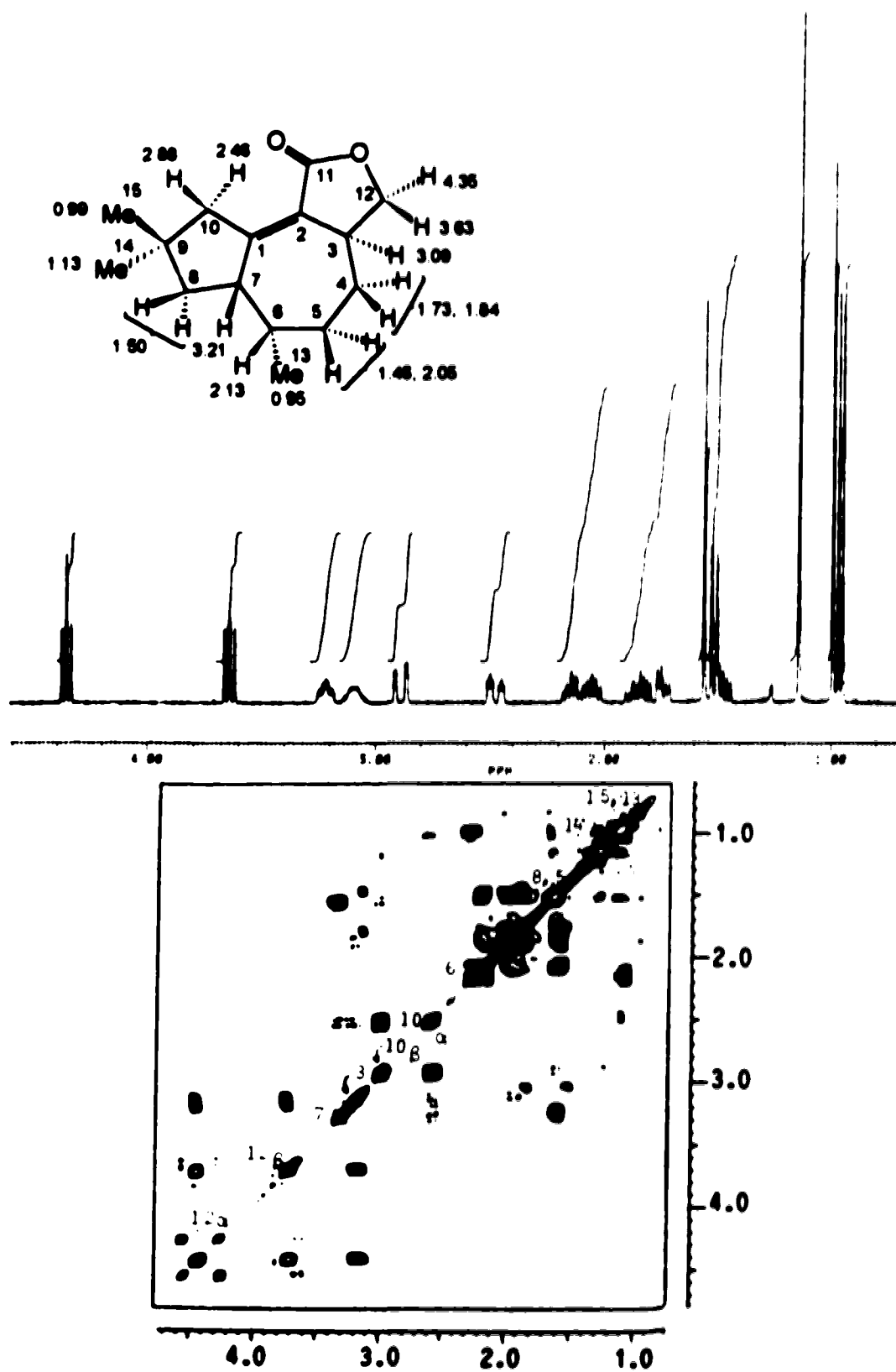


Figure 7. ¹H NMR, ¹H-¹H COSY spectra (CDCl₃) and chemical shift assignment of 23.

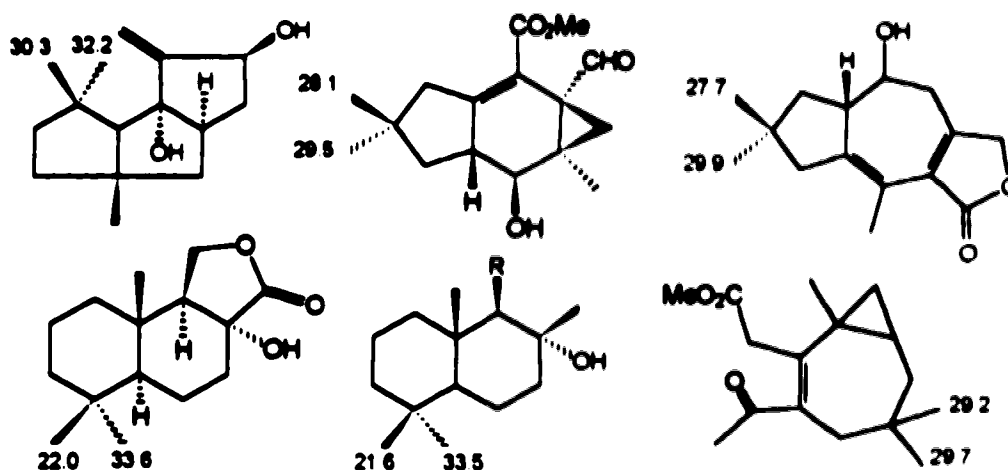
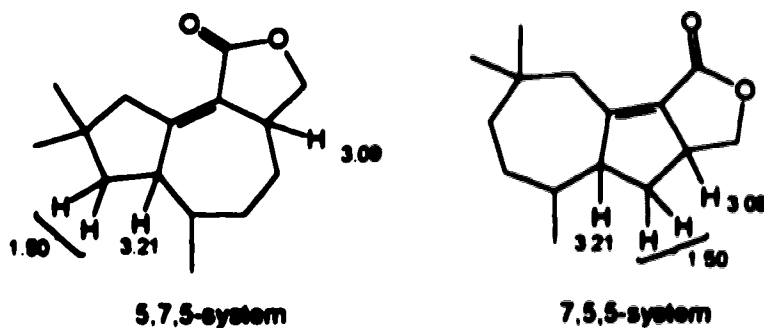


Figure 8 - ^{13}C chemical shift of *gem*-dimethyl groups in five-, six-, and seven-membered rings.

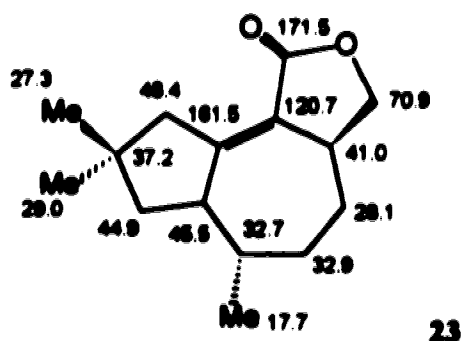
Consequently, there are two possible tricyclic systems that account for the data discussed so far, a 5,7,5- or a 7,5,5-system.



The first step in distinguishing between these two structures is to examine further the coupling patterns of the protons already assigned. For example, there is no evidence of coupling between the allylic proton at δ 3.09 and the signal at δ 1.50 which would be expected in the 7,5,5-system. Irradiation of the 3.09 resonance changes the multiplicity of the hydrogens at δ 1.84 and 1.73. These are also coupled to the hydrogens at δ 1.46 and 2.05 and these in turn are coupled to the methine at δ 2.13 (Figure 7). This coupling pattern is consistent with the 5,7,5-system. Furthermore, it was subsequently established

that ozonolysis of tremulenolide A affords a substituted cyclopentanone bearing a *gem*-dimethyl group (discussed later) consistent with the 5,7,5-structure **23**.

The multiplicities of the signals in the ^{13}C NMR spectrum (APT) are consistent with constitution **23**. It shows four singlets (three sp^2 and one sp^3 hybridized), three doublets, five triplets, one of which is oxygenated, and three quartets (Table 4). The assignment of the carbon resonances was based on the previously assigned proton spectrum and on an HMQC experiment which correlates protons and the directly attached carbons. Figure 9 shows the HMQC spectrum of **23**. This 2D spectrum presents the proton domain in the vertical axis and the carbon domain in the horizontal. The first signal in the carbon domain is at δ 70.9 and it shows two cross peaks which intercept the hydrogen resonances at δ 3.63 and 4.35. These are assigned to C-12. Using the same procedure with the remaining cross peaks, the carbon assignment shown in structure **23** below follows.



Analysis of the HMBC ^{13}C spectrum was extremely useful in supporting this structural assignment. This 2D experiment is very similar to HMQC, except that it shows correlations of protons and carbons which are separated by two and three bonds. An example of an HMBC spectrum is provided later in the discussion of compound **26**. The long range ^1H - ^{13}C correlation of H-7 with C-1, C-2, C-5, C-6, C-8, and C-13 (Figure 10, A) and H-6 with C-1, C-4, C-5, and C-13 (Figure 10, B), were particularly important to support the positioning of the methyl at C-6 relative to the 5-membered ring. Other useful correlations

are exhibited by H-10 β with C-1, C-2, C-7, C-8, C-9, and C-15, and these strongly support the assignment of the size of ring A.

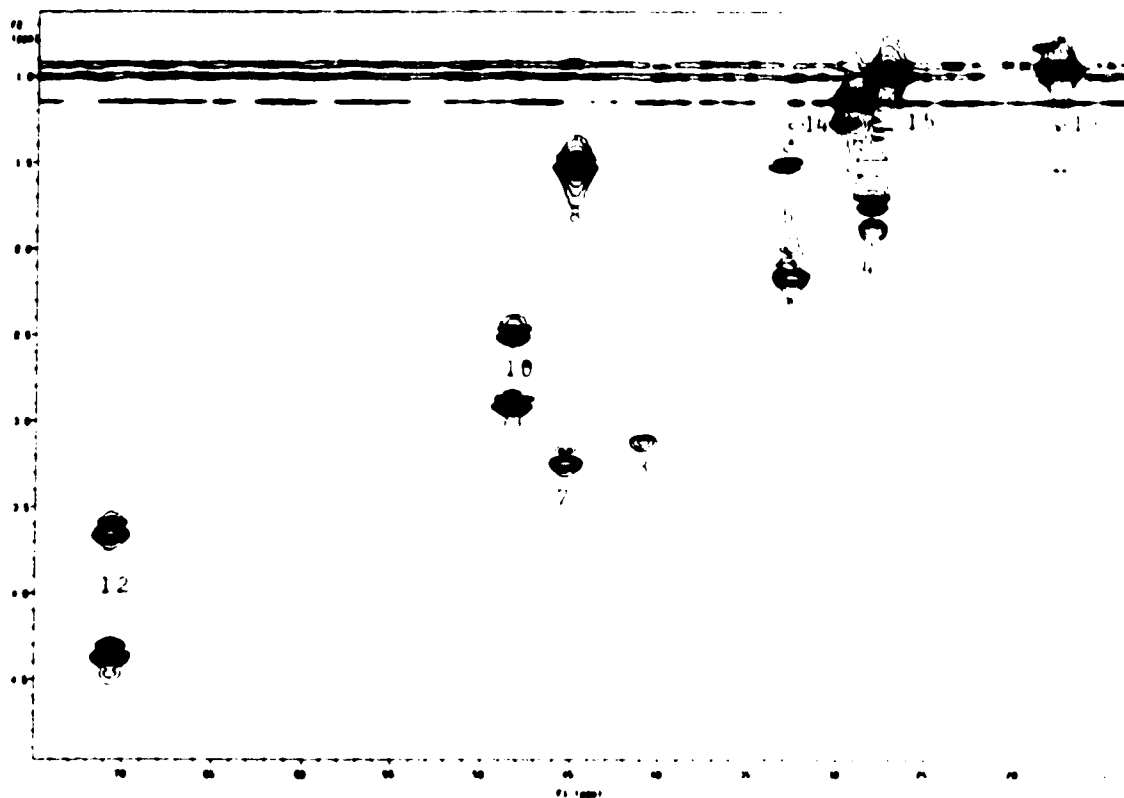


Figure 9 - HMBC spectrum of tremulenolide A (23).

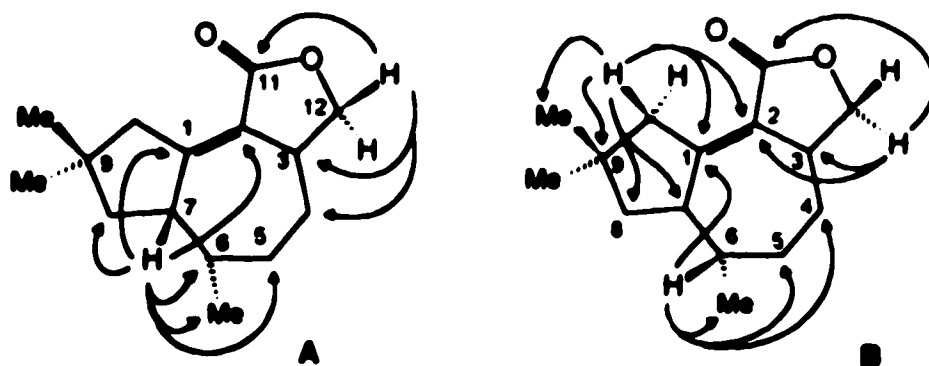


Figure 10 - Significant HMBC correlations of tremulenolide A (23)

Several interesting ^1H - ^1H couplings were important in establishing the relative stereochemistry. The coupling between H-3 and H-12 β is 10.5 Hz and that between H-3 and H-12 α is 8.5 Hz, reflecting dihedral angles approaching 180° and 0° , respectively, and is consistent with the *trans* relationship of H-3 and H-12 β . The assignment of H-12 β at higher field (δ 3.63) than H-12 α (δ 4.35) is based on the fact that it is in the shielding region of the C-2,C-3 and C-11,O bonds and in an antiperiplanar relationship to one of the oxygen lone pairs, which causes an upfield shift due to an $n\text{-}\sigma^*$ interaction⁴⁰. The protons on C-10 (δ 2.88, 2.46) both show pronounced long range couplings with H-3 ($^5J = 2.5, 4.5$ Hz, respectively). Since homoallylic coupling is at a maximum for C-H bonds parallel to the π orbitals⁴¹ the proton at δ 2.46, exhibiting the larger coupling constant, should be that in the α position (Figure 12).

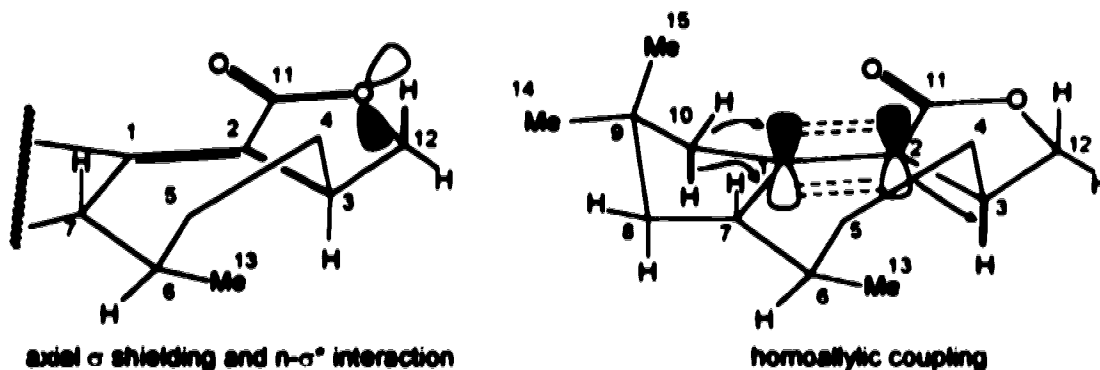


Figure 12 - Shielding of H-12 β and homoallylic coupling between H-3 and H-10 α in 23.

The β H-10, which is in the deshielding cone of the lactone carbonyl, is at δ 2.88. Another important long range coupling of H-10 α is with H-7, which can be explained in terms of an axial-axial zig-zag coupling. This diaxial configuration permits maximum $\sigma\text{-}\pi$ overlap involving the central π -bond at C-1, enhancing the normal spin transmission across four bonds⁴² (Figure 13). The large magnitude of these coupling constants can be attributed to the rigid geometry of this molecule which is optimal for $\sigma\text{-}\pi$ overlap⁴¹.

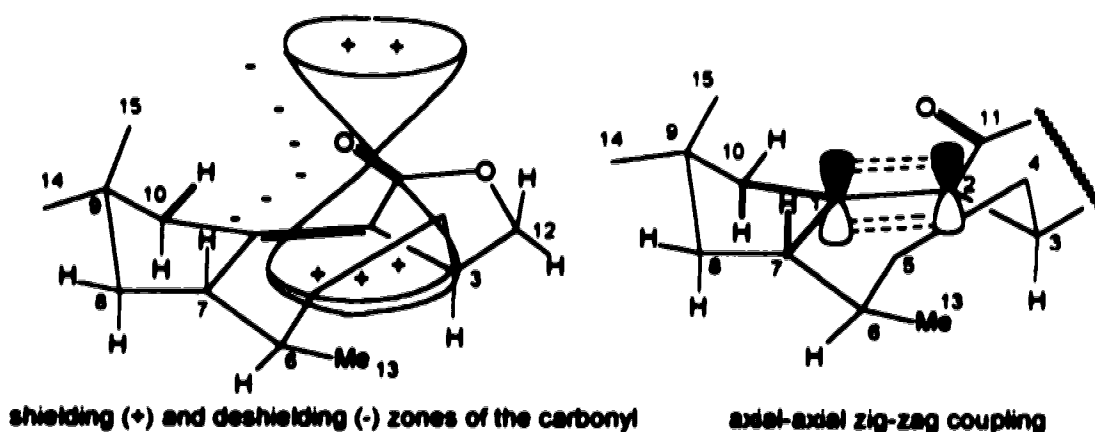


Figure 13 - Carbonyl cone effect and axial-axial zig-zag coupling in compound 23.

The small *vicinal* coupling between H-7 and H-6 ($^3J = 2$ Hz, dihedral angle approaching 90°) indicates that H-6 is also β . In NOE experiments on tremulenolide A (Figure 14), the H-7 and H-6 protons exhibit 4.5% NOE, and H-3 shows a 10 % NOE upon irradiation of the methyl at C-13. Additional NOEs have been observed between H-3 and H-12 α (5.6%), and between H-10 α and the methyl at δ 1.13 (8.7%). This latter NOE was useful in assigning the chemical shifts of the *geminal* methyls at C-9.

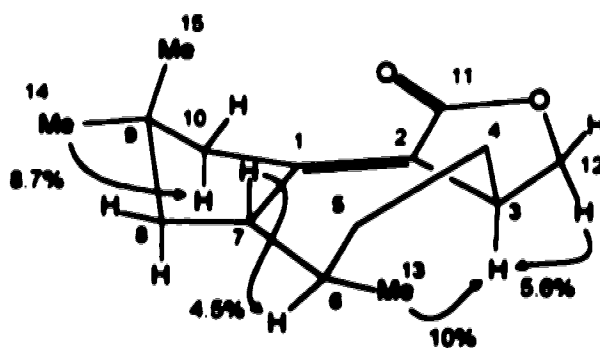
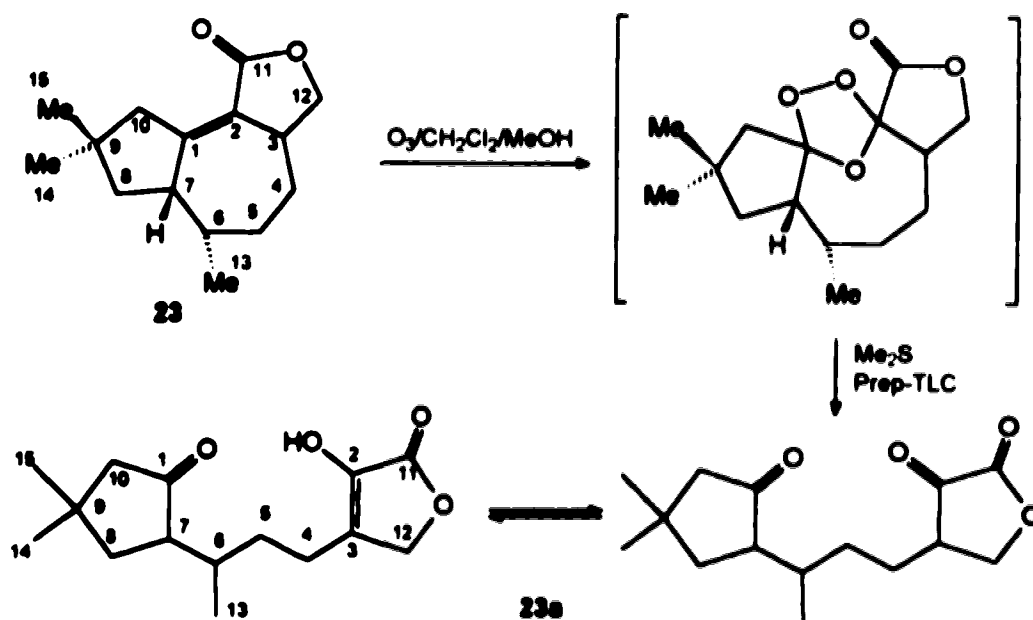


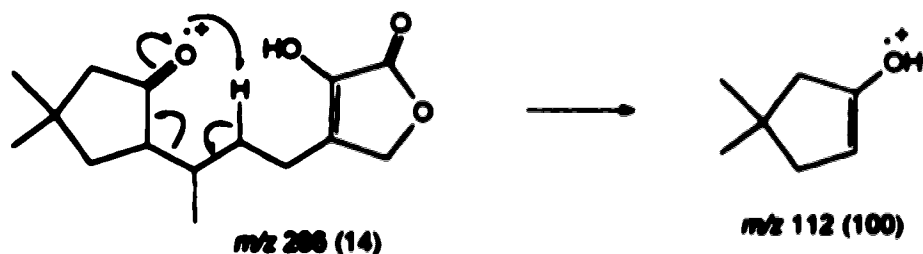
Figure 14 - NOE enhancements observed in tremulenolide A (23).

Ozonolysis of tremulenolide A (**23**) afforded compound **23a** which shows a molecular ion at m/z 266, corresponding to $C_{15}H_{22}O_4$. This is consistent with the introduction of 2 oxygens into the molecule. An AB quartet for the oxygenated methylene in the 1H NMR (δ 4.66) and an OH absorption in the FTIR spectrum indicate that the ketone formed in the lactone ring is enolized (Scheme 4). The same numbering system is adopted to facilitate comparison.



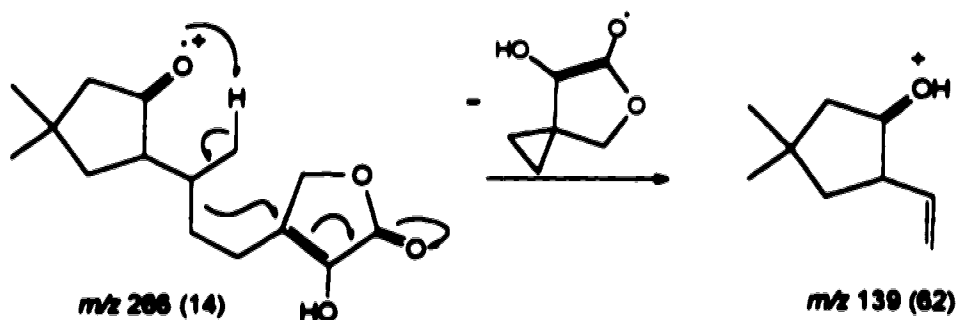
Scheme 4 - Ozonolysis of tremulenolide A (**23**).

The base peak in the HREIMS at m/z 112 arises from the McLafferty rearrangement of the ketone at C-1 (Scheme 5). This rearrangement can take place either with the 5-methylene hydrogens or with the 13-methyl hydrogens.



Scheme 5 - Base peak formation in the mass spectrum of **23a**.

Another interesting fragmentation occurs to form the ion at m/z 139. In this case the rearrangement may proceed as illustrated in Scheme 6.



Scheme 6 - Mass spectral fragmentation of 23a to form the fragment m/z 139.

In addition to the AB quartet at δ 4.66, the ^1H NMR spectrum of 23a shows the presence of four additional methylene pairs, two vicinally coupled (ABXY system, δ 2.36 and δ 1.46), and two long range coupled (AM system, δ 2.16, 1.96, and δ 1.84, 1.57). Irradiation at δ 2.36 (H-4) reveals its long range coupling with the oxygenated methylene at δ 4.66 ($^4J = 1$ Hz) and its proximity to δ 1.46 (H-5) is consistent with the assignments (Table 6). The AM methylene pair at δ 2.16 and 1.96 ($J_{gem} = 18$ Hz) is assigned to C-10 due to the deshielding effect of the carbonyl group (C-1). By exclusion, the other set (δ 1.84 and 1.57, $J_{gem} = 13$ Hz) is assigned to C-8. The remaining signals in the spectrum are due to two methines (δ 2.42 and 1.93) and 3 methyls (δ 0.99, δ 1.04, and 1.21). The methyl at δ 0.99 is secondary and its multiplicity changes to a singlet upon irradiation of the methine at δ 1.93, therefore these are assigned to H-13 and H-6, respectively. As a result, the methine at δ 2.42 is assigned to H-7, which is in accord with the deshielding effect of the C-1 carbonyl. The presence of this carbonyl is evident in the FTIR spectrum as part of a very broad and strong absorption centered at 1733 cm^{-1} . In the ^{13}C NMR spectrum the sp^2 carbons are not observed. It is possible to identify the other 11 carbons which show the expected multiplicity. The triplet at δ 69.6 was assigned to the oxygenated

methylene carbon (C-12). The doublets at δ 53.4 and 32.3 are assigned to C-7 and C-6, respectively, considering that C-7 is deshielded by the carbonyl C-1. For the same reason, the triplet at δ 54.5 is assigned to C-10. The remaining triplets at δ 33.7, 30.5, and 22.7 cannot be assigned with certainty. Table 6 summarizes the ^1H and ^{13}C NMR assignments for 23a.

Table 6 - ^1H and ^{13}C NMR data for ozonolysis product 23a

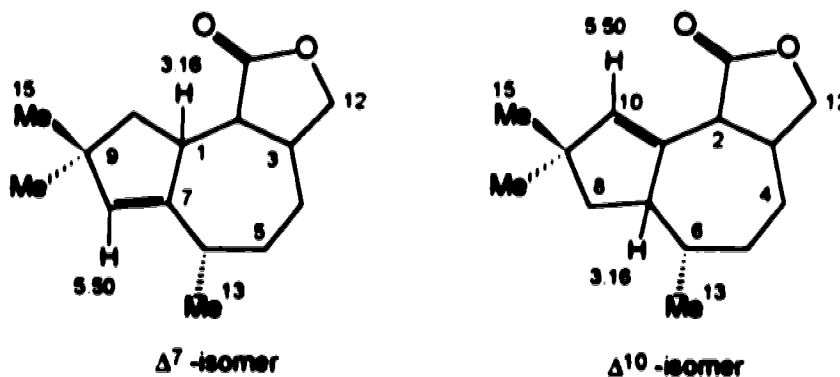
^1H NMR (δ , mult, J in Hz)		^{13}C NMR (δ , mult)	
H-4	2.36, 2H, m	C-4	22.7 (t)*
H-5	1.46, 2H, m	C-5	33.7 (t)*
H-6	1.93, 1H, m	C-6	32.3 (d)
H-7	2.42, 1H, m	C-7	53.4 (d)
H-8	1.57, 1H, dd, $^2J=12$, $^3J=12$	C-8	30.5 (t)*
	1.84, 1H, ddd, $^2J=12$, $^3J=9$, $^5J=2$		
H-10	1.96, 1H, d, $^2J=18$	C-10	54.5 (t)
	2.16, 1H, dt, $^2J=18$, $^4J=2$		
H-12	4.66, 2H, ABq, $^2J=16$, $^4J=1$	C-12	69.6 (t)
H-13	0.99, 3H, d, $^3J=7$	C-13	17.2 (q)
H-14	1.21, 3H, s	C-14	29.9 (q)
H-15	1.04, 3H, s	C-15	27.7 (q)

* may be interchanged.

The data for 23a are consistent with the cleavage of the seven-membered ring of tremulenolide A (23). This provides additional support for the skeleton proposed for this new group of sesquiterpenes. As noted previously, the observation of the base peak at m/z 112 in the mass spectrum of 23a provided early evidence that the *gem*-dimethyl group was located on a five-membered ring.

Tremulenolide B (24)

Tremulenolide B (24) was eluted in very small amounts, usually combined with tremulenolide A. It was obtained as a colorless oil and crystallized from hexanes as colorless needles. The HREIMS showed that it is isomeric with tremulenolide A (23), exhibiting a molecular ion at m/z 234 ($C_{15}H_{22}O_2$). The FTIR spectrum reveals that the lactone carbonyl (1775 cm^{-1}) is not conjugated. The ^1H NMR spectrum (Figure 15) shows the presence of one olefinic proton at δ 5.50 indicating a trisubstituted double bond. This hydrogen exhibits long range coupling (2.2 Hz) to the allylic hydrogen at δ 3.16 and no *vicinal* coupling is observed. Considering that only long range coupling is involved and assuming that 24 is a positional isomer of tremulenolide A (23), two structures were considered, Δ^7 - and Δ^{10} -isomers.



These structures are readily differentiated by the coupling pattern of the hydrogen at the remaining allylic position. In the Δ^7 -isomer, this hydrogen would be coupled to the secondary methyl group whereas in the Δ^{10} -isomer it is coupled to a methine hydrogen. Since the allylic signal at δ 3.63 is a doublet, the Δ^7 -structure was discarded. Furthermore, a decoupling experiment indicates that the secondary methyl is coupled to a hydrogen at δ 1.81 which is too shielded to be an allylic proton. This suggests that tremulenolide B is the β,γ -unsaturated lactone 24 (Δ^{10} -isomer). This structure is consistent with the downfield position of the allylic resonance at δ 3.63 (H-2) since in the Δ^{10} -isomer it is α to the lactone carbonyl.

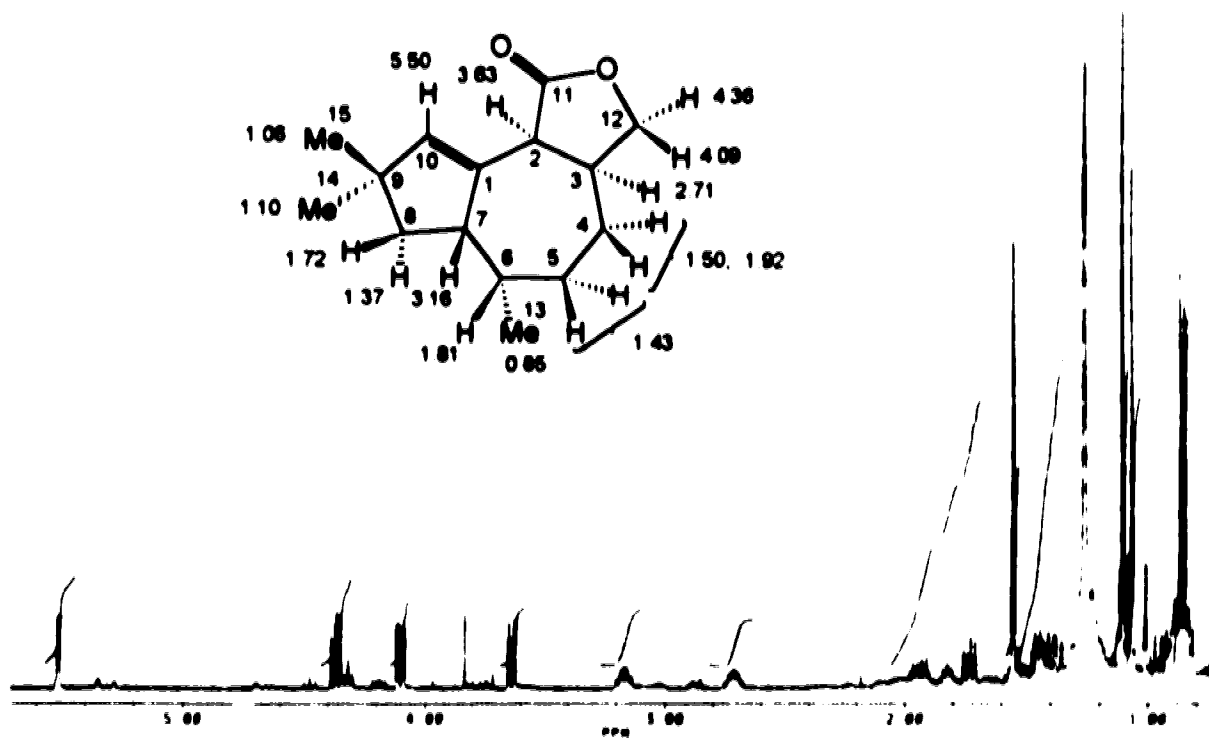
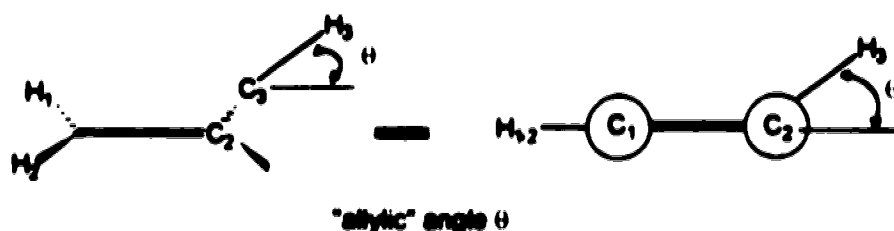


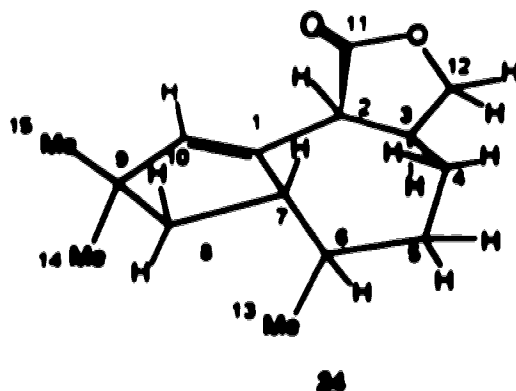
Figure 15 - ^1H spectrum (400 MHz, CDCl_3) and chemical shift assignment of tremulenolide B (24).

The splitting of H-2 in the spectrum is due to coupling to the methine hydrogen at δ 2.71 (H-3, $^3J = 9.5$ Hz). This, however, does not allow the assignment of configuration at C-2, since both *cis* (dihedral angle $\sim 0^\circ$) and *trans* (dihedral angle $\sim 180^\circ$) couplings in five-membered rings may be large⁴³. The assignment of the *cis* stereochemistry is based on the assumption that tremulenolide B (24) has the same stereochemistry at C-2 as the dial 25 (discussed later) where NOE experiments clearly demonstrate the *cis* relationship of H-2 and H-3. The proton at C-7 is also vicinally coupled to the methine hydrogen at δ 1.81 and to both hydrogens at C-8 (δ 1.37 and 1.72). The signal with larger coupling (δ 1.37, $^3J =$

10 Hz) is assigned to H-8 α since it reflects a dihedral angle approaching 180°, which is consistent with a *trans* relationship. This is also supported by the NOE results of **25**. The signal at δ 1.72 ($J = 7.5$ Hz) is assigned to H-8 β . The assigned stereochemistry also explains the small coupling constant observed between H-3 and H-12 β ($J = 3.2$ Hz), since in this way the dihedral angle approaches 90°. The coupling constant between H-3 and H-12 α is 7 Hz. The magnitude of these coupling constants allows us to predict the probable conformation of **24**. The large allylic coupling between H-7 and H-10 indicates that H-7 is aligned almost perpendicular with respect to the plane of the double bond. This is based on the fact that allylic coupling is maximum (3 Hz) when the "allylic" angle θ (shown below) is close to 90° and is zero when the angle is 0° and 180°⁴². Since allylic coupling between H-7 and H-10 has a value of 2.2 Hz, it requires an allylic angle close to 90° to provide maximum σ - π orbital overlap. Also, no coupling is observed between H-10 and H-2 indicating that the allylic angle between them is close to 0°.



The same behavior is observed in tremulenedial (**25**) where this rationale is supported by NOE experiments.



The intense signal observed at δ 1.25 in the ^1H NMR spectrum (Figure 15) is due to an impurity often eluted during silica gel chromatography. The ^{13}C NMR resonances of **24** was assigned by combining the ^1H NMR assignment shown in Figure 15 with the correlations extracted from the HMQC spectrum (Figure 16). An expansion of the high field portion of the HMQC spectrum is provided in order to distinguish between the methyl signals and the impurity signal (supposedly hydrocarbon grease). The correlations are consistent with the proposed structure for **24**. Comparison of the ^1H and ^{13}C NMR data (Tables 5 and 4, respectively) with those for tremulenolide A (**23**) confirms the relationship

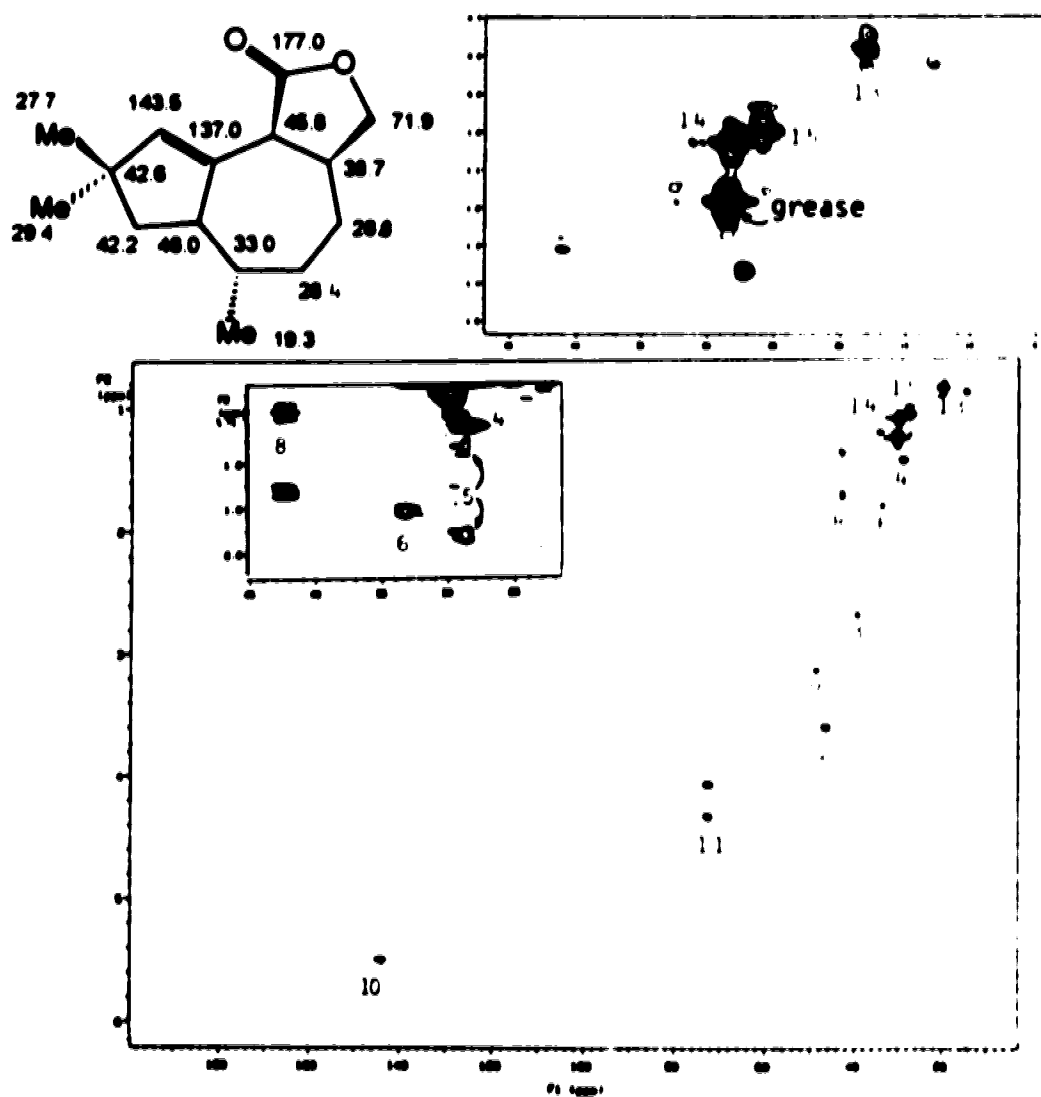
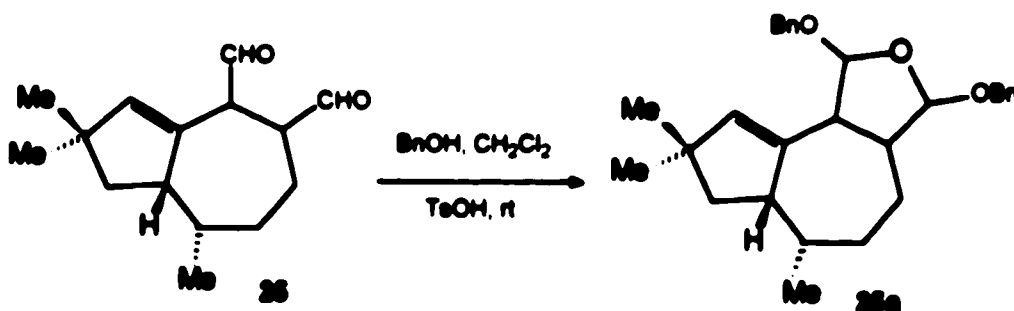


Figure 16 - HMQC spectrum and ^{13}C shift assignment for tremulenolide B (**24**).

Tremulenodial (25)

The compound which eluted after tremulenolides A and B was rather unstable as shown by its TLC behavior. The ^1H NMR spectrum of the crude material indicated the presence of an aldehyde signal at δ 9.72 integrating 2:1 with respect to an alkenic proton at δ 5.58. The remaining signals in the spectrum were very similar to those of tremulenolide B (24). This suggested that 25 was the dialdehyde precursor of 24 and it was found that treatment of the crude compound with either methanol or benzyl alcohol in the presence of acid gave a diacetal which was amenable to purification. The reaction with benzyl alcohol was chosen because it gave a single product, the dibenzyl acetal 25a, which is UV active and easily separated by PTLC. The CIMS indicated a molecular weight of 432, consistent with the formula $\text{C}_{29}\text{H}_{36}\text{O}_3$. The highest peak in the HREIMS corresponds to $\text{C}_{22}\text{H}_{29}\text{O}_2$, m/z 325, reflecting the loss of a benzyloxy radical from the molecular ion. The cyclic acetal was apparent from the ^{13}C NMR spectrum which shows two dioxygenated carbons (δ 107.5, 107.9) each carrying a hydrogen. The structural studies were carried out on the dibenzyl derivative 25a (Scheme 7), but it is assumed that the natural product is the dialdehyde, tremulenodial (25).



Scheme 7 - Benzylation of the dialdehyde tremulenodial (25).

The ^1H NMR spectrum of 25a (Figure 17) shows the alkenic hydrogen at δ 5.47 long range coupled to the hydrogen at δ 2.93 ($^4J = 2.2$ Hz) and a readily analyzed spin system correlating H-11, H-2, H-3, and H-12. The signal for H-2, for example, appears as

a double doublet at δ 3.52 which collapses to a doublet upon irradiation of H-11 (δ 5.20) and on irradiation of H-3 (δ 2.48). This last irradiation also converts the doublet at δ 4.98 (H-12) into a singlet. The J values involved in these couplings (Table 5) along with NOE and NOESY^{34b} experiments clearly establish the *cis* relationship between H-2 and H-3, being both α , and provide information on the relative stereochemistry at C-11 and C-12. Saturation of H-2, for instance, enhances the signals of H-3 and H-11 by 11.4% and 3.4%, respectively. The small enhancement of H-11 may indicate that these protons are not *syn*, since both H-3 and H-11 would have a similar arrangement in space relative to H-2. In addition, the dihedral angle between H-2 and H-11 in a *syn* configuration is almost 0°, about the same as the angle existent between H-2 and H-3, and one would expect similar coupling constants. However, the actual coupling constants are $J_{2,3} = 8$ Hz and $J_{2,11} = 5.2$ Hz. These differences in coupling constant and NOE enhancement suggest that H-11 is β . This is supported by further correlation of H-11 with H-7 (δ 2.93) and H-4 (δ 1.84) in the NOESY spectrum (Figure 18) which is only possible for a β hydrogen at C-11. This correlation allows us to assign the resonance at δ 1.84 as β . NOE enhancement is also observed between H-3 and H-12 (4.1%) but again the magnitude is small compared to the value between H-2 and H-3 (11.4%). Additionally, the coupling constant between H-3 and H-12 is small (1.5 Hz) indicating a dihedral angle approaching 90°. This is consistent with a β orientation for H-12 and is supported by the presence of cross peaks in the NOESY spectrum between H-12, H-7 and H-4 β . The influence of substituent electronegativity on the magnitude of *vicinal* coupling constants was also examined. In general, J_{vicinal} decreases with increasing electronegativity of the substituents⁴⁴. However, the effect in saturated cyclic systems is dependent on the orientation of the electronegative group, which will exert its maximum effect (resulting in minimum J_{vicinal}) when an antiperiplanar relation exists between a part of the "coupling path" and the bond by which the electronegative substituent is attached⁴⁴. In the case of 25a an antiperiplanar relationship between the benzyloxy group and H-2 or H-3 would result in an unfavourable *periplanar* orientation

of the substituents. Even though the decrease is not too pronounced for $J_{2,11}$ it is very pronounced for $J_{3,12}$ ($J = 1.5$ Hz) requiring a maximum interaction of the benzyloxy group at C-12 with H-3 (180°). This would destroy the spatial interactions observed in the NOESY spectrum (Scheme 8) involving H-7, H-4, H-11, and H-12. These correlations contributed to the assignment of the relative stereochemistry at C-4, C-7, C-8, and C-9.

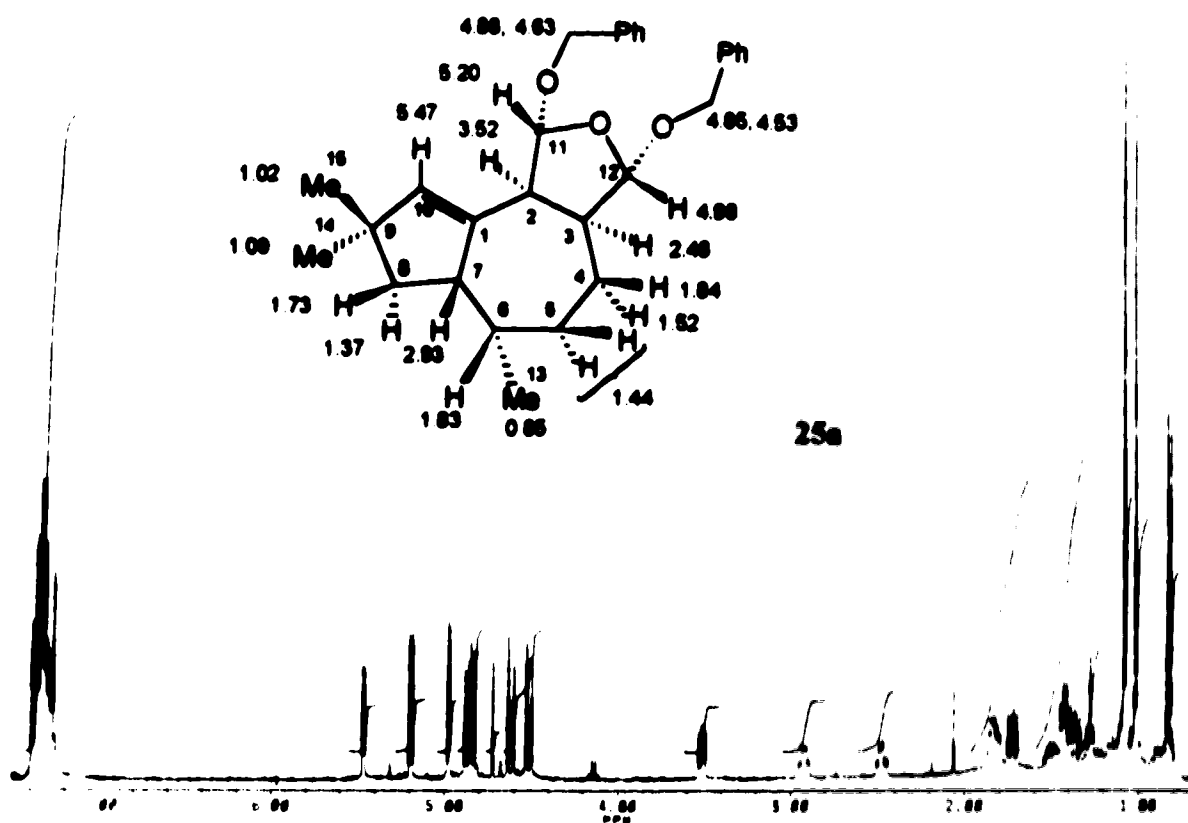
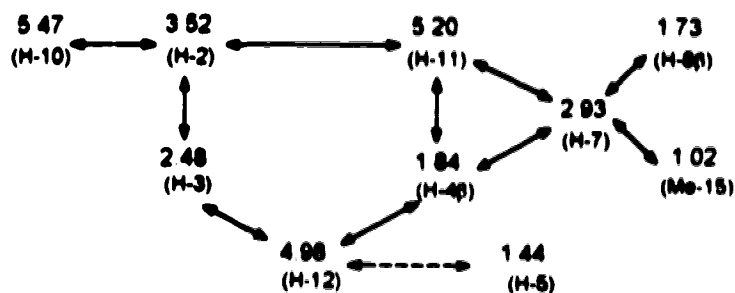


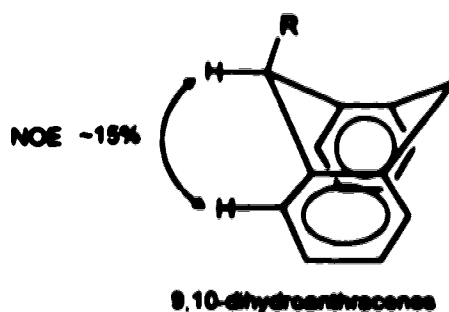
Figure 17 - ^1H NMR spectrum (400 MHz, CDCl_3) and chemical shift assignment of 25a.

The intense cross peak intersecting the signals at δ 5.47 and 3.52 corresponds to a large NOE enhancement (14.3%) of H-10 (δ 5.47) when H-2 (δ 3.52) is saturated. The cross peak between δ 4.98 (H-12) and 1.44 (H-5) may be due to a three-spin effect⁴⁵, which is transmitted through coupling between H-4 and H-5.



Scheme 8 - Cross peaks observed in the NOESY spectrum of 25a.

These results indicate that 25a is in a boat conformation as illustrated in Figure 18. The rationale is based on the fact that allylic coupling is maximum (3 Hz) when the "allylic" angle θ (shown in page 35) is close to 90° and is zero when the angle is 0° and 180° ⁴². Since allylic coupling between H-7 and H-10 has a value of 2.2 Hz, it requires an allylic angle close to 90° to provide maximum σ - π orbital overlap, as discussed previously for 24. Also, no coupling is observed between H-10 and H-2 indicating that the allylic angle between them is 0° or 180° , and the latter is not possible. This conformation places the protons H-7 and H-4 very close in space, as it brings H-11 and H-12 close enough to explain the NOESY results. Additional evidence for the quasicoplanar position of H-2 relative to H-10 is the large NOE enhancement (14.3%) observed between H-10 and H-2. This value approaches those found in disubstituted 9,10-dihydroanthracenes⁴⁶, shown below, in which the relative position and distance between the allylic and alkenic protons are comparable to those in 25a (Figure 18).



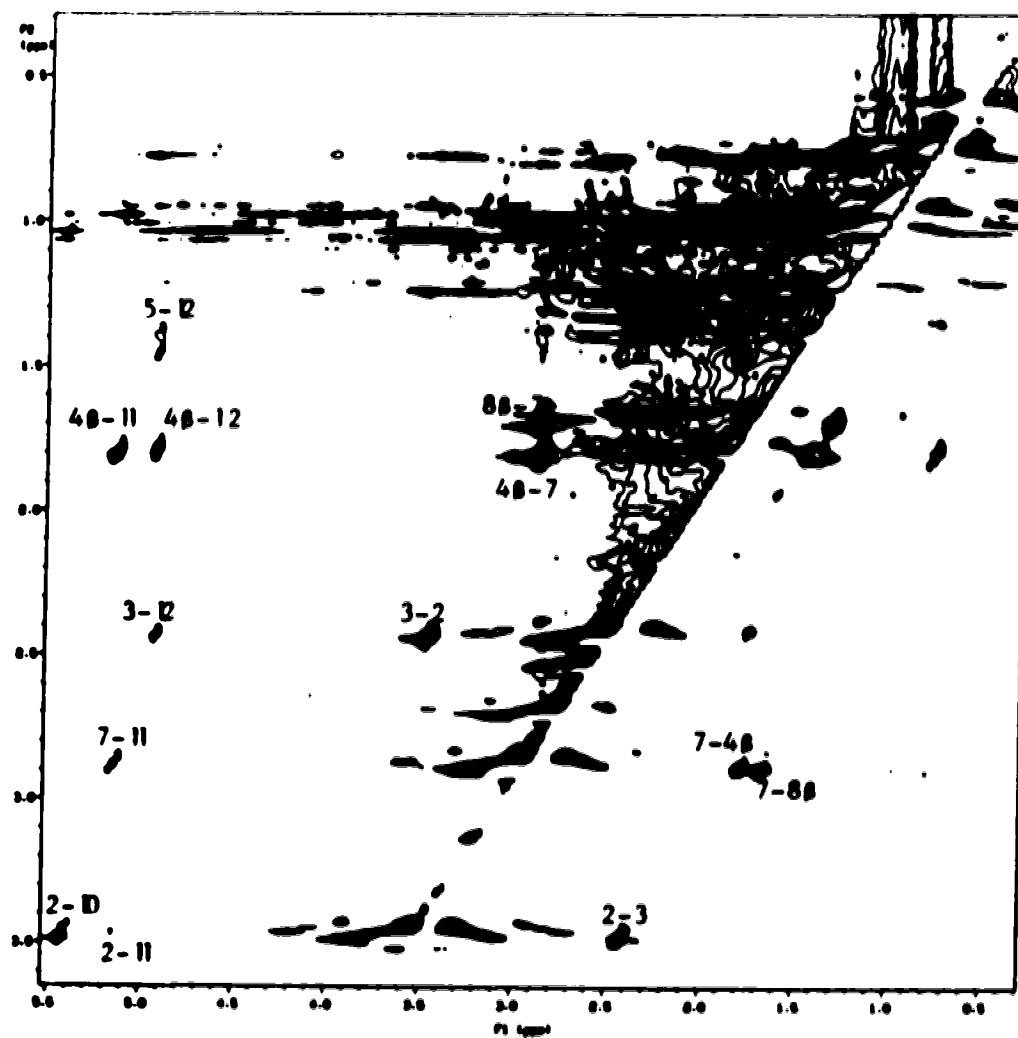
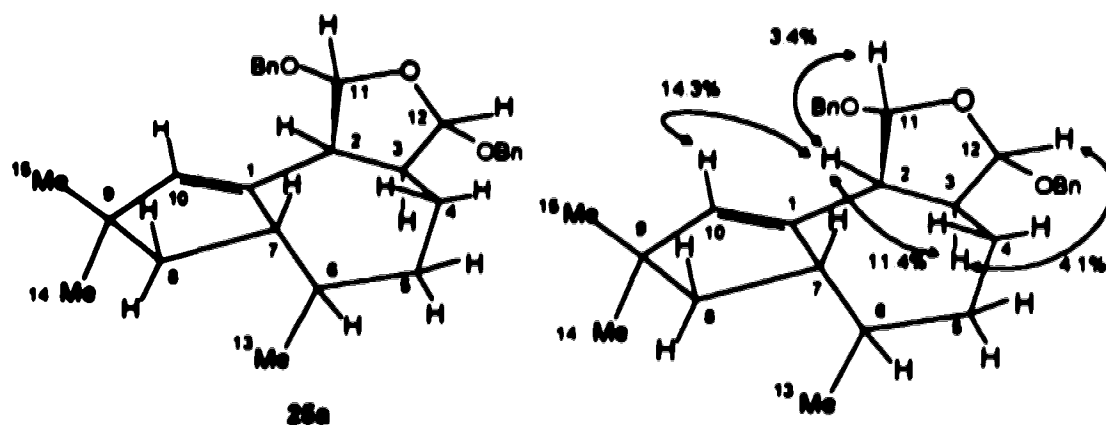


Figure 18 - Proposed configuration of 25a, NOE enhancements, and NOESY spectrum of 25a.

The benzyl resonances occur at δ 4.88 and 4.63 for one methylene group and at δ 4.85 and 4.53 for the other methylene pair, with the aromatic signals absorbing between δ 7.41 and 7.25. The remaining connectivities were secured by selective decoupling, APT, HMQC, and HMBC experiments. A complete assignment is shown in Tables 4 and 5. Figure 19 shows the HMQC spectra that supports the ^{13}C assignment of 25a based on the previously assigned ^1H NMR.

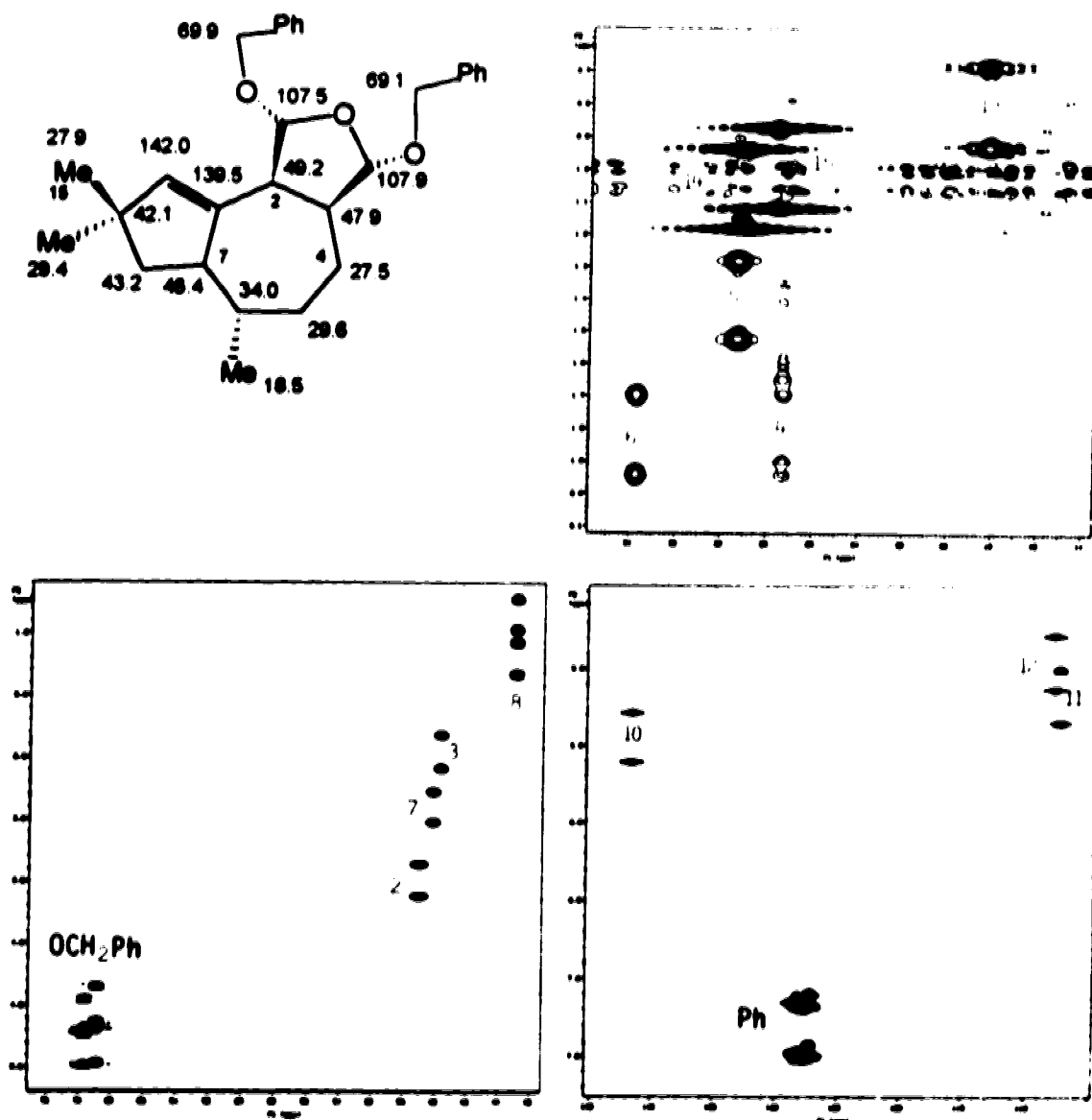


Figure 19 - HMQC spectrum (expanded regions) and ^{13}C NMR assignment of 25a (the double signals are due to an improper set up during data acquisition).

The precise assignment of the benzylic methylenes is based on the long range correlations obtained from the HMBC experiment (Figure 20). For example, three-bond correlation is observed between H-12 and the methylene group at δ 69.1 and between H-11 and the methylene group at δ 69.9. Other important three-bond correlations of H-11 and H-12 are with C-12 and C-11, respectively. This is additional evidence for the formation of a cyclic acetal. A mid point between the signals of similar shape was taken for analysis of the HMQC spectrum.

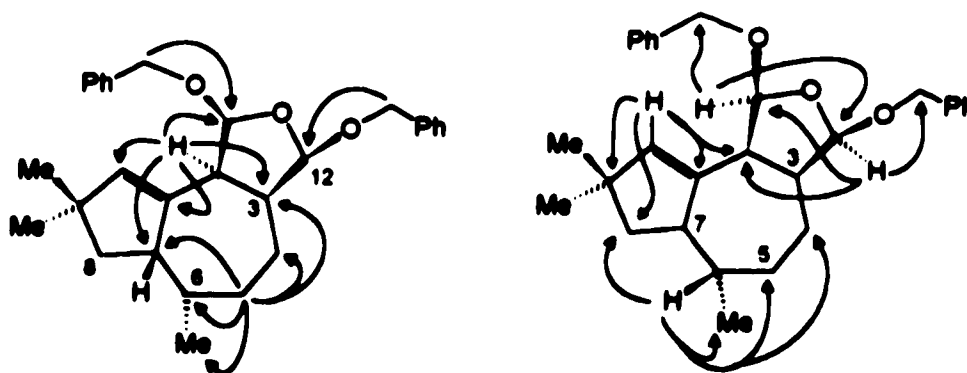
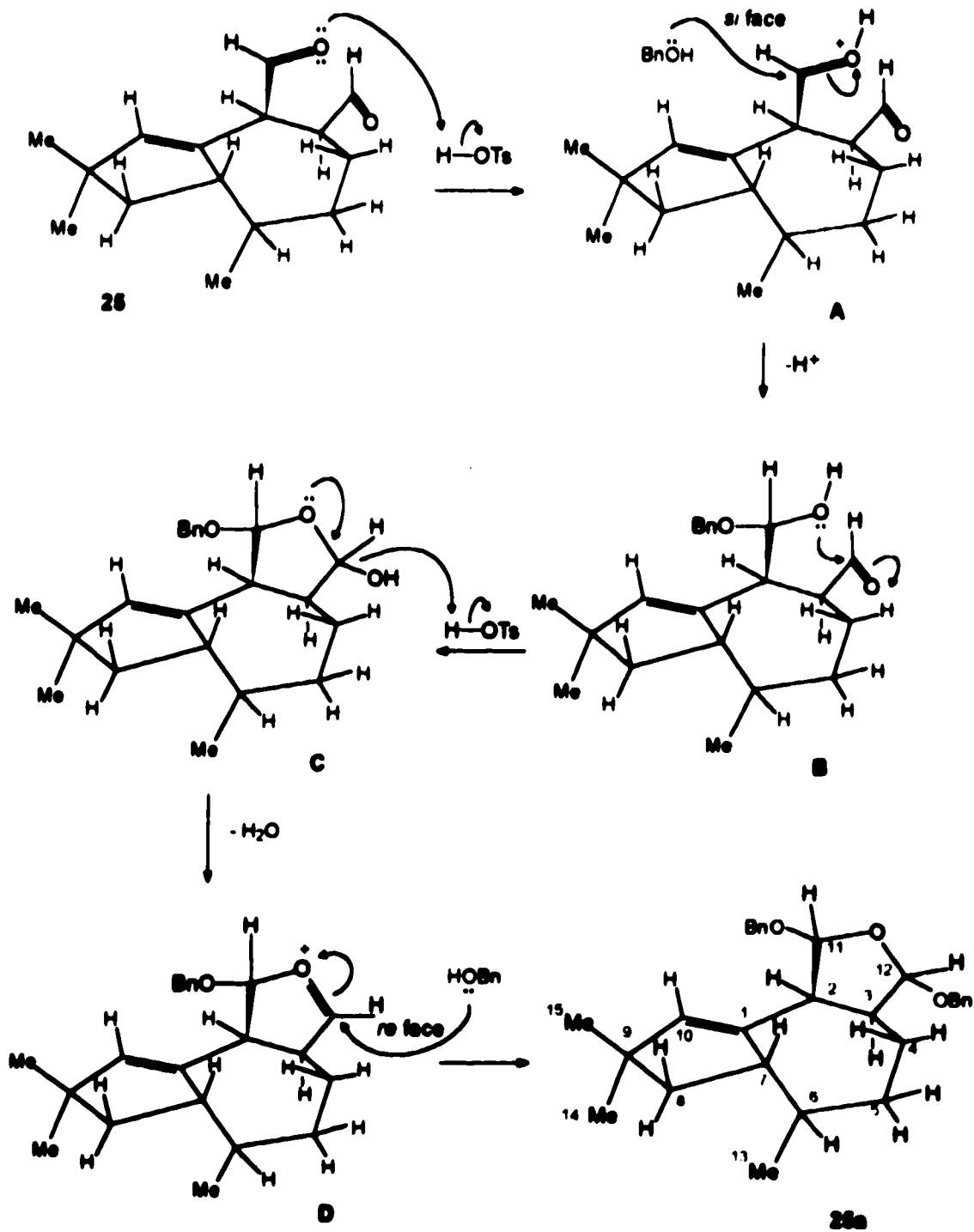


Figure 20 - Significant HMBC correlations of tremulenedial dibenzyl acetal (25a).

A possible mechanism for the formation of 25a that accounts for the assigned relative stereochemistry at C-11 and C-12 is given in Scheme 9. In order to facilitate representation it was assumed that the dial 25 is in a boat conformation and that the carbonyl groups are in perpendicular planes. The first molecule of benzyl alcohol adds on the *si* face of the protonated C-11 carbonyl (A) to form the hemiacetal B which then adds to the C-12 carbonyl to afford C. Dehydration of C gives the cyclic oxonium ion D. The dibenzyl acetal 25a is formed by the nucleophilic attack of a second molecule of benzyl alcohol on the *re* face of C-12 (D), which is the less hindered side since the hydrogens at C-4 are blocking the *si* face of C-12.

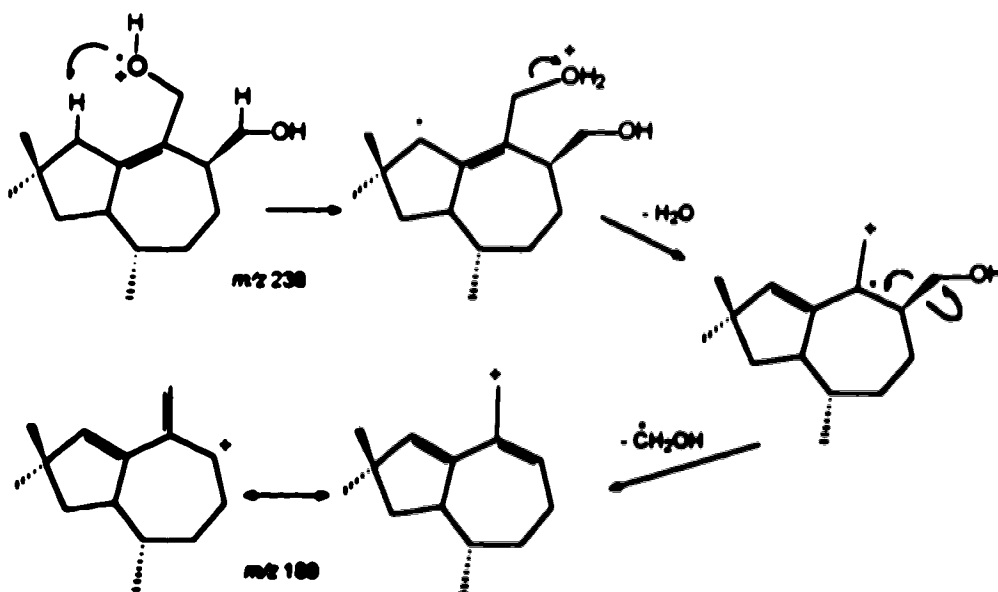


Scheme 9 - Possible mechanism of formation of the dibenzyl acetal 25a.

Tremulenediols A (26) and B (27)

Tremulenediols A and B are not separable by chromatography, both exhibiting the same R_f in several solvent systems. Crystallization from hexanes gave partial separation of tremulenediol A (26). However, the derived di-*p*-bromobenzoates (26a and 27a) are amenable to separation by PTLC. CIMS of the di-*p*-bromobenzoates shows the $[M+18]^+$ peak at m/z 620 (17%) and peaks at m/z 622 (35%) and 624 (17%) consistent with the presence of two bromine atoms in the molecule ($C_{29}H_{32}O_4Br_2$). The ^{13}C NMR spectra of 26 shows the presence of a fully substituted double bond (δ 145.6 and 132.3), while that of 27 shows a trisubstituted double bond. The double bond accounts for one of the three units of unsaturation, therefore these diols are bicyclic. 1H and ^{13}C NMR spectra indicate that these alcohols are primary and suggest that they are the reduced forms of the lactones previously described. The following evidence supports this assumption.

The HREIMS of 26 indicated a formula $C_{15}H_{26}O_2$ (mw 238) whereas that of 27 shows the highest mass peak at m/z 220 corresponding to the loss of water from the molecular ion. Further loss of a CH_2OH radical from this stable radical ion at m/z 220 affords the base peak at m/z 189, as illustrated in Scheme 10.



Scheme 10 - Fragmentation of tremulenediol A (26) to form the base peak at m/z 189

Tremulenediol A (26)

The ^1H NMR spectrum of **26** (Figure 21) shows the presence of four protons on oxygenated carbons. The doublet at δ 4.24 which is geminally coupled (11 Hz) to the broad doublet at δ 3.83 represent the allylic carbonyl protons on C-11. The double doublets at δ 4.01 and 3.61 are geminally coupled by 9 Hz and vicinally coupled to the allylic proton at δ 2.53 (H-3) and are assigned to H-12. The large chemical shift difference of these *geminal* protons and their distinct coupling patterns indicate that intramolecular hydrogen bonding may be holding this diol in a fixed conformation. Both the chemical shift difference and the coupling pattern disappear in the di-*p*-bromobenzoyl derivative **26a** discussed later. Intramolecularly bonded diols show two characteristic bands above 3000 cm^{-1} in the FTIR spectrum, a relatively sharp band between 3650 and 3600 cm^{-1} attributable to the vibration of the free hydroxyl group (denoted by $\nu_{\text{O-H}}^{\text{free}}$) and a much broader band below 3600 cm^{-1} which is assigned to the vibration of the hydrogen bonded hydroxyl group (denoted by $\nu_{\text{O-H}}^{\text{bond}}$)⁴⁷. The solution spectrum of **26** shows two bands above 3000 cm^{-1} in the absorbance IR spectrum, a sharp band between 3640 and 3550 cm^{-1} ($\nu_{\text{O-H}}^{\text{free}}$) and a broad band between 3550 and 3300 cm^{-1} ($\nu_{\text{O-H}}^{\text{bond}}$). On dilution the relative intensity of these two bands did not change indicating that intramolecular and not intermolecular hydrogen bonding is involved. Figure 22 shows this IR study. The shift in the OH vibration is denoted as $\Delta\nu$ and is a measure of the effect of the perturbation caused by hydrogen bond on the force constant of the O-H bond. The magnitude of $\Delta\nu$ increases as the distance between H and the proton acceptor group decreases. In the case of **26** this difference is calculated to be 190 cm^{-1} , as shown in equation 1, indicating that the hydroxyl groups are strongly H-bonded.

$$\Delta\nu = \nu_{\text{O-H}}^{\text{free}} - \nu_{\text{O-H}}^{\text{bond}} = 3615 - 3425 \quad \therefore \Delta\nu = 190\text{ cm}^{-1} \quad (1)$$

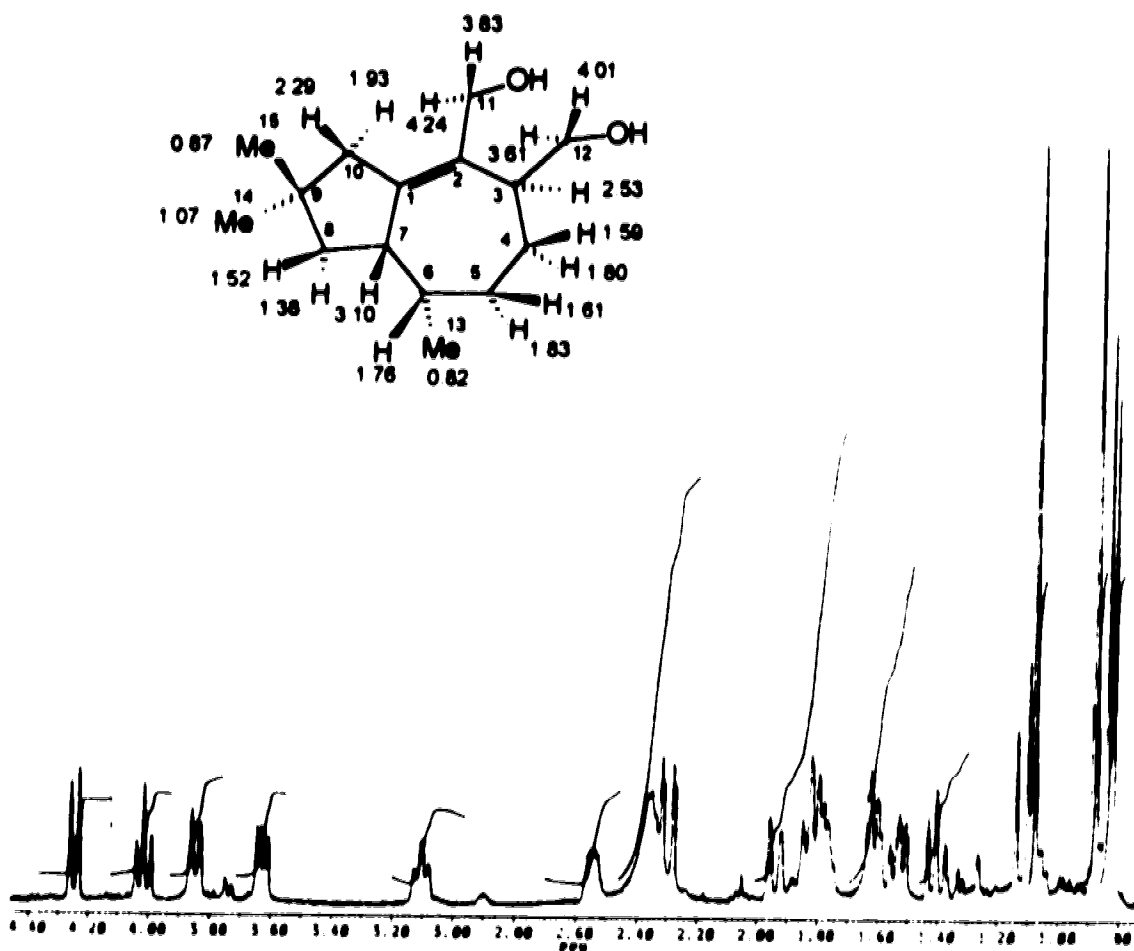


Figure 21 - ^1H NMR spectrum (400 MHz, CDCl_3) and chemical shift assignment of 26.

The coupling pattern in the ^1H NMR spectrum indicates that the allylic carbonyl proton at δ 3.83 is that held in the β -position since it exhibits long range coupling to H-7 (δ 3.10). This coupling is characteristic of an "allylic" angle approaching 90° (Figure 23). The carbonyl methylene protons at C-12 are differently coupled to H-3. The larger coupling (10 Hz) is exhibited by the proton at δ 4.01 suggesting a *trans* relationship with H-3. Correlations obtained from NOESY experiments (Figure 24) support these assignments as shown in Table 7. In particular, the cross peak between H-11 α and H-10 β shows that the methylene protons at C-11 are oriented towards C-10, and in the same way the methylene protons at C-12 are oriented towards C-7, as shown in Table 7 and Figure 23.

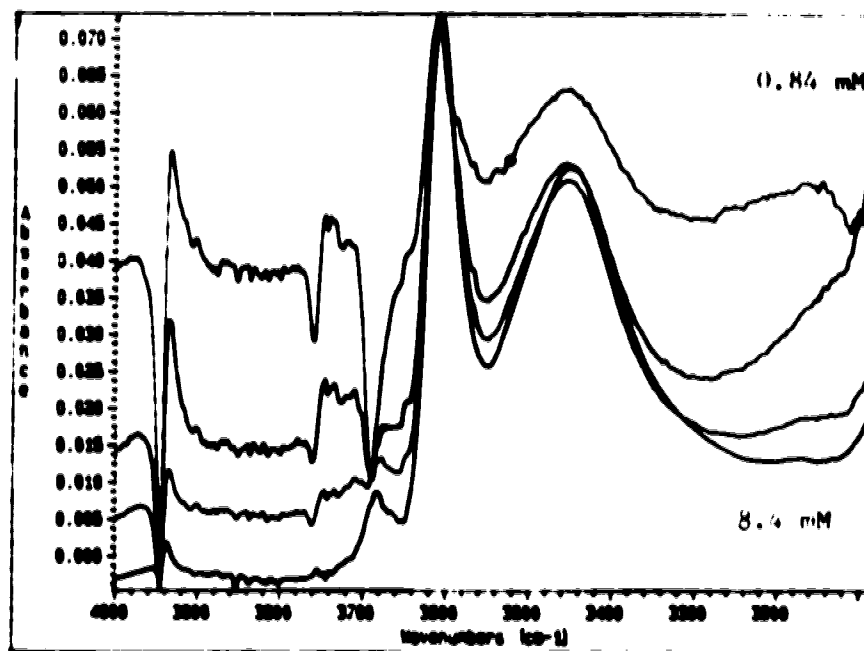
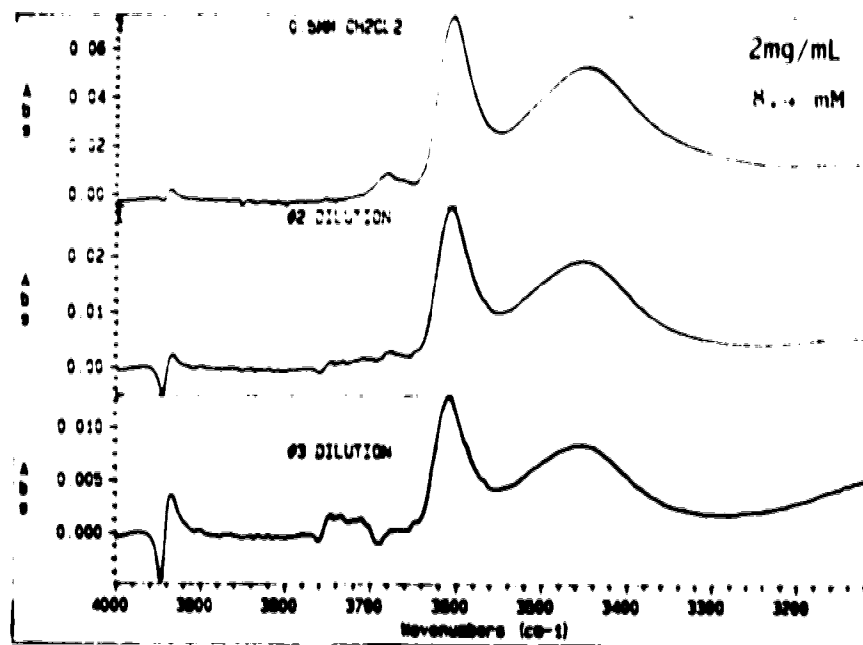
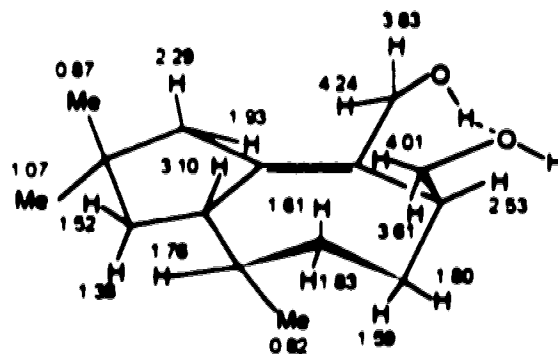


Figure 22 - Absorption IR spectra of diol 26 in CH_2Cl_2 at different concentrations indicating the presence of intramolecular hydrogen bonding.

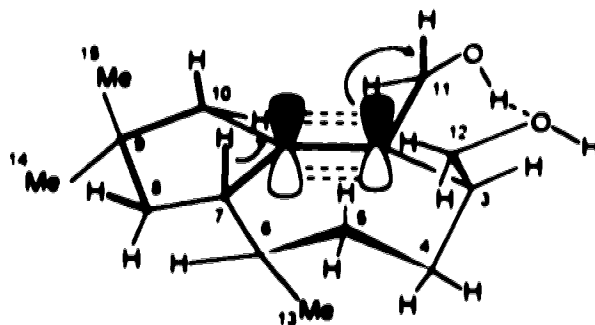
Table 7 - Correlations observed in the NOESY spectrum of diol 26



δ (atom)	NOESY cross peaks (intensity) ^a
2.53 (H-3)	4.01 (w), 3.83 (s), 3.61 (m), 1.80 (m), 1.59 (m)
1.59 (H-4 α)	2.53 (s)
1.80 (H-4 β)	4.01 (m), 3.61 (w), 3.10 (w), 2.53 (s), 1.59 (s), 0.82 (m)
1.83 (H-5 α)	1.61 (s), 0.82 (w)
1.61 (H-5 β)	3.61 (s), 1.83 (s)
1.76 (H-6)	3.10 (s), 0.82 (s)
3.10 (H-7)	4.01 (s), 3.83 (w), 3.61 (s), 1.76 (s), 1.52 (s), 1.38 (w), 0.87 (w)
1.38 (H-8 α)	1.93 (s), 1.52 (s), 1.07 (m), 0.82 (m)
1.52 (H-8 β)	3.10 (s), 1.38 (s), 0.87 (m)
1.93 (H-10 α)	4.24 (w), 2.29 (s), 1.38 (m), 1.07 (s)
2.29 (H-10 β)	4.24 (s), 3.83 (w), 1.93 (s), 0.87 (w)
4.24 (H-11 α)	3.83 (s), 2.29 (s), 1.93 (s)
3.83 (H-11 β)	4.24 (s), 3.10 (w), 2.53 (s)
3.61 (H-12 α)	4.01 (s), 3.10 (m), 2.53 (m), 1.59 (m)
4.01 (H-12 β)	3.61 (s), 3.10 (s), 2.53 (w), 1.80 (w)
0.82 (13-Me)	1.80 (s), 1.59 (w), 1.38 (w)
1.07 (14-Me)	1.93 (m), 1.38 (m)
0.87 (15-Me)	3.10 (w), 2.29 (w), 1.52 (w)

^a s = strong; m = medium; w = weak

A W-coupling of 2.5 Hz is observed between H-8 β and the allylic proton at δ 2.29, suggesting that they are *syn* (Figure 23). The remaining ¹H chemical shift assignments shown in Figure 21 and Table 5 are based on selective homonuclear decoupling and NOESY correlations.



W- and homoallylic couplings

26

Figure 23 - Representation of the W- and homoallylic couplings observed in compound 26

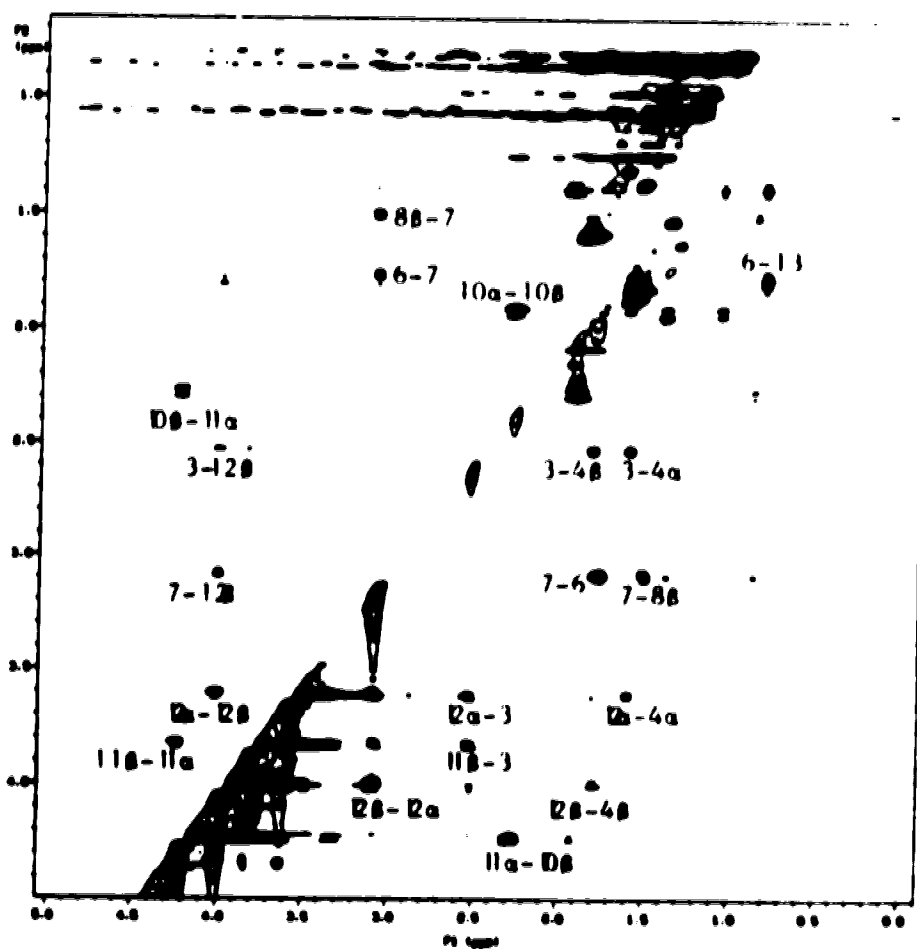


Figure 24 - NOESY spectrum of tremulenol A (26).

The conformation proposed for this compound is based on the spectroscopic data and accommodates all the observed correlations

Inspection of the ^{13}C NMR spectrum (APT) of **26** reveals two low field singlets at δ 145.6 and 132.3, assigned to the γ^2 quaternary carbons, and a high field singlet at δ 37.0 assigned to the γ^1 quaternary carbon bearing the *gem*-dimethyl groups. Two oxygenated triplets are observed at δ 65.6 and 63.2, the one at lower field is assigned to C-11 considering the deshielding effect of the *vicinal* double bond. The carbonyl carbon assignment is consistent with the results from the HMQC experiment. Direct ^1H - ^{13}C correlation is found between the signal at δ 65.6 and the allylic protons assigned to C-11. The same is observed for the carbonyl carbon at δ 63.2 which correlates with the oxygenated methylene protons at δ 4.01 and 3.61 (C-12), as indicated in Figure 25a. The middle region of the HMQC spectrum was expanded to provide a precise assignment of the carbons in that area (Figure 25b). The APT spectrum indicates that the signal at δ 48.0 is a triplet, which is supported by correlation with the proton signals at δ 2.29 and 1.93 in the HMQC spectrum. The signal at δ 46.0 is a doublet and it correlates with the allylic methine H-7. The next two signals in the APT spectrum are almost coincidental. However, they differ in multiplicity, the first is a triplet (δ 45.5) and the second a doublet (δ 45.4). Inspection of the expanded region of the HMQC spectrum indicates three correlations in the proton domain at δ 1.38, 1.52, and 2.53. Although further expansion provides a positive correlation between the first two protons and the methylene carbon (δ 45.5), the fact that they are geminally coupled establishes the correlation. Moving to the upfield region of the expanded HMQC spectrum, the triplet at δ 32.6 shows cross peaks with the *geminal* protons assigned to C-5 and the doublet at δ 31.6 shows cross peak with the methine proton H-6. The upfield signals in Figure 25a are readily correlated with the respective proton signals following the same rationale. The complete assignment of the

NMR spectra is provided in Tables 4 and 5. The assignment of the olefinic carbons was secured by HMBC correlations (Figure 26).

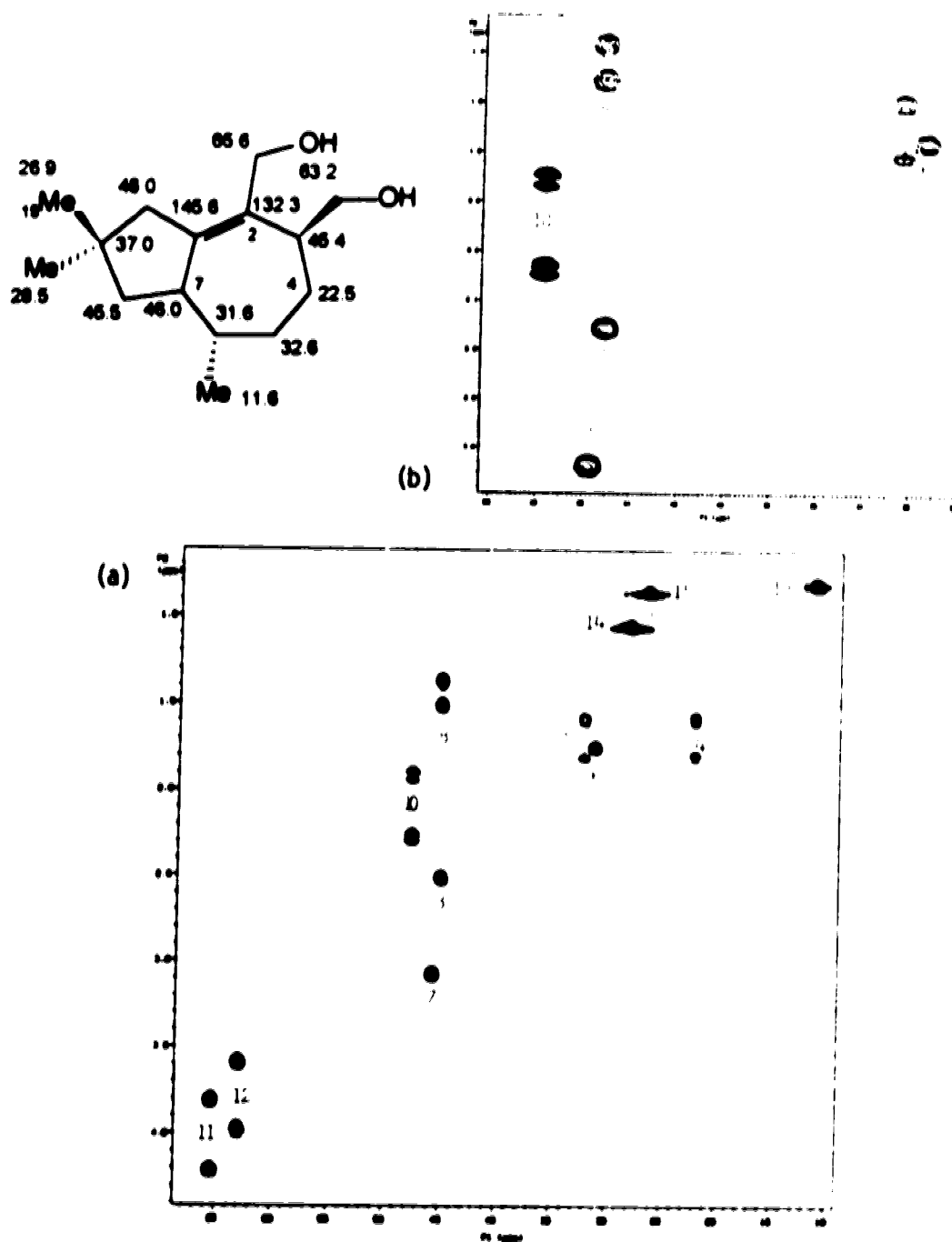


Figure 25 - HMQC spectrum and ^{13}C NMR chemical shift assignment of 26

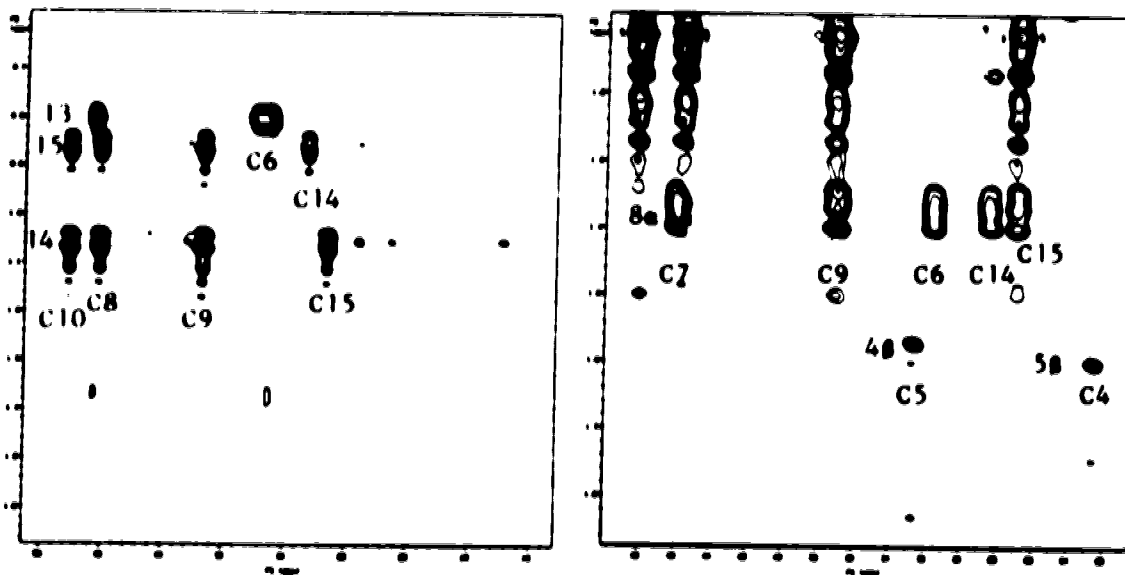
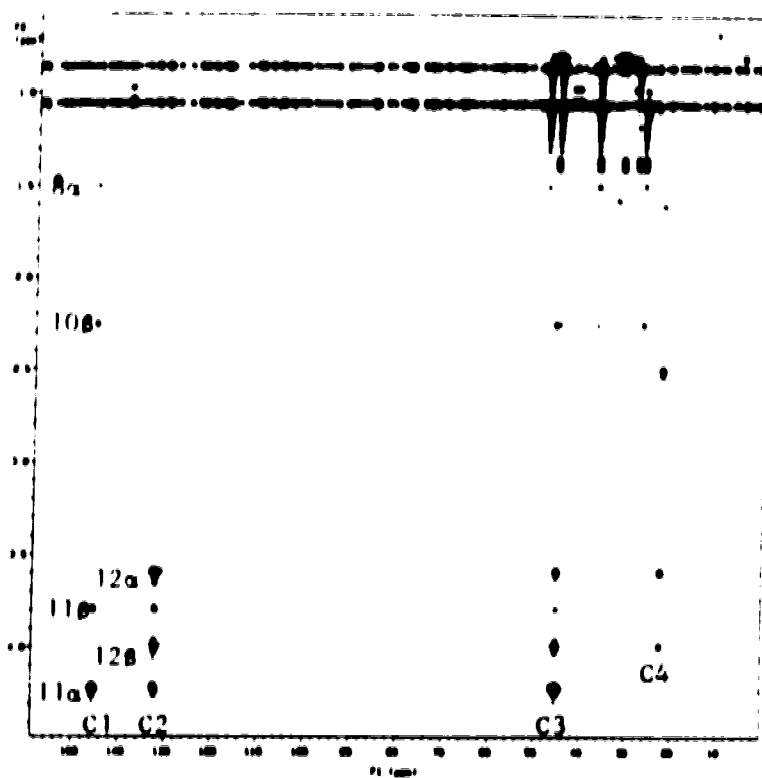


Figure 26 - HMBC spectrum of tremulenediol A (26) with expansion of the high field area.

In the HMBC spectrum shown in Figure 26, the proton resonance at δ 4.24 intersects the carbon resonances at δ 145.6, 132.3, and 45.4. Exactly the same correlation is found for δ 3.83. These are two and three bond correlations. The protons at δ 4.01 and 3.61 correlate with the carbon signals at δ 132.3, 45.4, and 22.5. Since of the carbinyl protons only those at C-11 (allylic) show correlation with the olefinic carbon at δ 145.6, this resonance is assigned to C-1. By exclusion, C-2 is assigned to δ 132.3. This assignment is supported by ^1H - ^{13}C long range correlation of H-10 β and H-8 β . The first correlates with both olefinic carbon resonances and the second uniquely with the carbon at δ 145.6. The remaining correlations are summarized in Figure 27. Confirmation of the structure and stereochemistry of tremulenediol A (26) was obtained by direct correlation with tremulenolide A (23). This transformation is described in section 3.3.

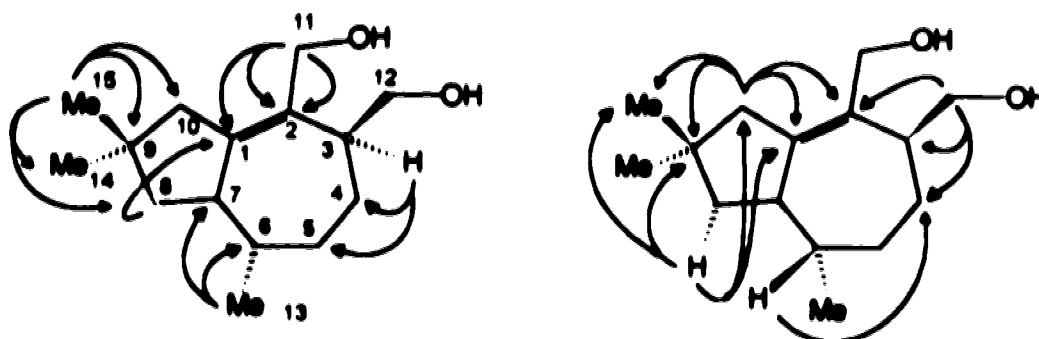


Figure 27 - Significant HMBC correlations of tremulenediol A (26)

Tremulemediol B (27)

The ^1H NMR spectrum of diol 27 (Figure 28) shows approximately 15% impurity of diol 26. This, however, did not interfere with its characterization and further purification was obtained by preparation of the di-*p*-bromobenzoate 27a. The alkenic proton is shown at δ 5.32, long range coupled (2.5 Hz) to H-7. This is the same kind of coupling observed in compounds 24 and 25a. The oxygenated methylene protons appear at different chemical shifts and exhibit different coupling patterns, which disappear in the di-*p*-bromobenzoyl derivative. This may be the result of intramolecular hydrogen bonding as proposed for the diol 26.

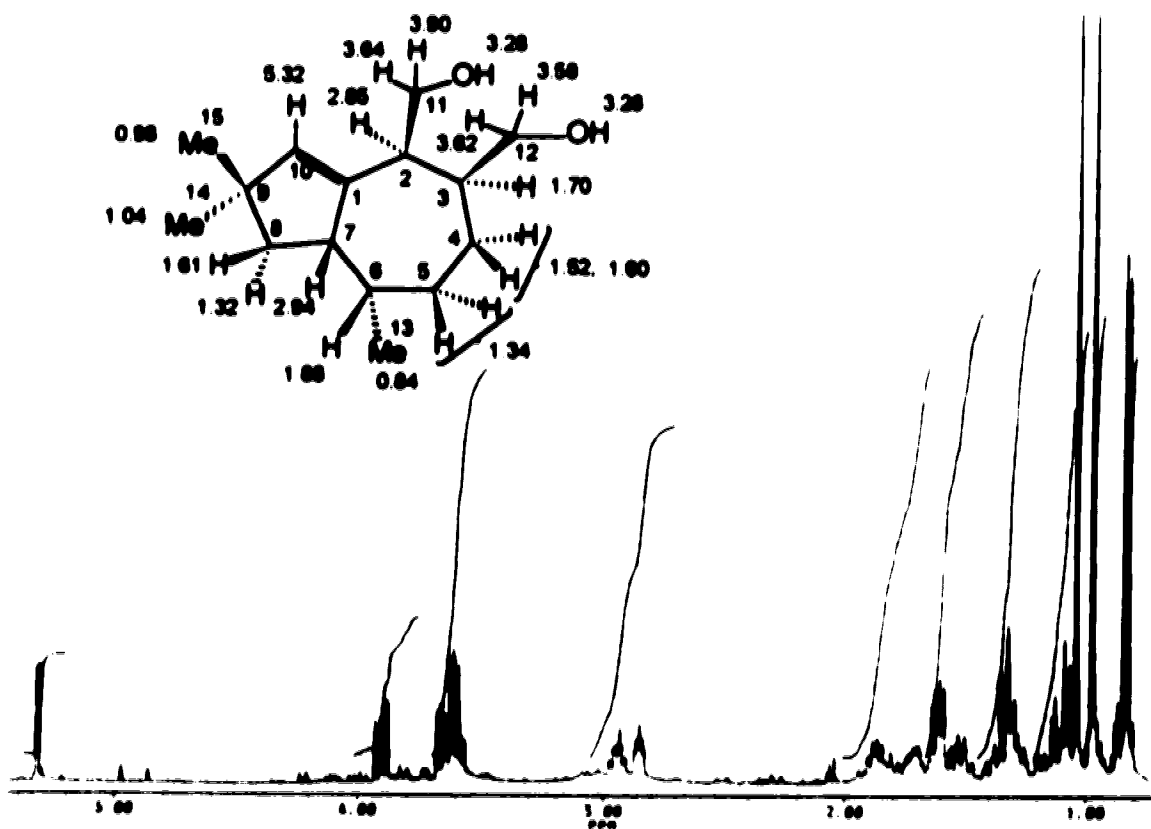


Figure 28 - ^1H NMR spectrum (400 MHz, CDCl_3) and chemical shift assignment of 27.

IR studies in solution were carried out for this compound and it was confirmed the presence of intramolecular hydrogen bonding was confirmed the relative intensities of the two bands above 3000 cm^{-1} did not change on dilution. The spectra are shown in Figure 29. The magnitude of $\Delta\nu$ ($\sim 180 \text{ cm}^{-1}$) indicates that strong hydrogen bonding is present in diol 27, similar to that observed for diol 26.

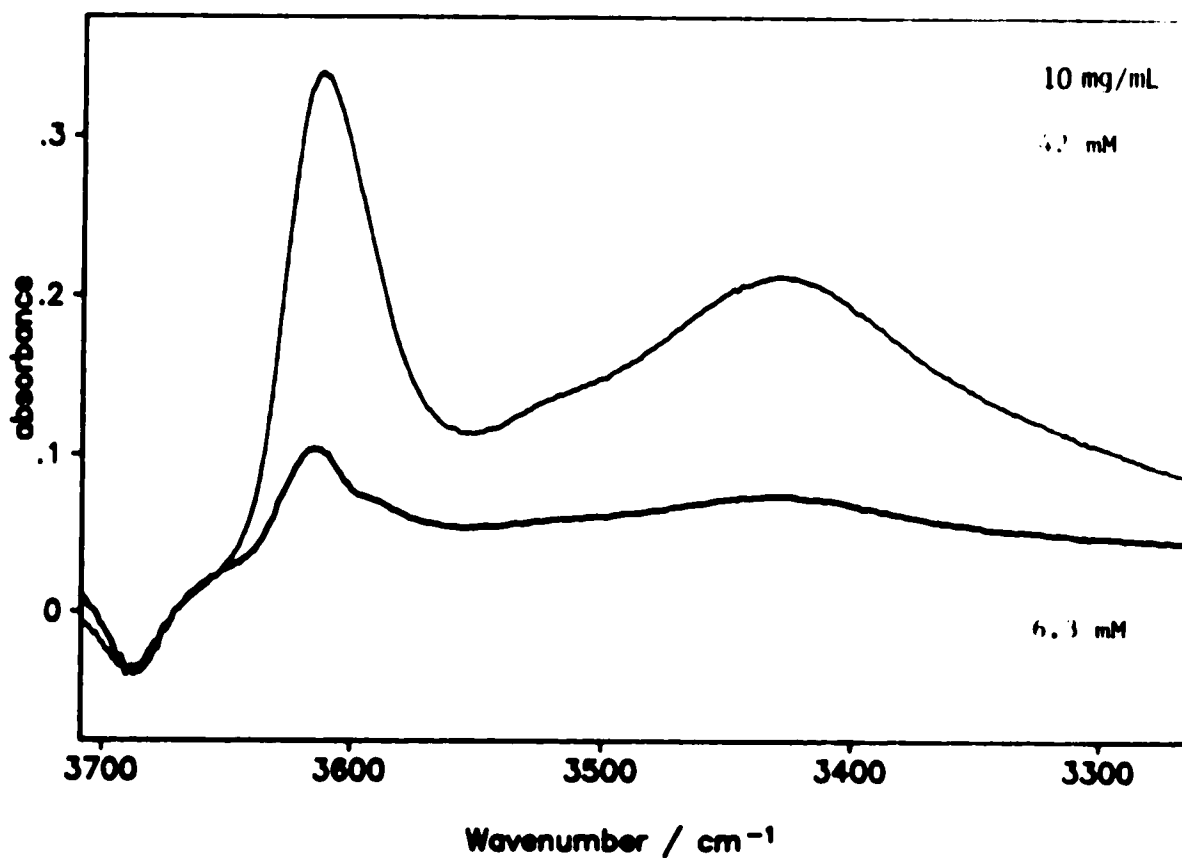
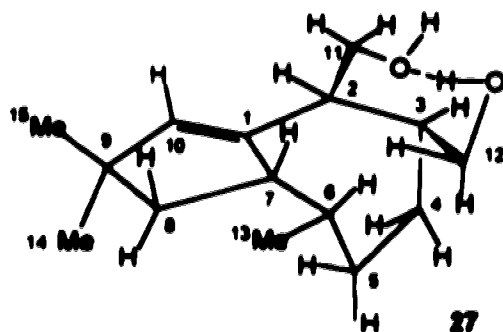


Figure 29 - Absorption IR spectrum of diol 27 in dichloromethane indicating the presence of intramolecular hydrogen bonding.

The carbinyl hydrogens at C-11 absorb at δ 3.90 and 3.64 in the ^1H NMR spectrum and are vicinally coupled to the allylic proton H-2 (δ 2.85) by 8.5 and 5 Hz, respectively. H-2 exhibits additional coupling to the methine H-3 (δ 1.70) but it is a small coupling, 4 Hz, suggesting a dihedral angle approaching 90° . H-3 is also coupled to the carbinyl protons at C-12 (δ 3.62 and 3.58, $^3J = 4$ and 6.5 Hz, respectively). An allylic coupling of 2.5 Hz is observed between H-7 (δ 2.94) and the alkenic proton at δ 5.32 (H-10). Since no such long range coupling is observed between H-10 and H-2, it is assumed that they lie on the same plane. H-7 is coupled to H-6 (δ 1.88) by 10 Hz which indicates that the dihedral angle between them is close to 0° . This coupling pattern is consistent with the conformation shown in structure 27 below. The remaining proton assignments shown in Figure 28 and Table 5 are based on selective decoupling experiments and on comparison with the previously assigned sesquiterpenes, particularly 24 and 25a (Table 5).



The assignment of the ^{13}C NMR spectrum of 27 was done in connection with the HMQC results following the ^1H NMR assignments. The different multiplicities of the olefinic carbons were sufficient to assign the sp^2 carbons. The singlet carbon at δ 145.6 is assigned to C-1 and the doublet at δ 138.6 to C-10. The methines are assigned by direct correlation with the protons at C-2, C-3, C-6 and C-7, and the same follows for the remaining signals. The complete ^{13}C NMR assignment is provided in Table 4 and Figure

30. The structure of tremulenediol B (27) was secured by its preparation from tremulenediol (25) as described in section 3.3

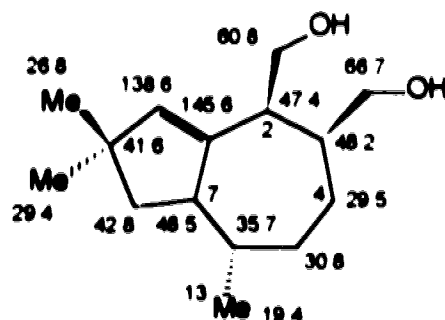
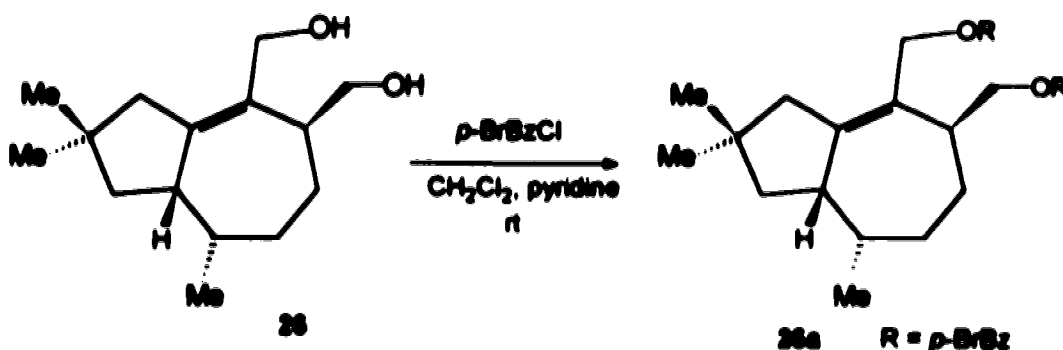


Figure 30 - ^{13}C NMR chemical shift assignment of tremulenediol B (27)

Purification of these diols was performed by preparation of their di-*p*-bromobenzoates. The derivatization was carried out using *p*-bromobenzoyl chloride and pyridine in dichloromethane, as exemplified in Scheme 11 for tremulenediol A (26).



Scheme 11 - Conversion of tremulenediol A into the di-*p*-bromobenzoate 26a

The di-*p*-bromobenzoates were purified by PTLC and characterized by NMR spectroscopy. The ^1H - ^1H -COSY and ^1H NMR spectra of 26a (higher R_f value component) are shown in Figure 31 and 32, respectively.

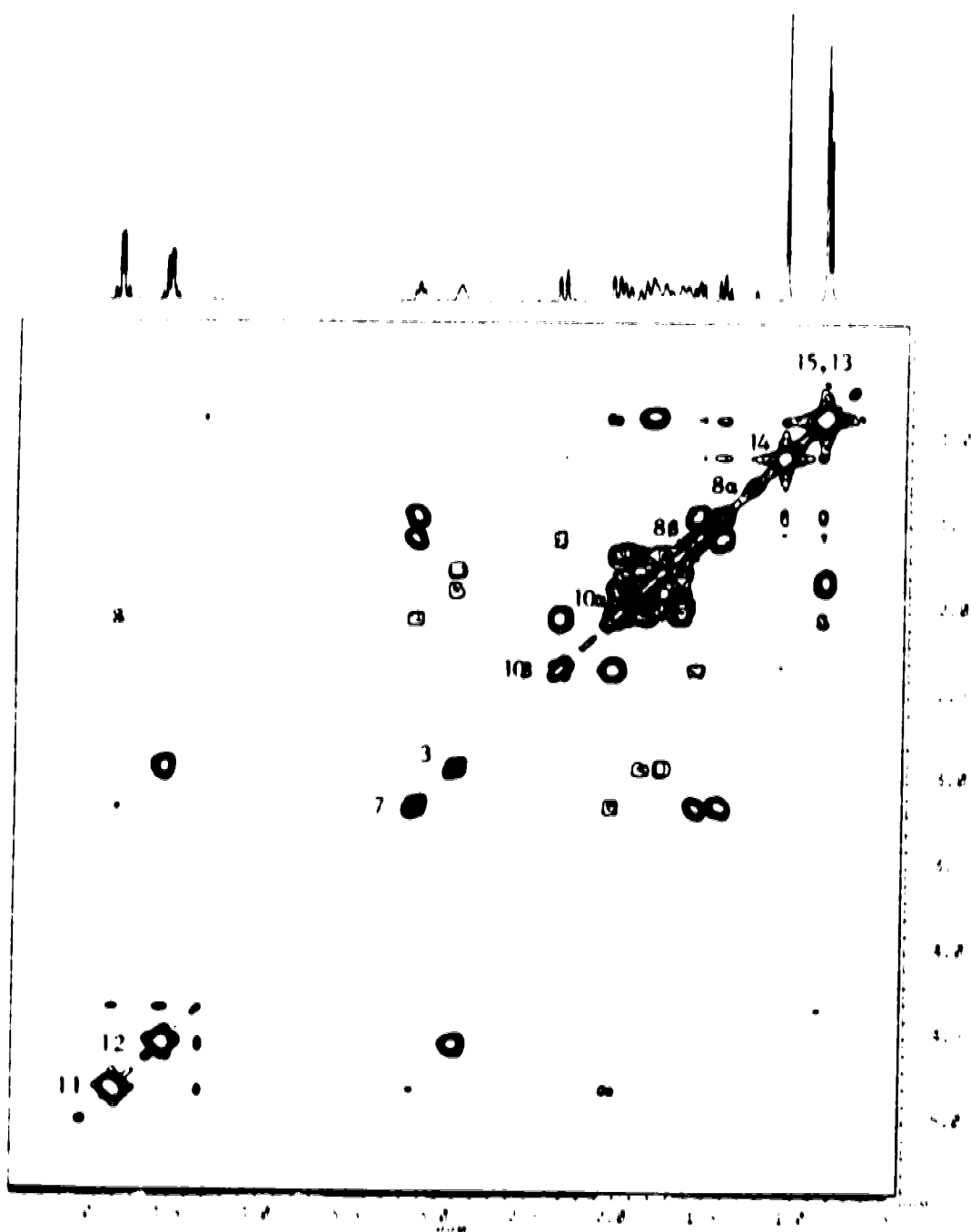


Figure 31 - ^1H - ^1H COSY spectrum of di-*p*-bromobenzoate 26a.

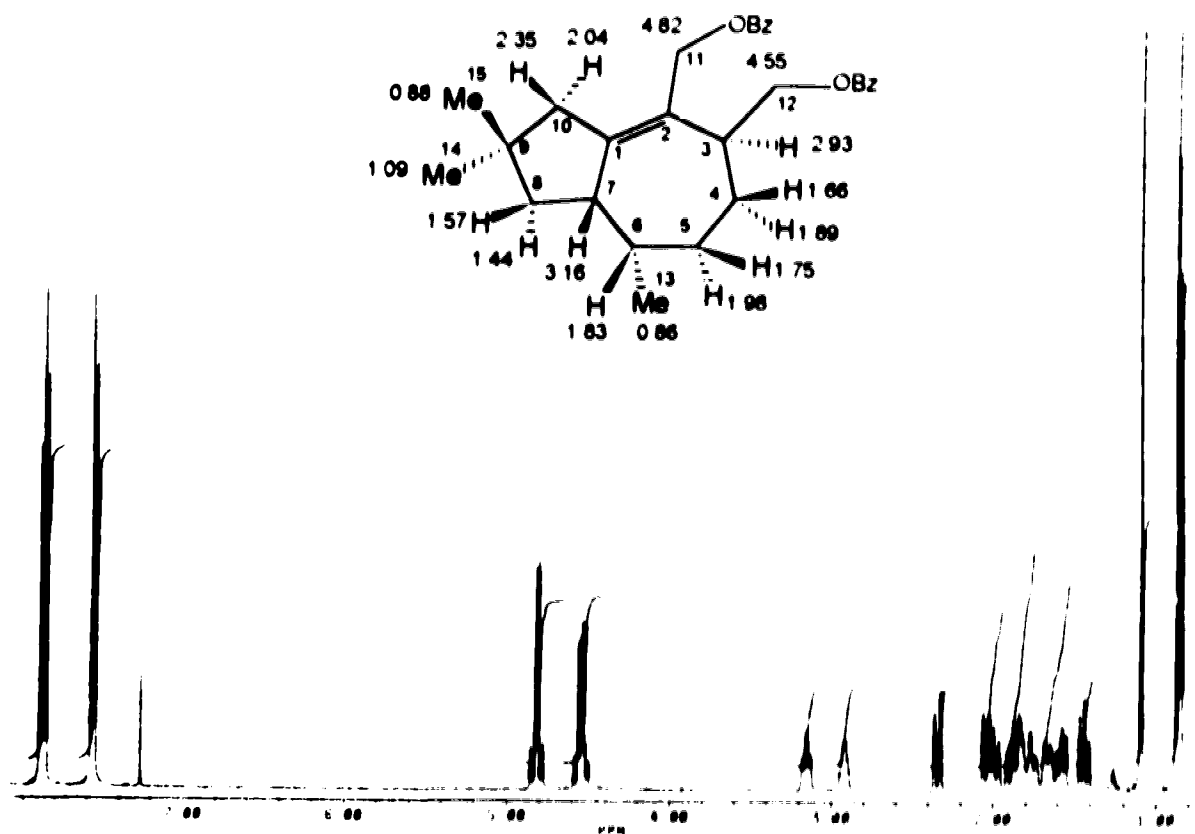


Figure 32 - ^1H NMR spectrum (400 MHz, CDCl_3) and chemical shift assignment of **26a**.

Analysis of these spectra indicates that the introduction of the *p*-bromobenzoyl groups in tremulenediol **A** causes an overall deshielding of all proton resonances, as summarized in Table 8. However, the main effect is observed on the oxygenated methylene hydrogens where the chemical shift difference between the *gem*-hydrogens becomes very small and the long range coupling exhibited by H-11 with H-3 and H-7 in the diol disappears. The ^1H - ^1H correlations observed in the COSY spectrum are consistent with the assignment shown in Figure 32 and Table 8. Selective homonuclear decoupling experiments also confirm the proton connectivities.

Table 8 - Comparison of ^1H NMR chemical shifts of **26** and **26a**

Atom	δ , multiplicity, J in Hz	
	26	26a
H-3	2.53, m	2.93, m
H-4 α	1.80, bd, 11.5	1.89, dt, 15, 2.5
H-4 β	1.59, dd, 11.5, 3.5	1.66, dm, 13.5, 2
H-5 α	1.83, m	1.98, dt, 13.5, 3
H-5 β	1.61, dd, 12, 3	1.75, ddd, 15, 13.5, 5
H-6	1.76, m	1.83, m
H-7	3.10, tm, 9	3.16, bdd, 11, 8, 2
H-8 α	1.38, dd, 12.5, 12	1.44, dd, 12, 11
H-8 β	1.52, ddd, 12.5, 8, 2.5	1.57, ddd, 12, 8, 2
H-10 α	1.93, bd, 15.5	2.04, bd, 15.5, 2
H-10 β	2.29, dd, 15.5, 2.5	2.35, dd, 15.5, 2
H-11 α	3.83, bd, 11	4.82, AB q, 11
H-11 β	4.24, d, 11	(2H)
H-12 α	4.01, dd, 10, 9	4.56, AB part of ABX
H-12 β	3.61, dd, 9, 5	(2H)
13-Me	0.82, d, 7	0.86, d, 7
14-Me	1.07, s	0.88, s
15-Me	0.87, s	1.09, s

The ^{13}C NMR spectrum of **26a** shows significant changes in the chemical shift for carbons C-1, C-2, C-3, and C-11. The remaining carbon resonances are very similar to those of the unprotected diol **26** (Table 4). HMQC correlations confirm the assignment of the ^{13}C resonances as shown in Figure 33, where the difference in chemical shift values for the carbons mentioned above with respect to the diol is given.

The correct carbon chemical shift assignment of this derivative is of great importance because it is the main compound used for the biosynthetic studies, described later.

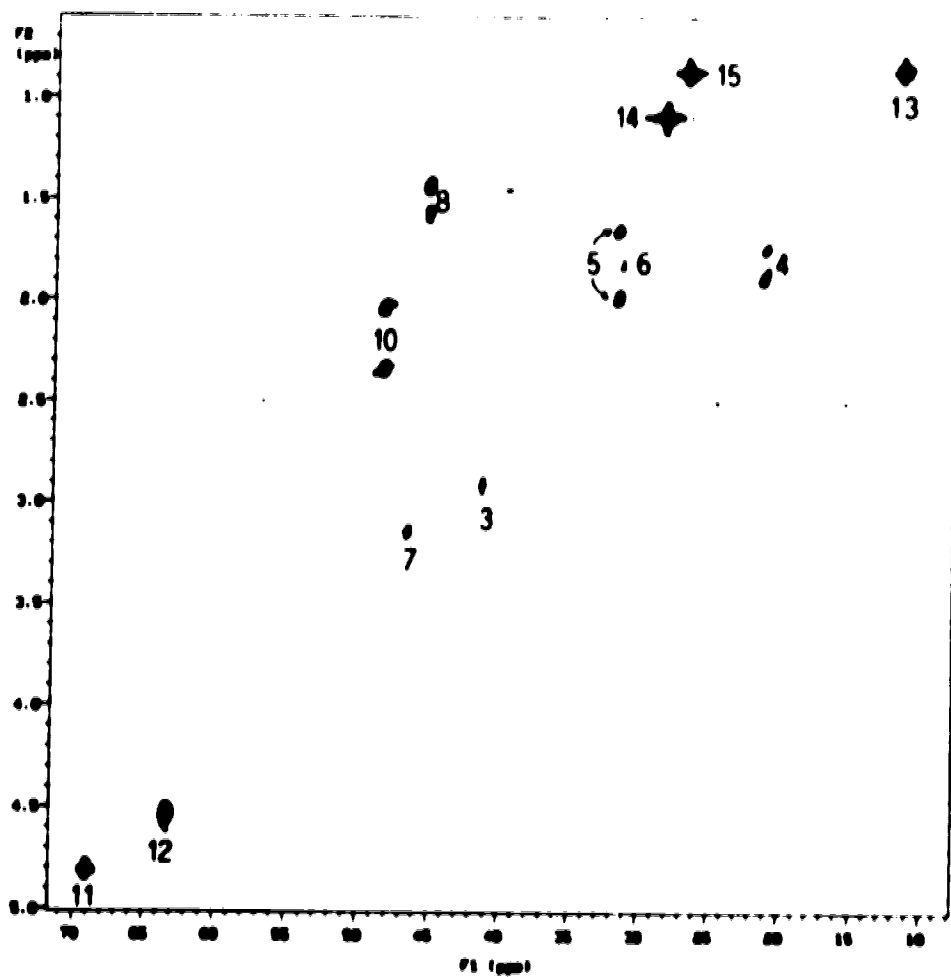
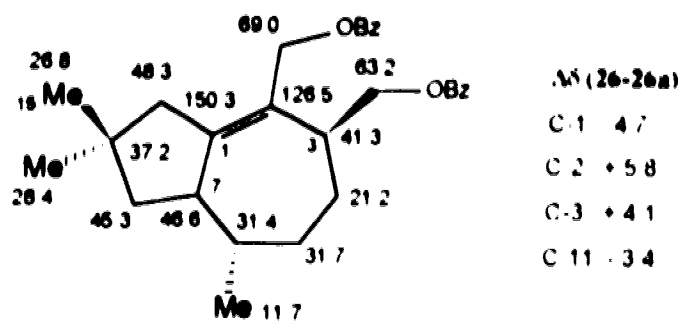


Figure 33 - HMOC spectrum, ¹³C NMR assignment of compound 26a, and chemical shift differences in relation to 26 (negative values indicate deshielding and positive values indicate shielding relative to 26)

The compound of lower R_f value (27a) has the ^1H NMR spectrum shown in Figure 34. In this derivative it was also evident that the aromatic ester exerts a deshielding effect on the majority of the proton resonances when compared with the values of the unprotected diol 27 (Table 9). The oxygenated methylene protons appear as doublets and exhibit only *vicinal* coupling indicating that they have the same chemical shift. The pair at δ 4.53 couples to the allylic proton at δ 3.26 and the pair at δ 4.30 couples to the methine proton at δ 2.11. This allows us to assign the lower field resonance to the homoallylic carbonyl C-11. The remaining chemical shifts are assigned based on comparison with compounds 25a and 27 and were confirmed by selective homonuclear decoupling. The proton assignment is shown in Figure 34.

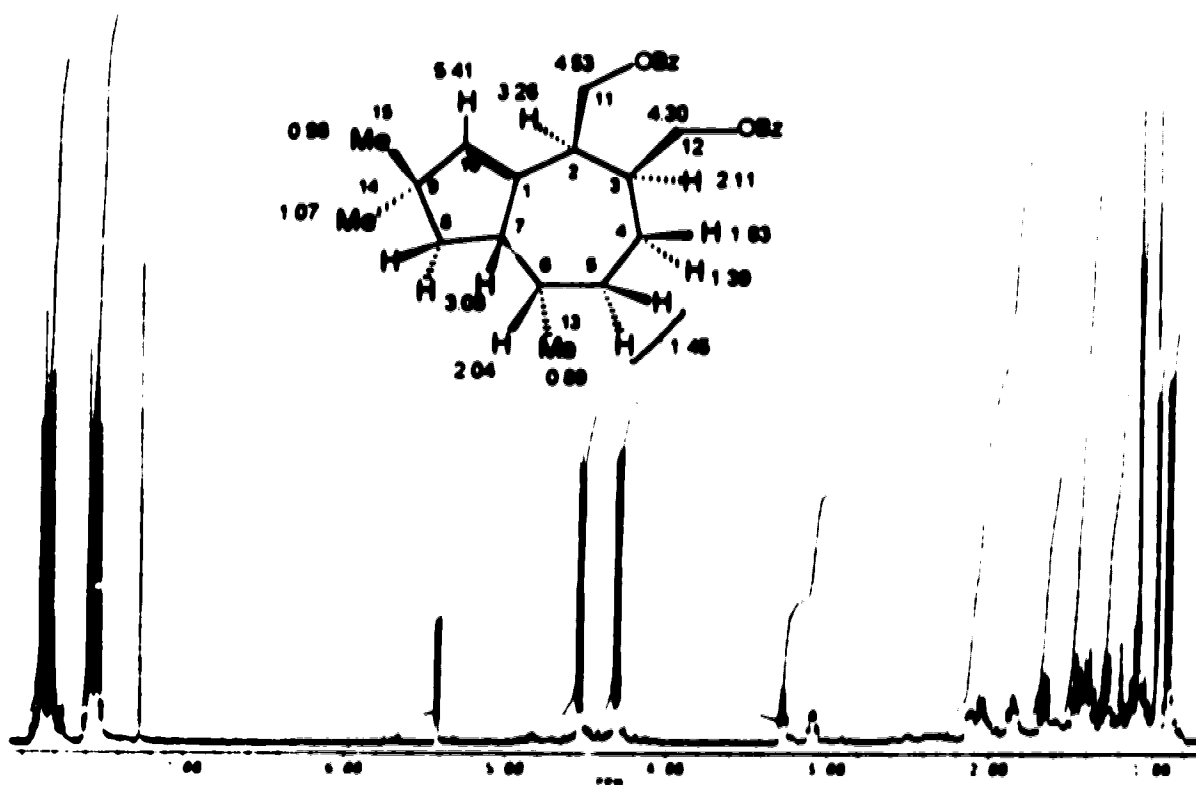


Figure 34 - ^1H and ^{13}C assignments for tremulenediol A dibenzoate (27a).

Table 9 - Comparison of ^1H NMR chemical shifts between 27 and 27a

Atom	δ , multiplicity, J in Hz	
	27	27a
H-2	2.85, ddd, 8.5, 5.4	3.26, td, 7.8, 3.5
H-3	1.70, m	2.11, m
H-4 α	1.52, m	1.39, m
H-4 β	1.60, m	1.83, m
H-5 α	1.34, m	1.45, dd, 10, 10
H-5 β	(2H)	(2H)
H-6	1.88, ddq, 10, 7.5, 7.5	2.04, bq, 7
H-7	2.94, dddd, 11.5, 10.6, 5.2, 5	3.08, m
H-8 α	1.61, dd, 11.5, 6.5	1.37, dd, 11, 11
H-8 β	1.32, dd, 11.5, 11.5	1.66, dd, 11, 7
H-10	5.32, d, 2.5	5.41, d, 2.5
H-11 α	3.90, dd, 11, 8.5	4.53, d, 7*
H-11 β	3.64, dd, 11, 5	(2H)
H-12 α	3.62, dd, 11, 4	4.30, d, 7
H-12 β	3.58, dd, 11, 6.5	(2H)
13-Me	0.84, d, 7.5	0.89, d, 7
14-Me	1.04, s	1.07, s
15-Me	0.98, s	0.98, s

The ^{13}C chemical shift assignment of 27a is shown in Table 4 and Figure 35 and is based on comparison with the data for 27. The chemical shift differences observed relative to 27 are given in the Figure

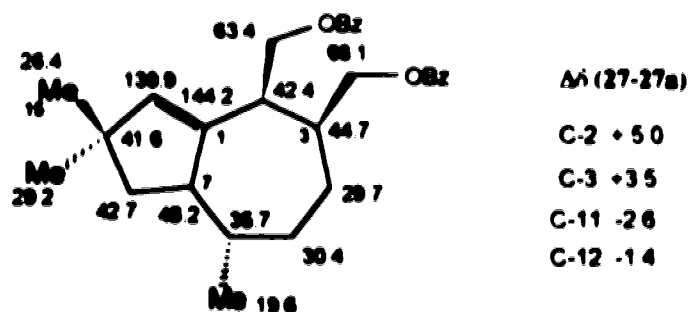


Figure 35 - ^{13}C NMR assignment of compound 27a and chemical shift differences in relation to 27 (negative values indicate deshielding and positive values indicate shielding relative to 27).

Tremulenediol C (28) and tremuladienol (29)

Tremulenediol C (28) was the last sesquiterpene to be eluted from the flash chromatogram. HREIMS showed it to be isomeric with diols A and B (26 and 27) exhibiting a weak molecular ion at m/z 238 equivalent to $C_{15}H_{26}O_2$. The ^{13}C NMR spectrum of 28 indicates the presence of a fully substituted double bond (δ 140.1 and 134.5). The 1H NMR spectrum (Figure 36) shows the presence of a vinylic methyl group (δ 1.94) long range coupled (2 Hz) to a methine proton (δ 4.03) of an allylic secondary alcohol. This suggests that this diol is the allylic isomer (28) of tremulenediol A (26).

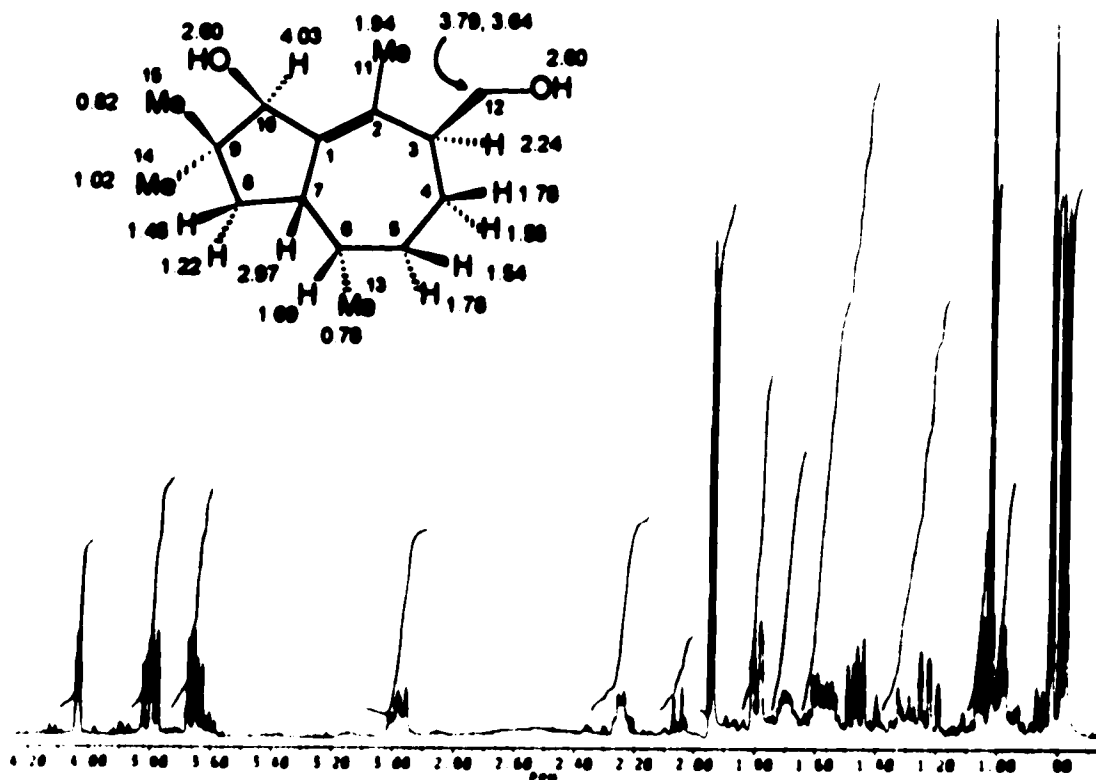
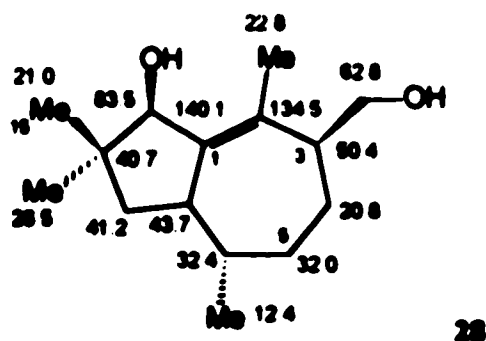


Figure 36 - 1H NMR spectrum and chemical shift assignment for tremulenediol C (28).

H-10 (δ 4.03) shows further long range coupling (2 Hz) to the proton at C-7, similar to that described for H-10 α in tremulenolide A (23). Assuming that the five-membered ring in 28 is in the envelope conformation, this indicates that the C-10 hydroxyl group is β -oriented. Other evidence for this is the absence of W-coupling between the protons at C-10 and C-8, as observed in tremulenediol A (26). The oxygenated methylene protons appear at δ 3.79 and 3.64 and are vicinally coupled to the allylic proton at δ 2.24 (H-3) by 8 and 7 Hz, respectively. The remaining proton assignments are based on selective homonuclear decoupling experiments and is given in Table 5 and Figure 36.

^{13}C NMR data are consistent with the proposed structure for compound 28. It shows two oxygenated carbons, a doublet at δ 83.5 and a triplet at δ 62.8 assigned to C-10 and C-12, respectively. The vinylic methyl group (C-11) resonates at δ 22.8. The complete carbon assignment (Table 4), was secured by HMQC (Figure 37) and HMBX' experiments and is shown in structure 28 below. The assignment of the olefinic carbons is based on the long range ^1H - ^{13}C correlation exhibited by H-8 β with the carbon at δ 140.1 and by H-12 with the carbon at δ 134.5. Another useful correlation is found between the *gem*-dimethyl groups and C-10, which supports the placement of the secondary alcohol at C-10. Cross peaks correlating the vinyl methyl group with both olefinic carbons and with the allylic carbon C-3 confirms the assignment of the vinyl methyl at C-11. Additional HMBX' correlations are summarized in Figure 38.



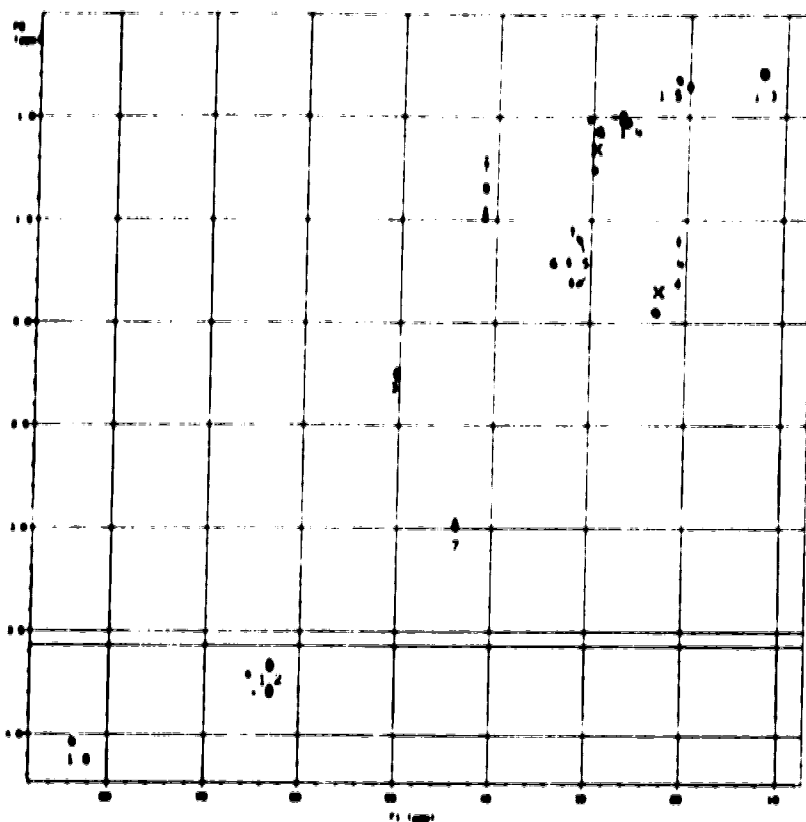


Figure 37 - HMBC spectrum of tremulenediol C (28).

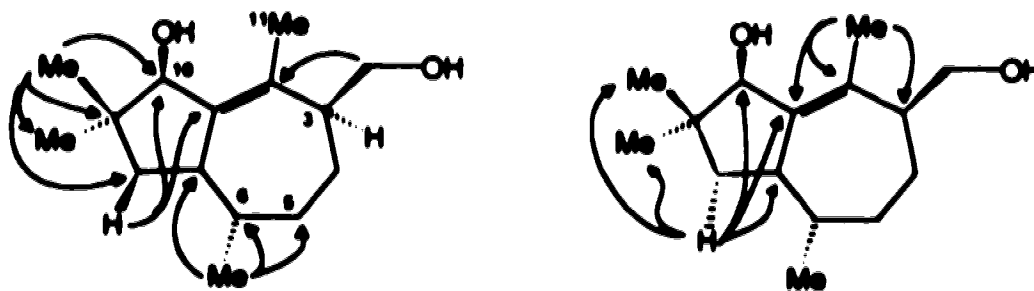
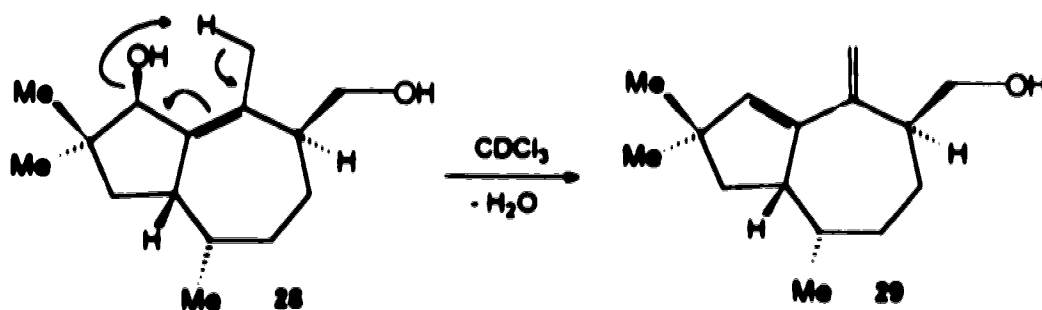


Figure 38 - Significant HMBC correlations of tremulenediol C (28).

On standing in chloroform at room temperature for some days tremulenediol C (28) underwent dehydration to give the dienol 29, also isolated directly from the original chromatography following tremulenolide A (Figure 3). The transformation of 28 to 29 (Scheme 12) has been monitored by NMR where the disappearance of the methyl signal at δ 1.94 is observed, concomitant with the appearance of the alkenic signals at δ 5.71, 5.22, and 4.80 which are characteristic of dienol 29.



Scheme 12 - Conversion of tremulenediol C (28) into tremuladienol (29).

The ¹H and ¹³C NMR spectra of 29 (Tables 5 and 4, respectively) are consistent with structure 29 for this dienol. The proton assignment shown in Figure 39 is based on selective homonuclear decoupling and comparison with the chemical shifts of the previous tremulanes. Irradiation of the signal at δ 5.71 affects the multiplet at δ 3.13. Assuming that this is due to allylic coupling (⁴J = 2.5 Hz) as described for the other Δ^{10} -sesquiterpenes, these resonances are assigned to H-10 and H-7, respectively. The exomethylene protons absorb at δ 5.22 and 4.80. The lower field proton is assigned *enak* due to its greater exposure to the deshielding cone of the C-1,C-10 double bond.

The ¹³C NMR spectrum confirms the presence of an exomethylene at δ 112.6 (triplet). The other signals for the diene appear at δ 139.5 (doublet), 142.8 (singlet), and 147.4 (singlet). The assignment of the quaternary olefin carbons is based on the electron density distribution on the carbons involved. The lower field signal is assigned to C-2 considering

the higher polarization of the C-2,C-11 double bond. The carbon assignment is shown in Figure 40

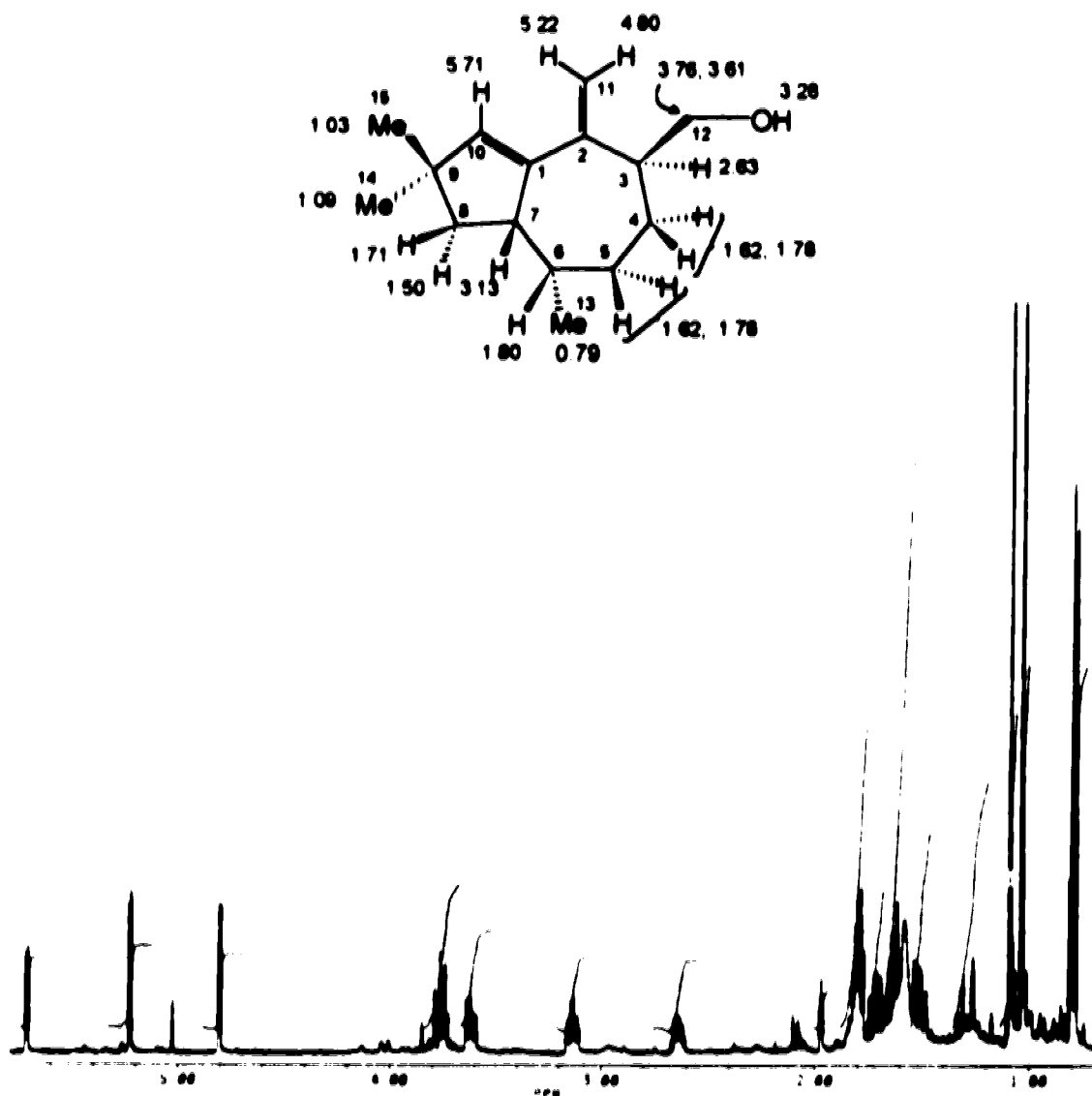


Figure 39 - ¹H NMR spectrum and chemical shift assignment for tremuladienol (29).

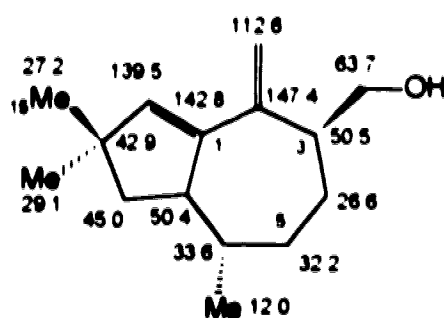


Figure 40 - ^{13}C NMR chemical shift assignment for tremuladienol (29).

The UV spectrum of **29** shows conjugated diene absorption at 244 nm. The molecular formula has been verified by HREIMS which gives a molecular ion at m/z 220 corresponding to $\text{C}_{15}\text{H}_{24}\text{O}$. This compound is very unstable and decomposes rapidly.

2.3.2. Absolute Stereochemistry

The X-ray crystallographic study of **23** did not establish its absolute configuration and we have used CD techniques for this purpose. Tremulenolide A (**23**) exhibits a positive Cotton effect at 252 nm. However, the chirality-sign relationship of ene lactones is not straightforward to analyze, since it seems to be dependent on the ring size and the *cis/trans* nature of the C=C-C=O system and a general quadrant rule cannot be applied⁴⁸. Another approach is to reduce the ene lactone to the corresponding diol⁴⁹. In this case, the chirality-sign relationship of allylic alcohols can be used and the sign of the Cotton effect can be predicted using the olefin octant rule^{50,51}. This approach has been used to determine the absolute configuration of the sesquiterpene lactone isolactarorufin and that of the sesquiterpene dialdehyde isovelleral⁴⁹.

The relationship between chirality and the sign of the Cotton effect for allylic alcohols is based on the C=C-C-O chromophore. A positive sign corresponds to a right-handed helix as shown in Figure 41.

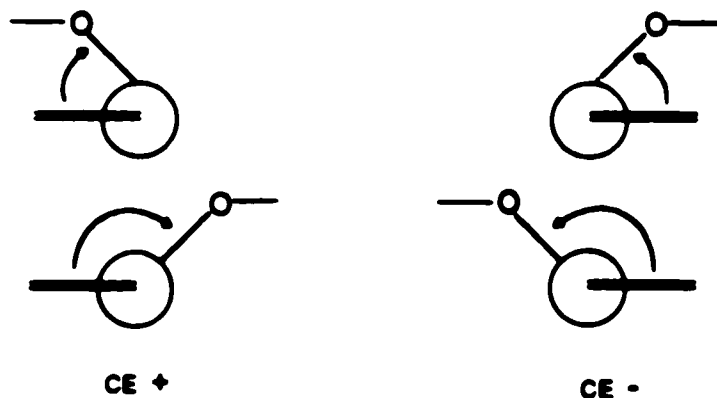


Figure 41 - Relationship between chirality and the sign of the Cotton effect in allylic alcohols.

Tremulenediol A (**26**) is the reduced equivalent of **23** and was used for this study. The CD spectrum of **26** shows a positive Cotton effect at 210 nm, which is associated with a right-handed helical arrangement of the C=C-C-O chromophore⁵⁰ (Figure 41). Since the

hydroxyl group is not attached to the rings, the original olefin octant rule can be applied¹¹

The octant projection, as viewed along the Z and Y axes, is represented in Figure 42

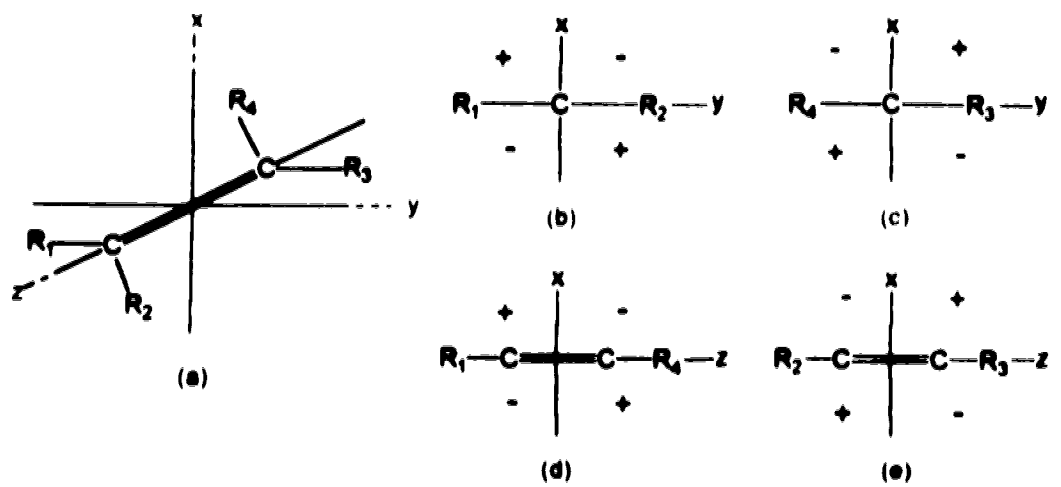


Figure 42 - The olefin octant rule (a) intersecting symmetry planes, (b) front octants viewed along the Z-axis, (c) rear octants viewed along the Z-axis, (d) rear octants viewed along the Y-axis, (e) front octants viewed along the Y-axis

The conformation proposed for tremulenediol A (26) is shown in Figure 43 along with its intersecting symmetry planes as demonstrated in Figure 42

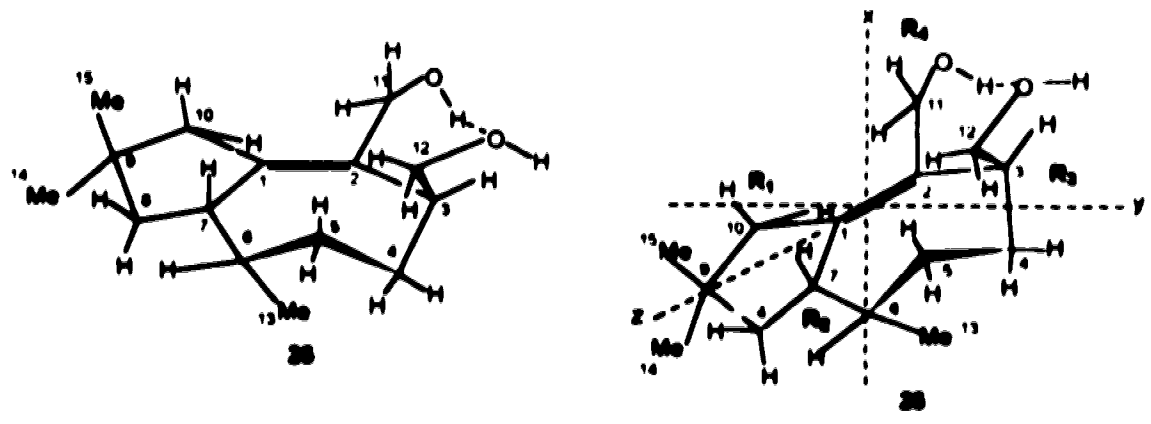


Figure 43 - Conformation of tremulenediol A (26) and the intersecting symmetry planes for the octant projection.

If an *S*-configuration is assigned to the chiral center at C-3 of **26** and the molecule is viewed along the Z-axis from C-1 to C-2 (Figure 44a,b) the heavily populated regions of the front and rear octants are in positive octants. The same is true when the molecule is viewed along the Y-axis (Figure 44c)

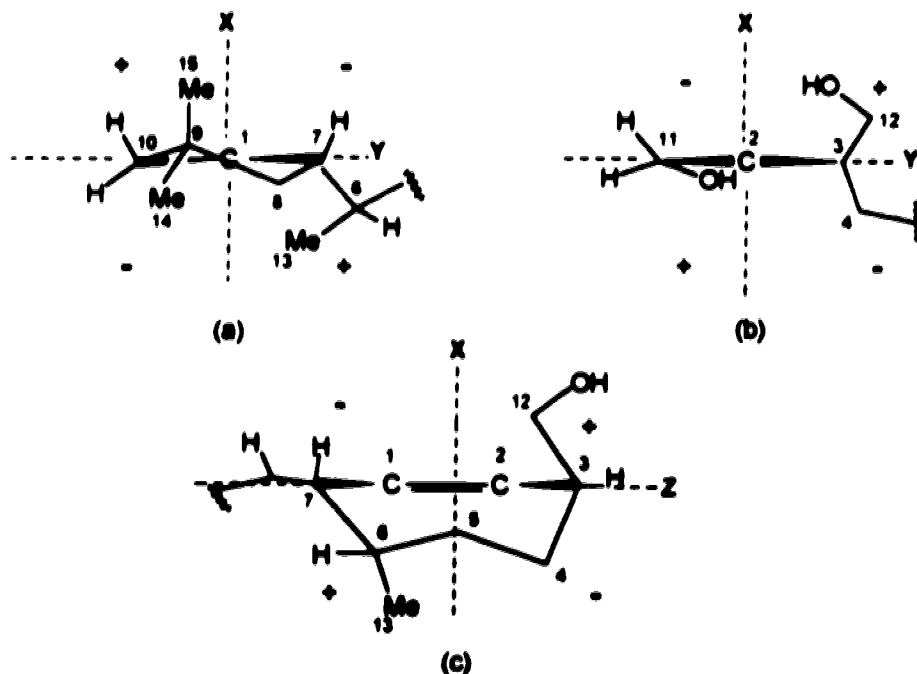
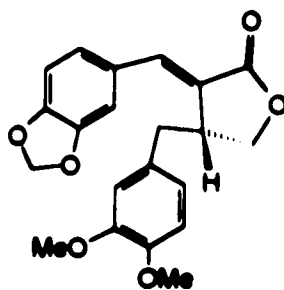
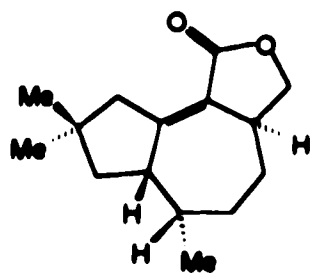
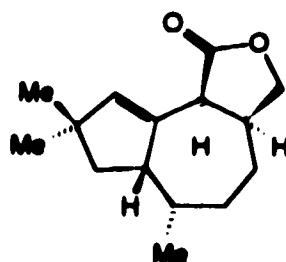
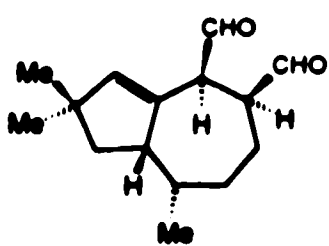
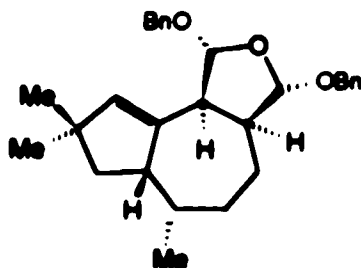
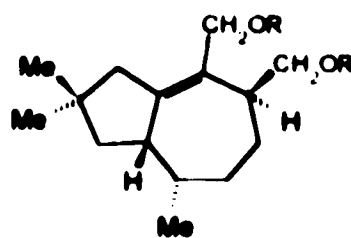


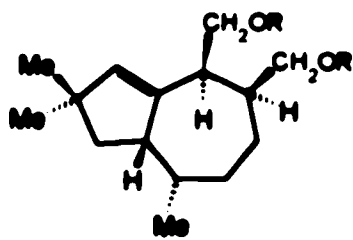
Figure 44 - Olefin octant rule projection for tremulenediol A (**26**): (a) front octants viewed along Z-axis from C-1 to C-2; (b) rear octants viewed along Z-axis from C-1 to C-2; (c) front octants viewed along Y-axis.

If a *3R*-configuration is assigned, the populated regions are in negative octants. This analysis suggests that the absolute stereochemistry of **26** is *S* at all three chiral centers (C-3, C-6, and C-7) by relating the relative configuration of the other asymmetric centers to C-3. Therefore, tremulenediol A has the absolute configuration shown in structure **26**. The positive Cotton effect observed for tremulenolide A (**23**) is consistent with this absolute stereochemistry. Comparing the CD spectrum of **23** (positive) with that of (-)-*3R*-hibelactone (**30**),⁵² a model *cisoid* γ -lactone, we find that they have Cotton effects

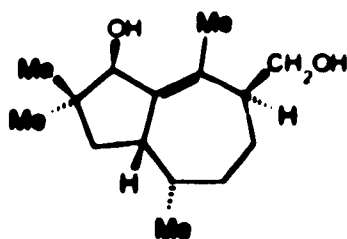
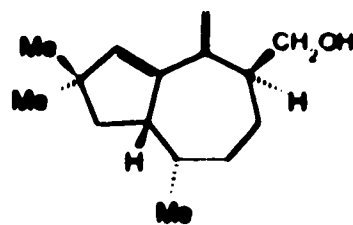
of opposite sign, indicating the opposite (and thus *S*) absolute stereochemistry at C-3 of **23**. Extrapolation of the results to all the natural tremulanes indicates they possess the absolute stereochemistry indicated in the structural formulas **23-29**

**30****23****24****26****26a**

26 R = H
26a R = OCOPh



27 R = H
27a R = OCOPh

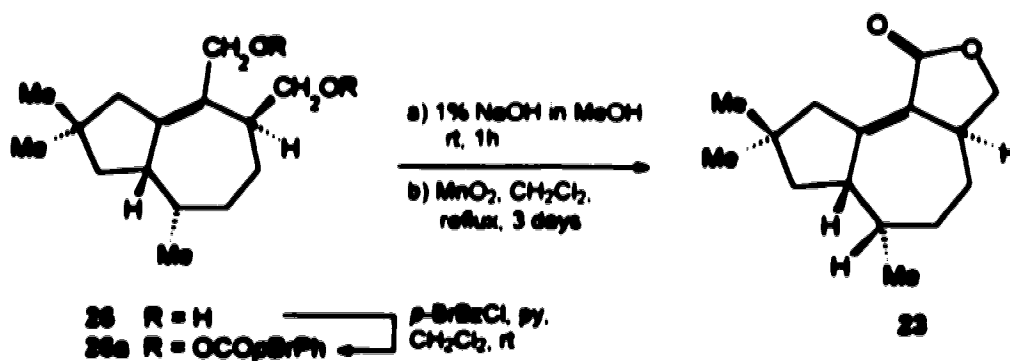
**28****29**

2.3.3. Chemical conversions

It has been noted that the tremulane sesquiterpenes are structurally correlated on the basis of NMR evidence. However, a more elegant way to confirm the structural relationships is to perform suitable chemical reactions which interconvert members of the series. In this regard, two pairs of tremulanes have been interrelated.

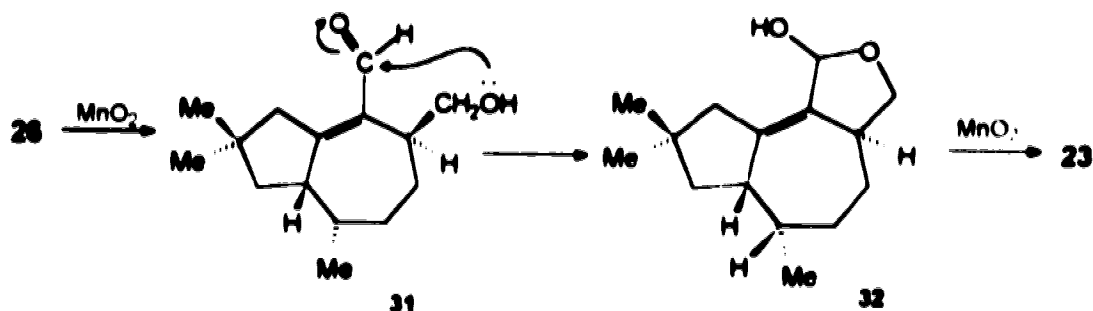
2.3.3.1. Oxidation of tremulenediol A (26) to tremulenolide A (23)

By taking advantage of the different type of alcohols present in tremulenediol A (26), an attempt was made to oxidize it to the corresponding lactone. To avoid interference by tremulenediol B (27), usually present in small amounts in the diol A (26), the di-*p*-bromobenzoate derivative of 26 was used as starting material. Deprotection of the di-*p*-bromobenzoate 26a under basic conditions (1% NaOH in MeOH)⁵³ afforded a compound with the same R_f of the diol A (26). Evaporation of the methanol followed by oxidation of the crude reaction mixture with manganese dioxide⁵⁴ in dichloromethane gave tremulenolide A, identical (R_f , NMR) with the natural product. This is illustrated in Scheme 13



Scheme 13 - Conversion of tremulenediol A (26) into tremulenolide A (23).

The formation of tremulenolide A is a result of two successive allylic oxidations (Scheme 14). In a first step the allylic alcohol at C-11 is oxidized to the monoaldehyde 31, which undergoes nucleophilic attack by the primary alcohol at C-12 to form the hemiacetal 32. This hemiacetal, being an allylic alcohol itself, is again oxidized to give the lactone 23.



Scheme 14 - Possible intermediates involved in the oxidation of diol 26 with MnO_2 .

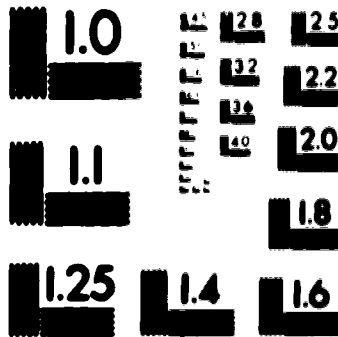
The formation of tremulenolide A from tremulenediol A confirms the relationship between these two tremulane sesquiterpenes.

2.3.3.2. Reduction of tremulenediol (25) to tremulenediol B (27)

The crude dialdehyde 25 was reduced with $NaBH_4$ in dichloromethane to give a compound with the same R_f value as diol 27. Treatment of the reaction mixture with *p*-bromobenzoyl chloride in the presence of pyridine afforded a di-*p*-bromobenzoate which exhibits the same NMR spectrum as the di-*p*-bromobenzoate 27a. Since it was possible that the crude dialdehyde 25 contained some of the diol 27 (they elute close together), the reduction was also carried out with $NaBD_4$. When deuterium incorporation takes place the product can be easily differentiated from the natural product by simple NMR techniques. The 1H NMR, for example, will show changes in multiplicity, since deuterium has a nuclear spin of 1, and in the integration for the carbinyl groups. In the ^{13}C NMR the effect

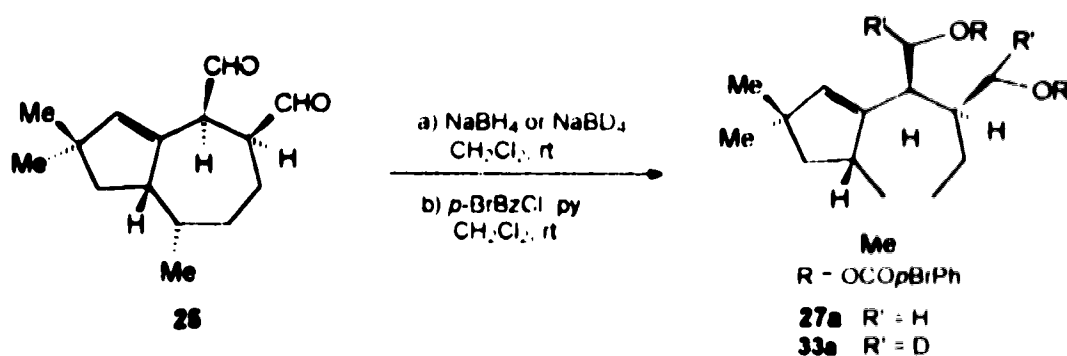
2 of/de 2

PM-1 3 1/2" x 4" PHOTOGRAPHIC MICROCOPY TARGET
NBS 1916a ANSI/ISO #2 EQUIVALENT



PRECISIONSM RESOLUTION TARGETS

of deuterium incorporation not only produces changes in multiplicity but also causes an upfield shift in the directly bonded carbon resonance. The magnitude of this isotope effect ranges from 0.3 to 0.6 ppm⁵⁵. The product was isolated as the di-*p*-bromobenzoate derivative and its ¹H and ¹³C NMR spectra are consistent with the incorporation of one deuterium at both C-11 and C-12 (Scheme 15).



Scheme 15 - Reduction of tremulenedial (**25**) with NaBH₄ and NaBD₄

In the ¹H NMR spectrum the signals at δ 4.53 and 4.30 each integrate for a single hydrogen and the multiplicity of each is changed from a doublet to an apparent triplet due to additional *geminal* coupling with deuterium. The multiplicity of the signal for H-2 (δ 3.26) is changed from a triple doublet to a double doublet indicating *vicinal* coupling with a single hydrogen at C-11, as shown in Figure 45. In the ¹³C NMR (APT) the resonances for C-11 and C-12 are shifted upfield (0.3 ppm) due to the isotope effect of deuterium, the phase is reversed, and the signals appear as triplets due to coupling with ²H.

This result with the reduction with NaBD₄ indicates that the diol formed indeed originated from the dial and hence confirms the correlation between this pair of tremulanes.

These chemical transformations serve to demonstrate that a common biosynthetic pathway governs the formation of all members of this new group of sesquiterpenes. This motivated studies on the biosynthesis of these compounds which is described next.

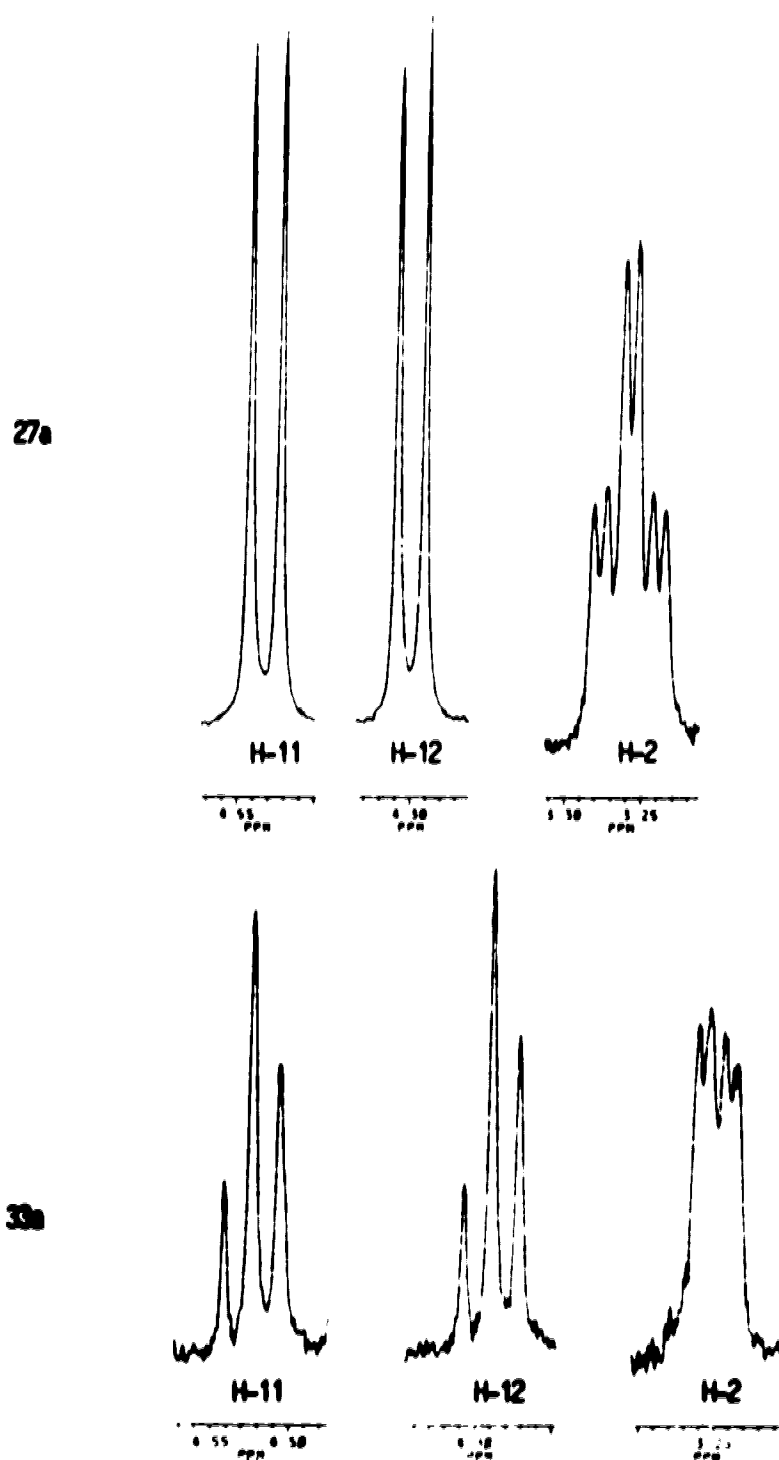
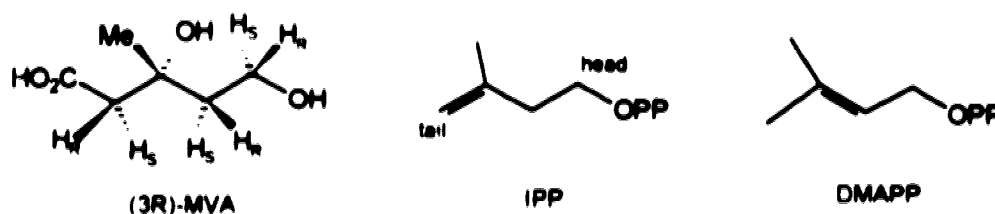


Figure 45 - Comparison of the partial ^1H NMR spectrum of tremulenediol B di-*p*-bromobenzoate (**27a**) with that of the diduteride **33a**.

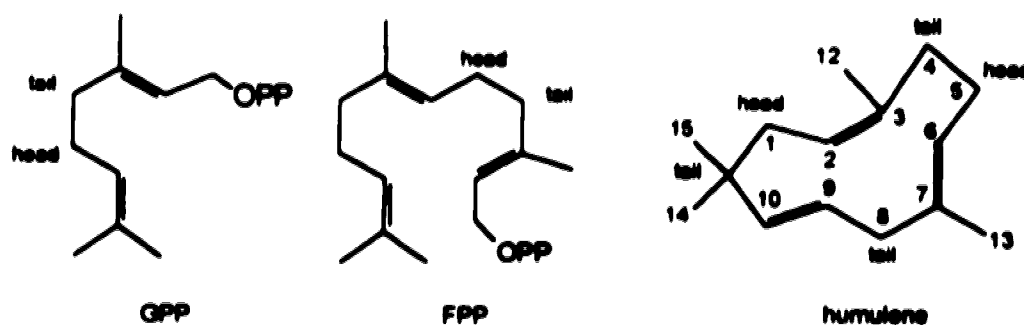
2.3.4. Biosynthesis

The isolation of new secondary metabolites brings an ongoing problem which is twofold^{12,56a} the identification of the primary source(s) from which the secondary metabolite has its genesis, and the identification of the mechanism and intermediates involved in the biogenesis. The two parts of the problem are partially solved with the structure of the secondary metabolite since it provides the first hint to identify the primary source and allows informed speculation about its mechanism of formation. However, the complete solution requires the use of special techniques. The most common technique involves the administration of likely precursors to the organism under study and examination of the uptake use of these precursors in the formation of the secondary metabolite. To follow the path of these precursors through to the metabolite it is necessary to use labelled precursors. One can choose between radioactive isotopic labels (^{14}C , ^3H) and stable isotopic labels (^{13}C , ^{15}N , ^2H , ^{18}O)^{56a}. The first group is assayed by liquid scintillation counting which is based on the conversion of β -radiation into light. The second group is assayed by NMR spectroscopy and/or mass spectrometry. Stable isotopes can yield more information more quickly than radioactive ones. Among the stable isotopes mentioned above, only ^{18}O does not give rise to NMR signal. However, its incorporation can be analyzed by ^{13}C NMR since its presence on a particular carbon atom causes an upfield shift of that carbon resonance compared to the spectrum when ^{16}O is present. The most common labelled precursor is carbon labelled sodium acetate, which is available in the form of 1- ^{13}C , 2- ^{13}C , and 1,2- $^{13}\text{C}_2$. The use of singly labelled acetate affords a ^{13}C NMR spectrum with enhanced signals for the positions where the incorporation occurred. In the case of doubly labelled acetate the ^{13}C NMR spectrum shows doublets for the carbons which originate from the incorporation of an intact acetate unit. These doublets flank the natural abundance singlet in the proton decoupled spectrum. The identification of these carbons is based on coupling constant measurements, selective decoupling, and/or 2D-techniques^{56a}.

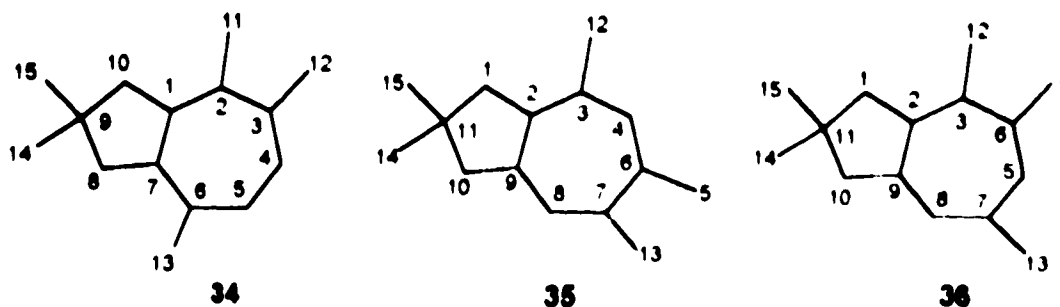
Terpenes are known to be derived from mevalonate (MVA) which is a product of acetate metabolism. They are characterized by the presence of repeated isoprene units usually linked in a head-to-tail manner⁵⁷. These C_5 units are isopentenyl pyrophosphate (IPP) and dimethylallyl pyrophosphate (DMAPP), which are the building blocks of the isoprenoids.



Sesquiterpenes are C_{15} compounds formed from the condensation of three isoprene units. Condensation of IPP with DMAPP gives geranyl pyrophosphate (GPP) which condenses further with IPP to produce farnesyl pyrophosphate (FPP). Cyclization of FPP yields the humulene skeleton which is the precursor of many cyclic sesquiterpenes.



Tremulane (34) is a perhydroazulene-type skeleton isomeric with the well-known lactarane skeleton (35)⁵⁸, and with the skeleton 36 produced by the fungus *Merulius tremellosus*⁵⁹. Skeletons 35 and 36 may be derived by cyclization and rearrangement of humulene^{58,59}. The numbering in 35 and 36 follows that of humulene. Since these sesquiterpene skeletons differ only in the position of the secondary methyl groups one might expect a similar biogenesis for all of them.



In order to investigate the biosynthetic origin of the tremulane skeleton labelling experiments were carried out, administering singly and doubly labelled acetate to liquid cultures of *P. tremulae* and investigating the incorporation using ^{13}C NMR spectroscopy

The cultures of *P. tremulae* were prepared as before (with added resin) and were periodically supplemented with injections of a sterile solution of labelled sodium acetate [$1\text{-}^{13}\text{C}$], [$2\text{-}^{13}\text{C}$], and [$1,2\text{-}^{13}\text{C}_2$]. After 16 days of growth, the culture was harvested and the crude extract was chromatographed as described previously. Since tremulenediol A (26) can be isolated in reasonable amount and in pure form as its di-*p*-bromobenzoate 26a, it was chosen to conduct the incorporation analysis. The procedure for separation and purification of 26a also allows the isolation of the di-*p*-bromobenzoate 27a, which was also analyzed to confirm the incorporation pattern found for 26a. In order to differentiate the labelled compounds from the non-labelled ones they will be referred as $1\text{-}^{13}\text{C}\text{-}26\text{a}$, $2\text{-}^{13}\text{C}\text{-}26\text{a}$, and $1,2\text{-}^{13}\text{C}_2\text{-}26\text{a}$: the same applies to compound 27a.

The ^{13}C NMR spectrum of enriched $1,2\text{-}^{13}\text{C}_2\text{-}26\text{a}$ exhibits six pairs of spin-coupled doublets appearing as satellites about the enhanced natural abundance singlets, as well as three enhanced singlets, as shown in Figure 46. The satellite-like signals that appeared for the resonances of C-12 and C-14 were neglected because the coupling constant of these "doublets" does not match with any other and also these carbons do not show any coupling in the INADEQUATE^{56b} experiment. The results are presented in Table 10, along with the data for compound $1,2\text{-}^{13}\text{C}_2\text{-}27\text{a}$.

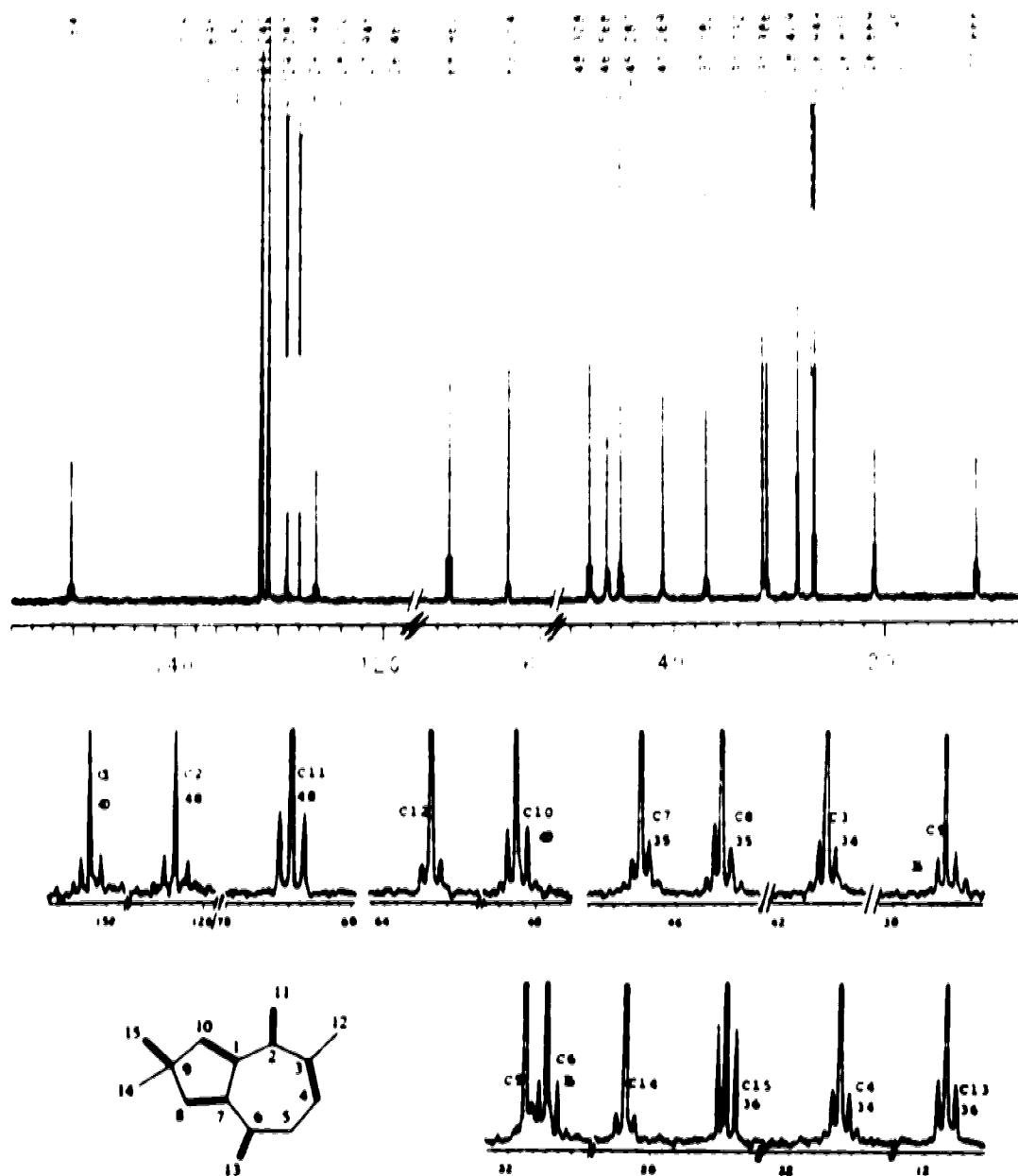


Figure 46 - ^{13}C NMR spectrum (125 MHz) of the doubly labelled tremulenediol A di-*p*-bromobenzoate (26a).

Table 10 - ^{13}C NMR data of doubly labelled **26a** and **B (27a)**

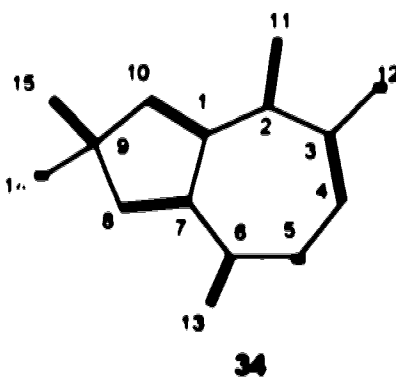
Carbon	26a		27	
	δ_{C}	J_{CC} , Hz	δ_{C}	J_{CC} , Hz
C-1	150.3 s	40	150.3 s	70
C-2	126.5 s	48	126.5 s	30
C-3	41.3 d	34	41.3 d	33
C-4	21.2 t	34	21.2 t	33
C-5	31.7 t	s	31.7 t	s
C-6	31.4 d	36	31.4 d	35
C-7	46.6 d	35	46.6 d	34
C-8	45.3 t	35	45.3 t	34
C-9	37.2 s	36	37.2 s	35
C-10	48.3 t	40	48.3 t	70
C-11	69.0 t	48	69.0 t	30
C-12 ^a	63.2 t	s	63.2 t	s
C-13	11.7 q	36	11.7 q	35
C-14 ^a	28.4 q	s	28.4 q	s
C-15	26.8 q	36	26.8 q	35

^a these signals show an undefined satellite about the natural abundance singlet which have been neglected based on INADEQUATE results

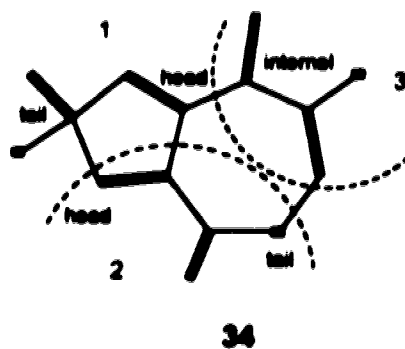
Doubly labelled acetate is a particularly useful precursor of isoprenoid metabolites in biosynthetic investigations. All carbons in any subsequent metabolite which are derived from paired atoms give rise to coupled doublets in the ^{13}C NMR spectrum, provided that the paired atoms remain connected. Adjacent carbon atoms derived from separate molecules of acetate will not show spin-spin coupling as long as there is a significant pool of unlabelled acetate. Furthermore, since C-1 of mevalonate is lost as carbon dioxide in the formation of IPP, all carbons in any subsequent metabolite which are derived from C-2 of mevalonate give rise to enhanced singlets. In the case of tremulane these singlet carbons are C-5, C-12, and C-14. A 2D ^{13}C - ^{13}C correlation experiment was carried out in order to confirm the results obtained by coupling constant measurements and also to observe

whether or not the satellites that appeared about the singlet resonances of C-12 and C-15 are real

An INADEQUATE experiment (Figure 47) confirms the spin-coupled carbons for the following pairs C-1,C-10, C-2,C-11, C-3,C-4, C-6,C-13, C-7,C-8, and C-9,C-15. Carbons C-5, C-12, and C-14 do not give rise to cross peaks with other carbon resonances, indicating that they are actually singlets. The same coupling pattern is observed for tremulanes **26a** and **27a**, as indicated in the tremulane skeleton (**34**) below.



This result with doubly labelled acetate indicates that tremulane does not obey the classical isoprene rule in a straightforward manner. Two units are linked by head-to-tail addition, but the third unit seems to be involved in internal linkage and it appears that the 2- ^{13}C singlet of this unit has migrated.



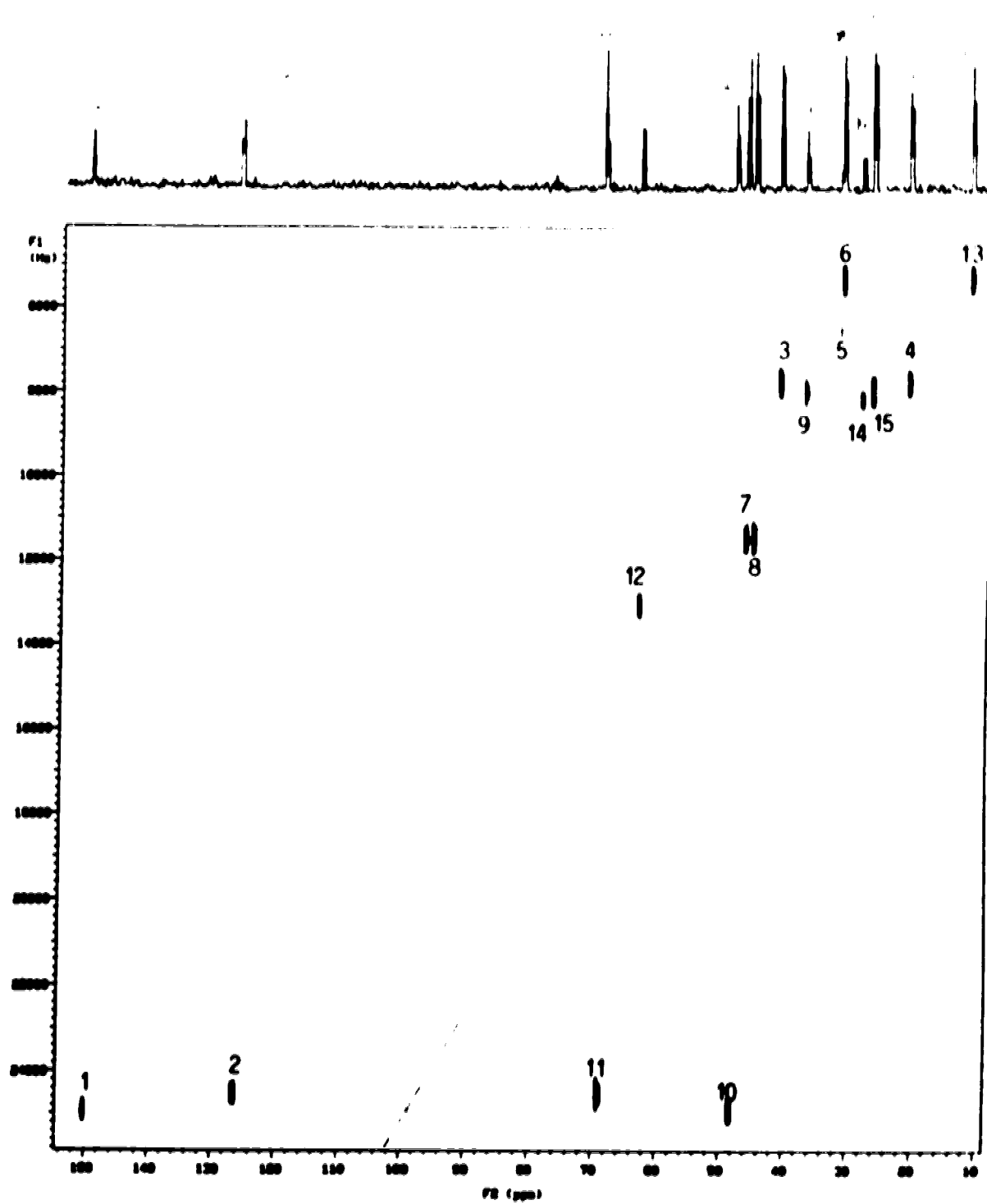
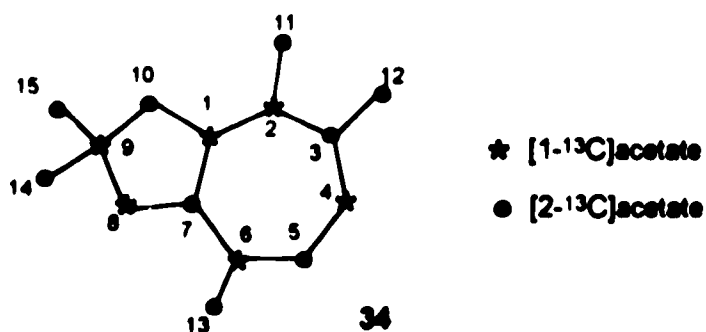


Figure 47 - INADEQUATE spectrum of the doubly labelled tremulenediol A di-*p*-bromobenzoate (26a).

In order to elucidate this unusual incorporation pattern administration of singly labelled acetate ($1\text{-}^{13}\text{C}$ and $2\text{-}^{13}\text{C}$) to cultures of *P. tremulae* was carried out in the same manner described previously. Singly labelled tremulenediols A and B were isolated as their di-*p*-bromobenzoates **26a** and **27a** and analyzed by ^{13}C NMR spectroscopy. The broad band ^{13}C spectrum was obtained using the same conditions for the unlabelled, $[1\text{-}^{13}\text{C}]$ labelled, and $[2\text{-}^{13}\text{C}]$ labelled compounds. The enriched signals were identified by subtracting the natural abundance spectrum (unlabelled) from the labelled spectra. Figure 48 shows the unlabelled and singly labelled spectra of **26a** which indicates the incorporation pattern shown in tremulane **34** below.



A summary of these labelled acetate incorporations is given in Figure 49.

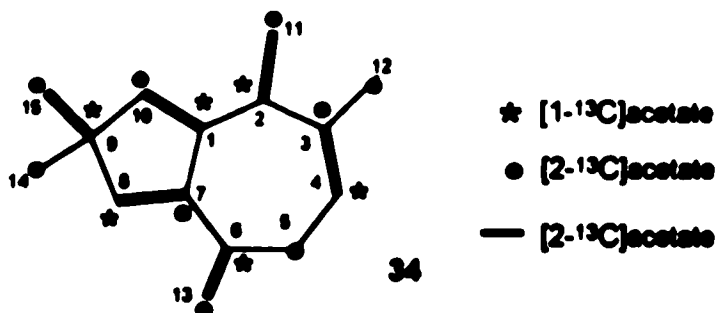


Figure 49 - Summary of incorporation of singly and doubly labelled acetate administered to cultures of *P. tremulae* in tremulane sesquiterpenes.

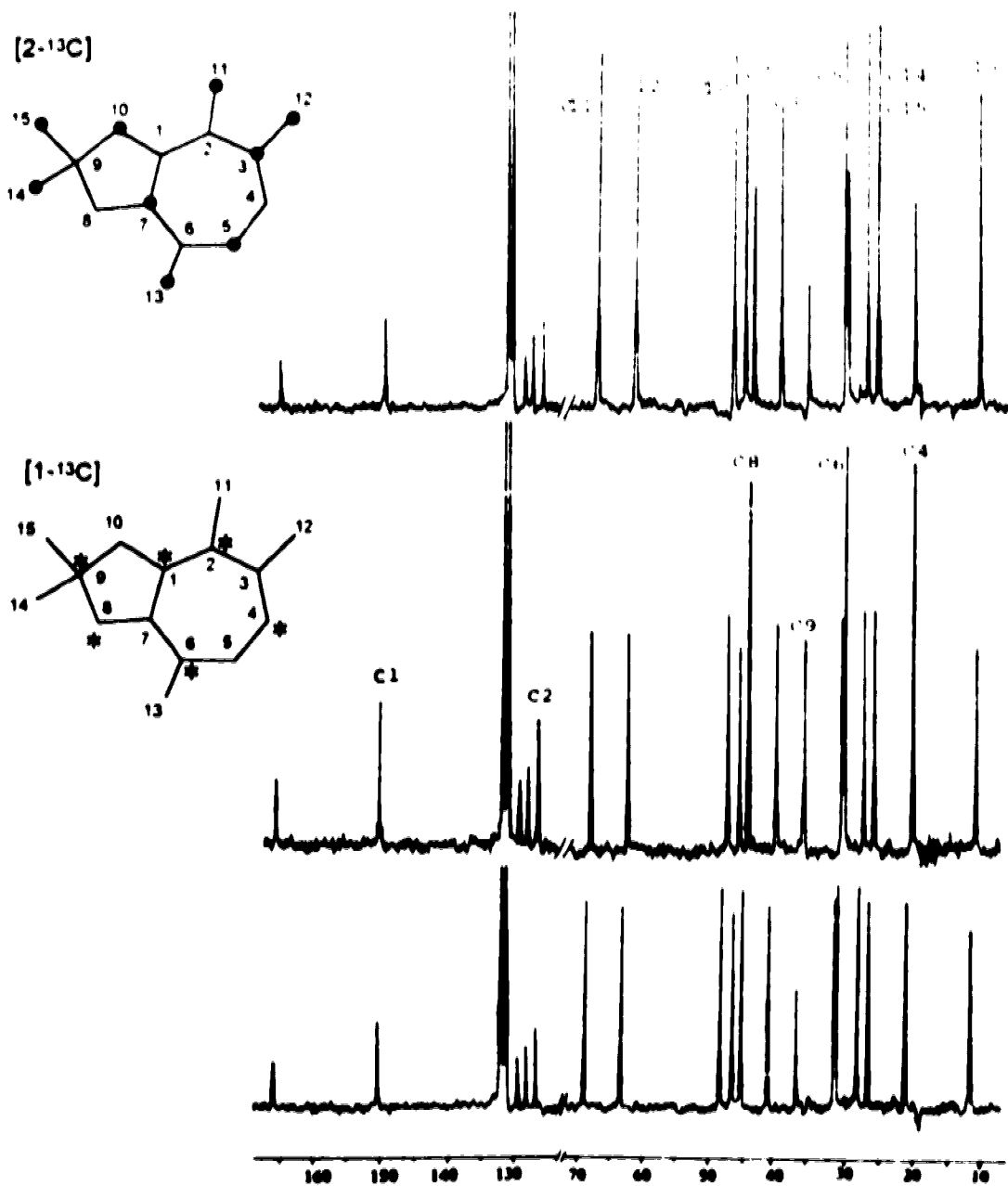


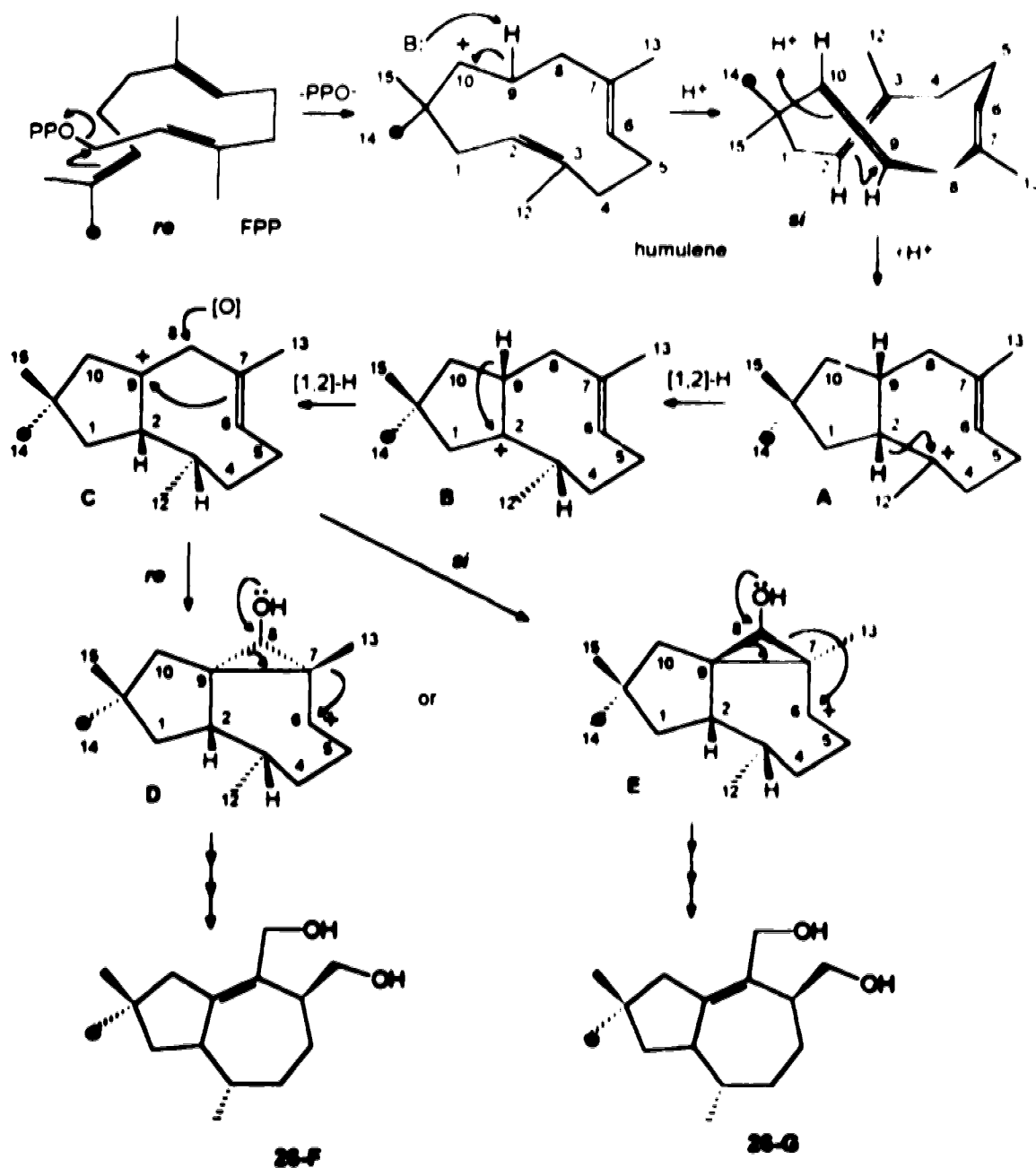
Figure 48 - ^{13}C NMR spectra of 26a natural abundance (bottom), $[1-^{13}\text{C}]$ labelled (center), and $[2-^{13}\text{C}]$ labelled (top)

These results strongly support the previous observation of migration of one of the *geminal* methyl groups in the third isoprene unit. There are two possible mechanisms that account for this rearrangement. One invokes the common pathway of sesquiterpenes biosynthesis from *trans,trans*-farnesyl pyrophosphate *via* humulene⁹ and the other involves the initial condensation of GPP and DMAPP. The stereochemical course of the biosynthesis is based on the work of Cane and Nachbar⁽¹⁰⁾, in which the condensation and cyclizations are related to the known absolute stereochemistry at each chiral centre.

In the FPP-mechanism, the cyclization of *trans,trans*-FPP may be envisaged as the electrophilic attack by the C-1 carbinyl carbon at C-11 which may occur on the *re* or *si* face of the distal double bond. If attack occurs on the *re* face, the methyl group derived from C-2 of mevalonate becomes the *pro-S* methyl of humulene. If the attack is on the *si* face the same methyl becomes *pro-R*. The cyclization of the five-membered ring can also occur by attacking the *re* or *si* face of the 9,10-double bond. In order to account for the absolute stereochemistry of the tremulane sesquiterpenes the cyclization of FPP has to occur at the *re* face of the distal double bond, as shown in Scheme 16. The humulene formed has a *pro-R* methyl derived from C-2 mevalonate (C-14). Then, humulene is folded as in A to promote a *si* attack on the 9,10-double bond after its protonation. This results in a *trans* relationship between the hydrogens on the fused rings and the labelled C-14 methyl. [1,2]-H shift from C-2 to the upper face of the carbocation C-3 (B) and then from C-9 to the upper face of the new-formed carbocation C-2 (C) sets the *S* absolute stereochemistry at C-2 and C-3. This corresponds to the observed *S* stereochemistry at C-7 and C-6 of tremulane, respectively. Oxidation at C-8 and electrophilic attack by the carbocation C-9 at C-7, generates the cyclopropanes D or E depending on whether the attack occurs on the *re* or *si* face, respectively. To achieve the proper stereochemistry at C-6 of humulene (C-3 of tremulane), the migration of the β -oriented group should take

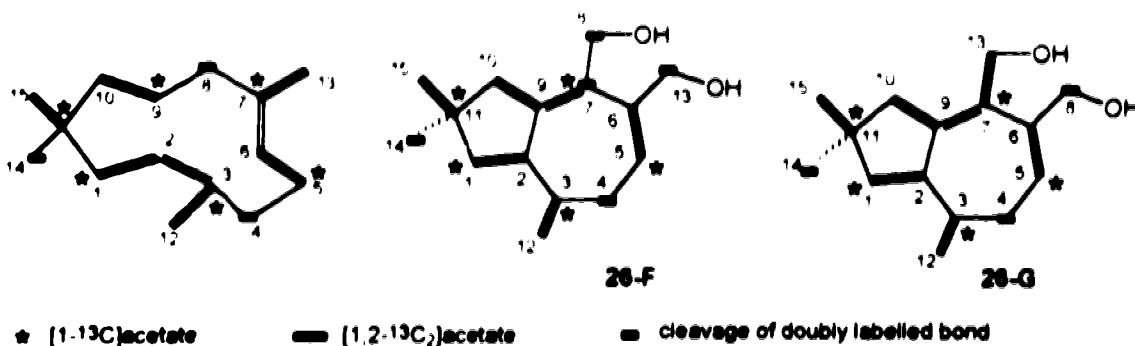
⁹ We thank Prof. David Cane for initially suggesting this pathway.

place. If a *re* attack occurs, C-13 of humulene migrates (D). If a *si* attack occurs, C-8 of humulene migrates (E).



Scheme 16 - Stereochemical course of the tremulane biosynthesis from FPP via humulene, exemplified for tremulenediol A (26).

After appropriate functionalization, one would expect to obtain **26-F** or **26-G**, whose labelling pattern from humulene is shown in Scheme 17, with the numbering of humulene

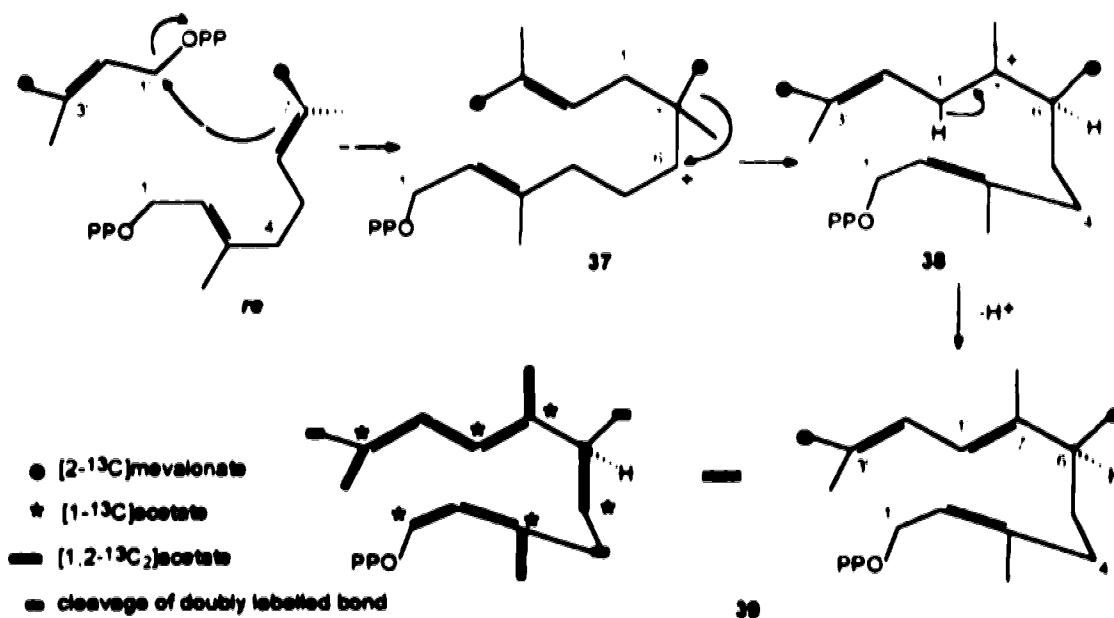


Scheme 17 - Labelling pattern expected for tremulane following humulene pathway (tremulane is numbered according to humulene).

The pathway which leads to the formation of **26-F** can be ruled out since it requires the cleavage of an acetate unit, contrary to the experimental results. The labelling pattern in structure **26-G** is consistent with that obtained for tremulane (Figure 49), favoring the *si* attack in the intermediate **C**. However, it seems unusual that the same center responsible for the cyclopropane ring opening is the one which migrates.

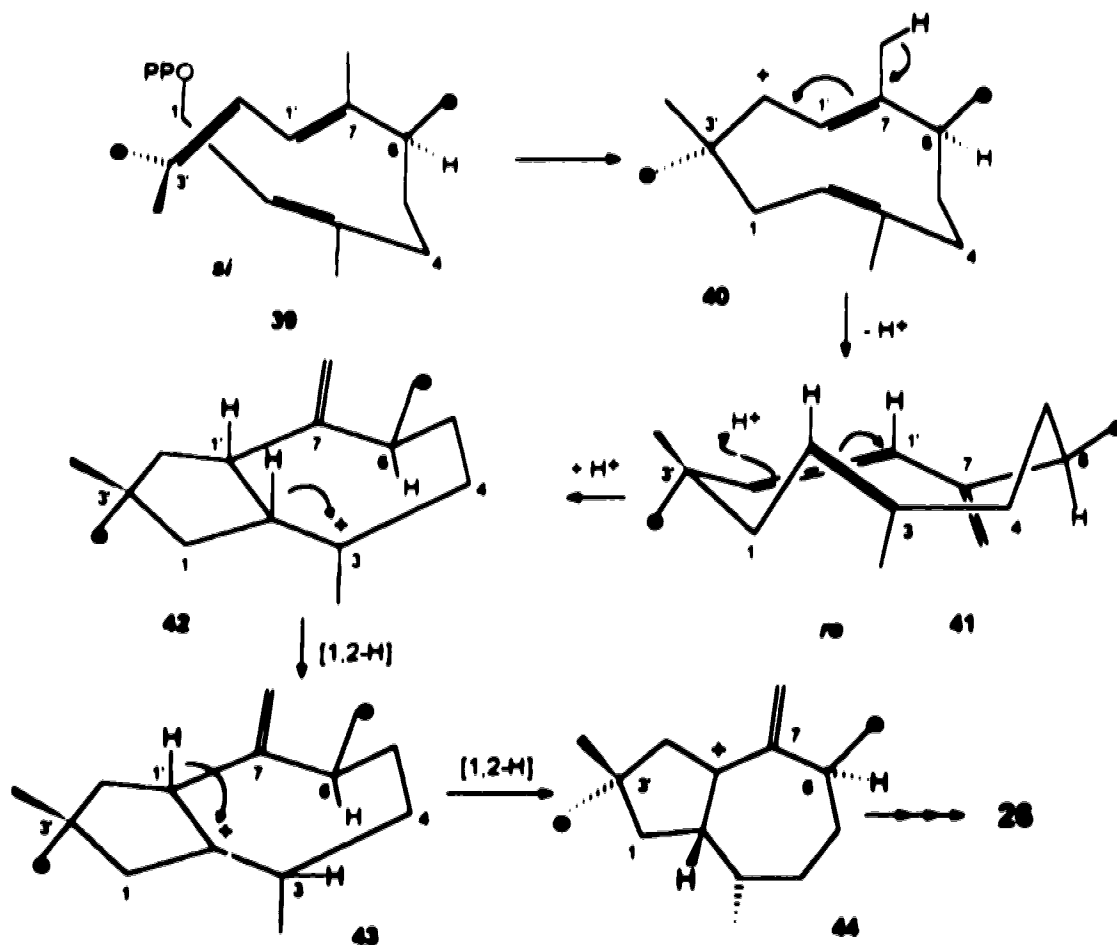
The formation of the tremulane skeleton can also be rationalized as the condensation of GPP and DMAPP. This process requires a larger pool of DMAPP compared to IPP which does occur in many organisms⁵⁷. This condensation-cyclization-rearrangement can occur *via* different pathways. One of the possible mechanisms will be presented. The first part is illustrated in Scheme 18. Electrophilic attack by the C-1' carbinyl of DMAPP at the *re* face of the distal double bond (C-7) of GPP generates the carbonium ion intermediate **37** in which the *pro-S* methyl at C-7 is derived from C-2 of mevalonate. Migration of the *pro-S* methyl to the *si* face of the carbocation C-6 yields **38**. Loss of a proton gives the

intermediate **39** In accordance with the labelling pattern of DMAPP and GPP, structure **39** has the labelling shown in Scheme 18



Scheme 18 - GPP-DMAPP-mechanism in the tremulane biosynthesis: generation of the acyclic intermediate **39**.

The intermediate **39** is then folded to allow an electrophilic attack by the carbinyl group on the *si* face of C-3' to afford the carbonium ion **40** (Scheme 19). Loss of a proton gives rise to the neutral intermediate **41**. Intramolecular cyclization of **41** takes place through a *re* attack by the 2,3-double bond to C-1' with concomitant protonation at C-2' to produce **42**. A double [1,2-H]shift from C-2 to the carbocation C-3 and from C-1' to C-2 gives **43** and **44**, respectively. Appropriate functionalization of **44** provides tremulenediol **26**. The resultant labelling pattern is the same as that found experimentally.



Scheme 19 - Stereochemical course of the tremulane biosynthesis in the GPP-DMAPP-mechanism of tremulane biosynthesis:

Both mechanisms account for the observed incorporation results. Since there is no precedent for the GPP-DMAPP condensation, and since humulene is involved as an intermediate in the formation of many sesquiterpenes, we tend to favor this route. However, further work will be required in order to completely define the pathway.

2.4. Additional Studies

The isolation of these new metabolites produced by *P. tremulae* prompted us to explore some related aspects of the work. Included are the bioactivity of the metabolites, the oxidase activity of fungus towards other aromatic carboxylic acids, and an attempt to isolate the metabolites from rotted aspen and from *Phellinus* conk

2.4.1. Bioactivity

Sesquiterpenes have a very diverse biological spectrum. Their activity varies from being very toxic to exhibiting remarkable antibiotic and antitumor activities. Amongst the potent antitumor sesquiterpenes are the sesquiterpene lactones. The marked biological activity of these lactones, or more particularly of α,β -unsaturated lactones, is thought to be due to their properties as Michael acceptors, that is as potent alkylating agents⁵⁷. In this respect, tremulenolide A is a possible antitumor agent. Sesquiterpene dialdehydes seem to be involved in the natural chemical defense systems of many organisms (antifeedant activity)⁵⁸. The small amounts of compounds available in this study allowed us to test only the antifungal activity against two fungi associated with aspen: *Pheniophora polygonia*, responsible for decay and discoloration of wood, and *Ophiostoma crassivaginum*, which causes grayish to blackish sapwood stains that often develop in stored logs³. The assays was performed in the North Forestry Centre. The antifungal activity of some of the metabolites isolated from *P. tremulae* is summarized in Table 11 and is related to the effect of these metabolites on the *in vitro* growth of the fungi.

Although the antifungal activity of the tremulanes against these two fungi is weak, it does not rule out their possible biological significance, since they may be produced directly where required as antifungal agents. It is remarkable that methyl benzoate and methyl

salicylate are the most active in this series. This indicates that the resistance of *P. tremulae* in nature may reside in something as simple as its ability to metabolize aromatic compounds by methylating and oxidizing them.

Table 11 - Bioactivity of compounds produced by *P. tremulae* against aspen occurring fungi^a.

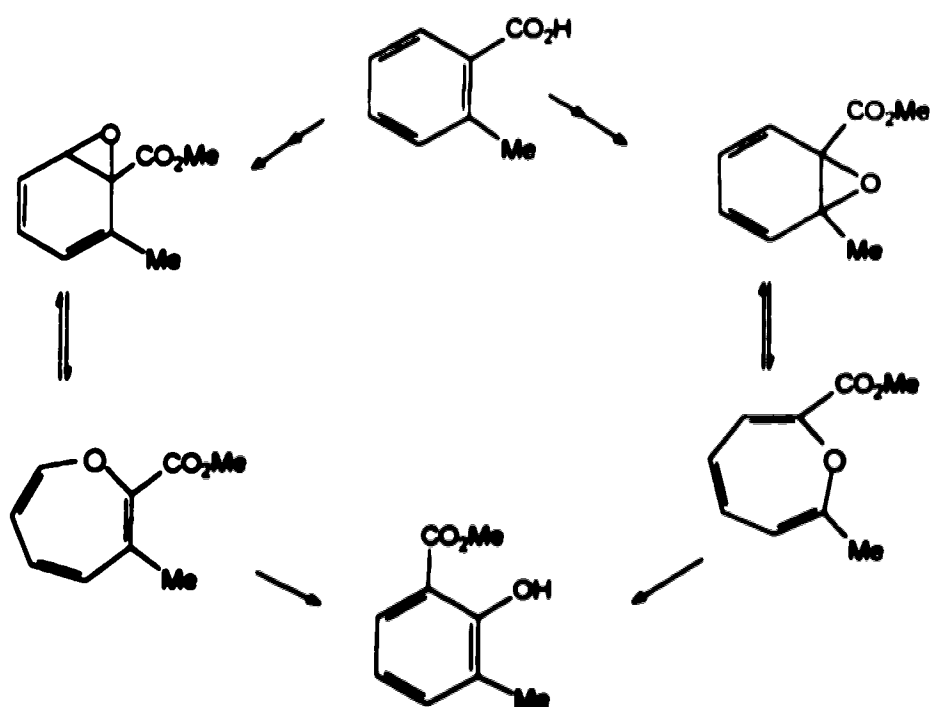
Compound	<i>P. poligonia</i>		<i>(.) crassivaginatium</i>	
	50 ppm	100 ppm	50 ppm	100ppm
Methyl benzoate (5)	+	++	-	+
Methyl salicylate (7)	+	++	-	+
2-Carbomethoxyoxepin (22)	-	+	-	-
Tremulenolide A (23)	-	+	-	+
Tremulenedial (25)	-	+	-	+
Tremulenediol A (26)	-	+	-	-
Tremulenediol B (27)	-	-	-	-

^a Reduction of growth from control: + = 25% ; ++ = 50% ; - = no effect.

This motivated further investigation of the ability of *P. tremulae* to oxidize aromatic compounds other than benzoic acid.

2.4.2 Oxidase activity

Harper *et al.* demonstrated that a number of aromatic and aliphatic carboxylic acids are converted to their methyl esters when administered to *Phellinus pomaceus*¹⁶. They showed that *o*-toluic acid was methylated by the fungus and we decided to see whether *P. tremulae* would also oxidize this compound to produce an oxepin (or substituted salicylate):



Two different experiments were conducted. In exp-1 *o*-toluic acid was incorporated into the malt extract medium (with added resin) prior to inoculation and the culture was grown for 16 days. In exp-2 *P. tremulae* was grown in 2% malt extract broth (without resin) for 16 days, after which the mycelium was filtered off, washed with water, and transferred to a citrate-phosphate buffer pH 4 containing *o*-toluic acid (procedure similar to that used by Harper *et al.*)¹⁶.

The workup of exp-1 was the same as used previously for a normal culture except that the crude extract was directly applied to a PTLC plate and the UV active zone with similar R_f to that of methyl *o*-toluate, methyl salicylate, and methyl benzoate was separated (exp-1a). The gas chromatogram and ^1H NMR spectrum were recorded. The workup of exp-2 was done after 4, 6, and 26 h of incubation. The buffer was extracted with dichloromethane and subjected to PTLC. The UV active components with similar R_f of to that methyl *o*-toluate, methyl salicylate, and methyl benzoate were separated and analyzed by GC and NMR (exp-2a). No major difference was observed in the different times of incubation, although no quantification was attempted.

The GC of exp-1a indicated the presence of two components, neither of which was methyl *o*-toluate. These two components were also present in the ^1H NMR spectrum of exp-2a in addition to the methyl *o*-toluate peaks. There was no indication of aromatic ring oxidation, since in both ^1H NMR spectra the aromatic protons were in the usual deshielding region. However, when these spectra were compared with that of methyl benzoate, a good match was found. Taking the two-component spectrum exp-1a and excluding the methyl benzoate signals, the remaining resonances were singlets at δ 2.68 (3H) and 10.28 (1H), a doublet at δ 7.81 (1H), two triplets at δ 7.56 (1H) and 7.47 (1H), and there was a signal partially hidden under the chloroform signal. The ^{13}C NMR of this mixture reveals an aldehyde carbonyl at δ 192.8. These data are consistent with *o*-tolualdehyde. Confirmation of the identity of these three components in exp-2a was obtained by GC-IR analysis. The identification of the two components in exp-1a was secured by GC. These results are summarize in Table 12. The control reaction of the citrate experiment (without added *o*-toluic acid) did not contain these compounds.

The reduction of *o*-toluic acid instead of its oxidation was surprising. However, it is known that *P. tremular* produces benzyl alcohol¹³, which may originate from reduction of benzoic acid. The absence of methyl *o*-toluate in the normal feeding experiment (exp-1)

suggests that the formation of *o*-tolualdehyde may proceed *via* reduction of the methyl ester instead of direct reduction of the carboxylic acid

Table 12 - Oxidase activity of *P. tremulae* using *o*-toluic acid

Compounds	exp-1a ^a	exp-2a ^b	control ^c
Methyl benzoate	+	+	-
Methyl <i>o</i> -toluate	-	+	-
<i>o</i> -Tolualdehyde	+	+	-

^a 2% malt extract broth, 2% w/v resin, 0.5 mM *o*-toluic acid incubated for 16 days (shake culture);

^b 20 mM citrate-phosphate buffer pH 4, 0.5 mM *o*-toluic acid, washed mycelium, incubated for 4, 6, and 26 h (shake culture);

^c same as (b) but in absence of *o*-toluic acid.

The presence of a methyl substituent α to the carboxyl group in *o*-toluic acid may be responsible for the non-recognition of this compound by the monooxygenase enzyme, which suggests that steric requirements are especially important for the enzymatic activity. The isolation of methyl benzoate in the citrate buffer experiment (exp-2) was unexpected. Although methyl benzoate is a normal metabolite of *P. tremulae* its formation was not detected in the citrate control, which may indicate that it was produced from *o*-toluic acid. However, this is pure speculation since biological demethylation is considered to be a minor pathway of secondary metabolism, but it is well established in cholesterol biosynthesis⁶¹.

Although a reductive process instead of an oxidative process took place, this ability of *P. tremulae* to metabolize aromatic compounds may have some relationship with the virulence of this pathogen.

2.4.3 Rotted aspen and conk study

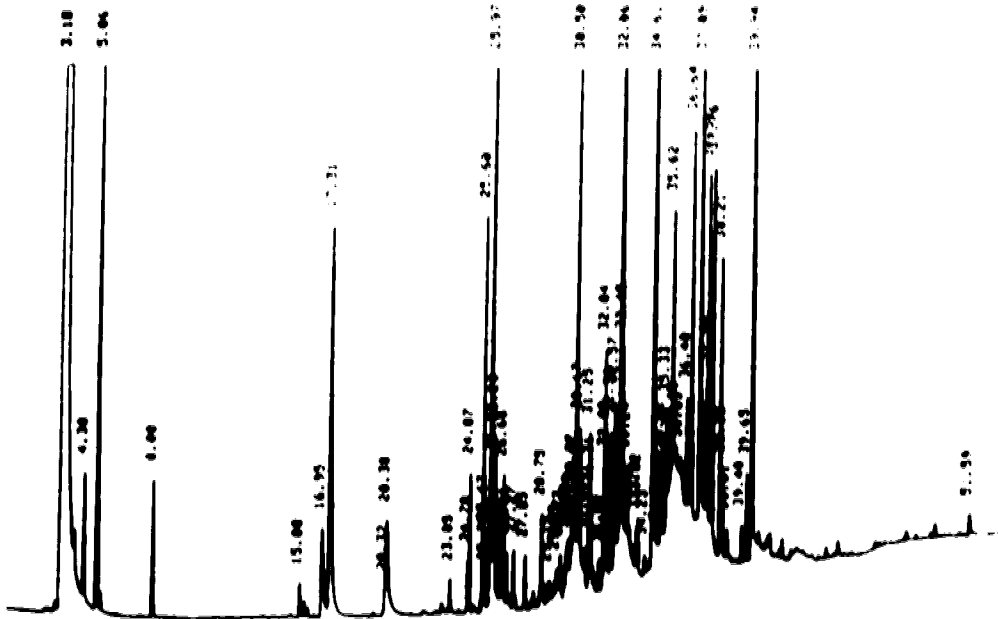
The purpose of this investigation was to analyze the extracts of rotted aspen and of *Phellinus* conks for the presence of the tremulanes. Rotted heartwood of aspen was powdered and shaken with dichloromethane for 1 day. The organic extract was separated, concentrated, and chromatographed. The fractions were analyzed by ¹H NMR. The sesquiterpenes could not be detected.

The crude rotted aspen extract was also analyzed by GC under the same conditions as for a liquid culture extract (Figure 50). The majority of the rotted wood extract peaks were identified by GC-MS, as shown in Figure 51. None of the peaks corresponds to any of the tremulanes. Methyl benzoate and methyl salicylate were detected. A molecular weight array was also examined, but no match was found for the sesquiterpenes.

The conk extract showed only three spots in the TLC corresponding to ergosterol peroxide, some di or triglycerides, and long chain fatty acids, as judged by ¹H NMR and HREIMS.

The absence of the tremulanes in the infected aspen and conks does not necessarily mean that they are not formed at all in these conditions. It may be that their formation occurs at a specific stage of growth or that they are formed in very small amounts compared to the detected compounds.

Liquid culture



methyl benzoate: $t_R = 16.8$

methyl salicylate: $t_R = 20.2$

tremulenolide A: $t_R = 39.4$

tremulenodiols A and B: $t_R = 25.9, 30.4, 37.0, 39.9$

(the diols apparently decompose in the column)

Aspen

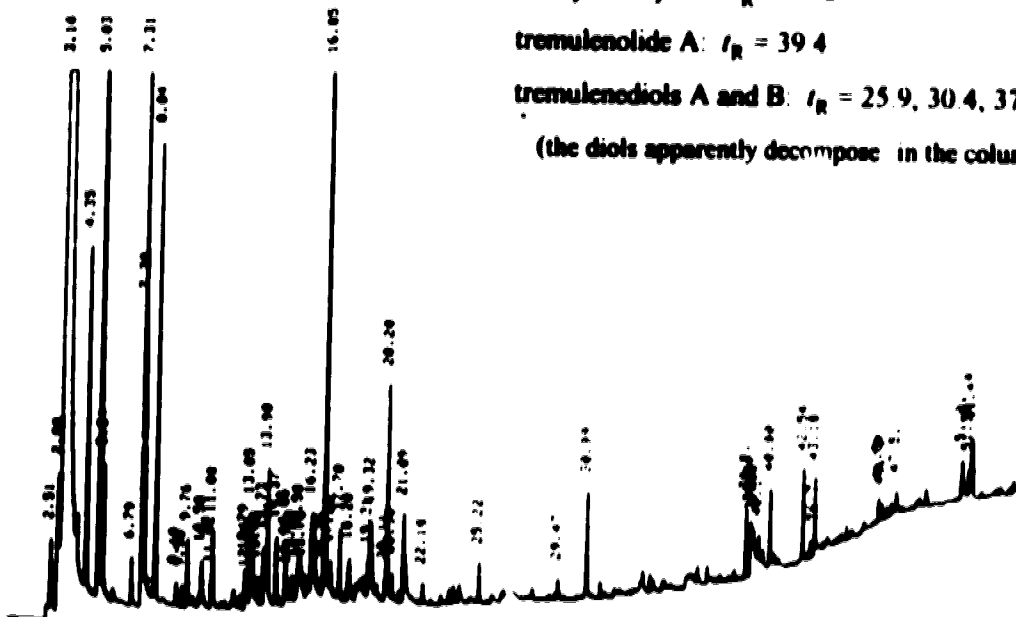


Figure 50 - GC of rotted aspen and liquid culture extract of *P. tremular*.

File: nov1b Creation Date: 11/3/93 Time: 8:14:05 Type: Lo Res Mass Data (PeakTop)
 File: R: Cruz Aspen 1 3µL on DB-5 50(2) to 260 at 5 d/m
 Desc: Res=1000 ScanP/s=20 Thresh=10 PeakWidth=10 MultWidth=4
 Delay=0.30 Int Start Scan Rate=1.0 (100%)
 Local Start Sol Delay=120.00 Fil Delay=0.00 Timed to = 1.00.00

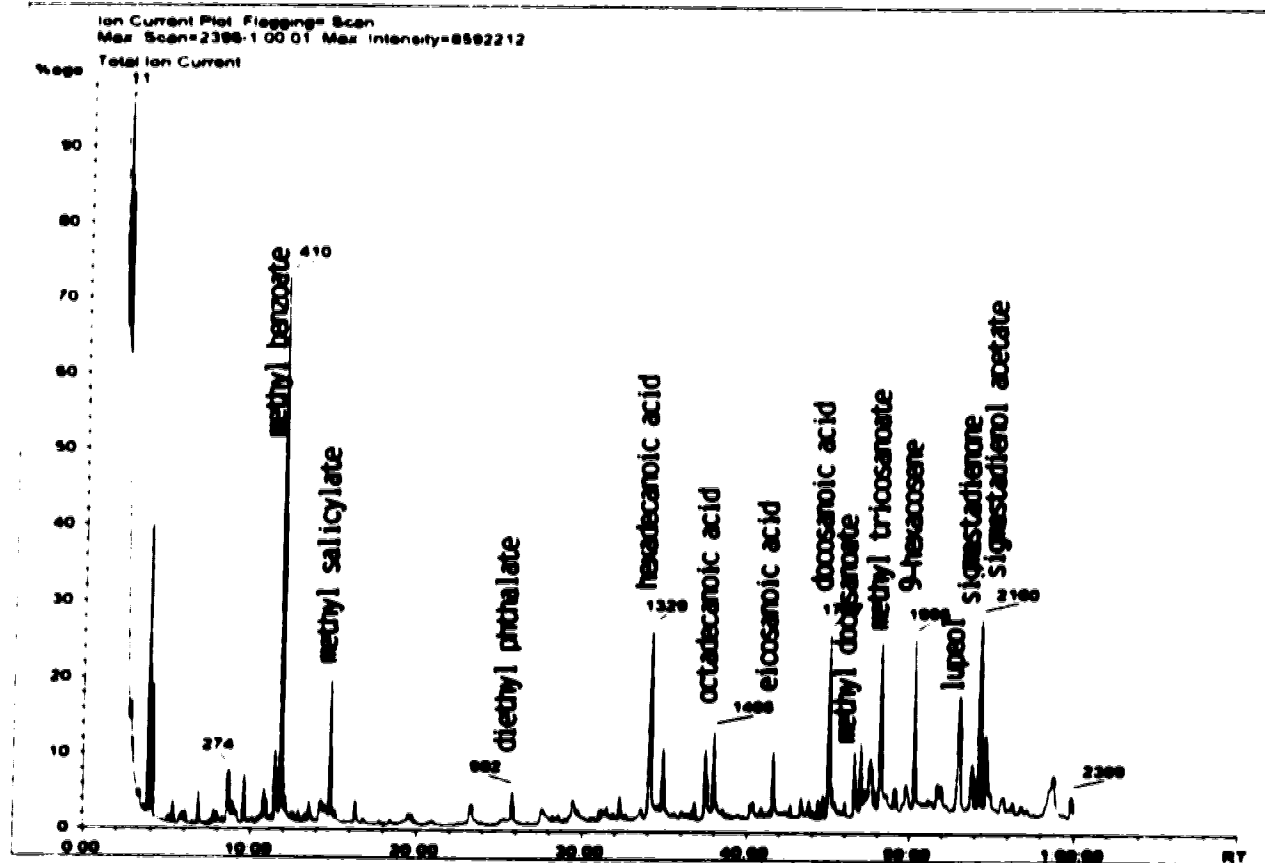


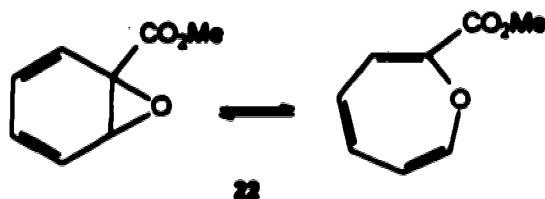
Figure 51 - GC-MS analysis of rotted aspen extract.

III. CONCLUSIONS

Our major goal in conducting this work was to provide some background information about the secondary metabolites of the fungus *Phellinus tremulae*. This was accomplished with the isolation of several new natural products including the compound postulated to be the biosynthetic precursor of methyl salicylate, 2-carbomethoxyoxepin, and a new group of sesquiterpenes possessing a previously unreported carbon skeleton, the tremulanes.

These metabolites were isolated along with two known metabolites from *P. tremulae* which are methyl benzoate and methyl salicylate. The volatility of these esters led us to study milder workup conditions which resulted in the utilization of the synthetic adsorbent DIAION HP 20 resin, a highly porous polymer of large surface area²⁴. This resin proved to be very efficient in adsorbing organic molecules from aqueous medium, simplifying considerably the harvest of liquid cultures. The metabolites extracted from liquid medium with added resin were similar to those extracted from liquid medium without resin.

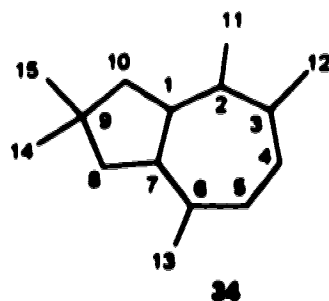
We showed that *P. tremulae* metabolizes benzoic acid to produce methyl salicylate and that this process involves the intermediacy of the arene oxide valence tautomer 2-carbomethoxyoxepin (22).



This result shows the pathway followed by *P. tremulae* to biosynthesize methyl salicylate and reveals that it indeed parallels the biosynthesis of salicylic acid in plants, since both methyl salicylate and salicylic acid are formed from a common biosynthetic

the systemic acquired resistance (SAR) that a plant develops in response to pathogen infection, we suggest that the esterification of benzoic acid may be a strategy used by *P. tremulae* to block the production of salicylic acid (a potential signal molecule in SAR) by the tree

The structure elucidation of the tremulanes (**34**) was mainly based on spectroscopic data and has been confirmed by X-ray crystallographic studies on tremulenolide A. Chemical transformations on tremulenediol A and tremulenediol gave tremulenolide A and tremulenediol B, respectively, proving the structural interrelation of these tremulanes. CD studies on tremulenediol A indicated that the absolute stereochemistry at C-3 is *S*, which dictates the same stereochemistry for the remaining chiral centers, based on their relative stereochemistry. This suggests a common biogenesis of these compounds. The biosynthetic results obtained for the tremulane sesquiterpenes are interesting. The labelling pattern is explained in terms of two possible mechanisms, one involving cyclization-rearrangement of a farnesyl precursor *via* humulene, and another involving condensation-cyclization-rearrangement of geranyl and dimethylallyl precursors. In both mechanisms migration of one of the *geminal* methyl groups is invoked. The establishment of the absolute stereochemistry allowed us to propose the stereochemical course of the tremulane biosynthesis which accounts for the chirality at the different centers.



Analysis of *Phellinus* conks and infected aspen shows that the tremulanes are not present in the diseased wood, at least in significant amounts. Bioassays indicate weak activity of the tremulanes and moderate activity of methyl benzoate and methyl salicylate against two aspen occurring fungi. The investigation on the oxidative ability of *P. tremulae* towards *o*-toluic acid reveals that a reductive process takes place leading to the formation of *o*-tolualdehyde in addition to the expected methyl *o*-toluate. The citrate buffer assay proved to be an efficient procedure to conduct substrate incorporation experiments since it allows us to follow more accurately the substrate transformations without interference of the normal metabolites produced in conventional medium.

The ability of *P. tremulae* to metabolize aromatic compounds may have some relationship with the virulence of this pathogen.

IV. EXPERIMENTAL

High resolution electron impact mass spectra (HREIMS) were recorded on a Kratos AEI MS-50 mass spectrometer. Chemical ionization mass spectra (CIMS) were obtained using a Kratos AEI MS-12 mass spectrometer with ammonia as the reagent gas. The data were processed using DS-55 software and a Nova-4 computer or Maspec data system software and a PC 386 computer. Fourier transform infrared (FTIR) spectra were recorded on a Nicolet 7199 FTIR, Nicolet MX-1 FTIR, Nicolet 750 FTIR, and on a Bruker IFS 113v FTIR spectrometer. Nuclear magnetic resonance (NMR) spectra (^1H and ^{13}C) were obtained on Varian Unity-500 spectrometer and/or Bruker WH-300, WM-360, or WH-400 spectrometers with either Aspect 2000 or Aspect 3000 computer systems. Carbon-13 multiplicities were determined using spin echo *J*-modulated experiments (APT, Attached Proton Test)^{25b}. Methyl and methine groups are shown as signals possessing opposite phase with respect to the deuteriochloroform signal, whereas methylene, quaternary, and carbonyl carbons appear in phase. Nuclear Overhauser Enhancement (NOE)^{34b} experiments were determined in the difference mode in which a control (unsaturated) spectrum was computer-subtracted from the irradiated spectrum after Fourier Transformation. Positive enhancements appear as signals possessing opposite phase with respect to the irradiated signal. Correlated Spectroscopy (COSY)^{25a} spectra were obtained on a Bruker WM-360 or WH-400. The following experiments were recorded on a Varian Unity-500 spectrometer: Heteronuclear Multiple Quantum Coherence (HMQC)^{25c}, Heteronuclear Multiple Bond Coherence (HMBC)^{38c}, Nuclear Overhauser Enhancement and Exchange Spectroscopy (NOESY)^{34b}, and Incredible Natural Abundance Double Quantum Transfer Experiment (INADEQUATE)^{56b}. Long-range CH correlations were established using the HMBC experiment optimized for $^nJ_{\text{CH}} = 10$ Hz. All NMR spectra were recorded in CDCl_3 solution. ^1H chemical shifts and coupling constants are reported as if they are first order. CDCl_3 chemical shift was used as

reference for ^1H and ^{13}C chemical shifts having tetramethylsilane as an internal standard. Differential NOE data are reported for signals exhibiting calculated values above 3%. Ultraviolet (UV) spectra were obtained on a Hewlett Packard 8450A diode array spectrophotometer and optical rotations in a Perkin Elmer 241 polarimeter. Circular dichroism (CD) spectra were measured on a JASCO SS-20-2 spectropolarimeter and are reported in molar ellipticity $[\theta]$ units. Gas chromatographic (GC) analyses were carried out on a Varian 3700 Gas Chromatograph using He as the carrier gas and equipped with flame ionization detector and a 50 m PONA column. GC-MS spectra were recorded on a Varian Vista 6000 Gas Chromatograph using He as the carrier gas and equipped with a 30 m DB-1 column and a VG 7070 mass spectrometer. GC-IR analyses were performed on a 5965 Hewlett-Packard IRD apparatus using He as the carrier gas and equipped with a 25 m Ultra 2 crosslinked column. Melting points are uncorrected and were determined on a Thomas model 40 melting point apparatus. Universal Scientific Incorporated silica gel 60 (40 microns) was used for flash chromatography. Preparative thin layer chromatography (PTLC) was performed on E. Merck precoated 20 x 20 glass plates of silica gel 60 F-254 or on prepared 20 x 20 glass plates using Aldrich silica gel for TLC with fluorescent indicator. Analytical thin layer chromatography (TLC) was carried out on cut sections of E. Merck precoated aluminium sheets of silica gel 60 F-254. Ultraviolet active materials were detected by visualization under a UV lamp (254 nm). The TLC plates were then dipped in a vanillin solution (2 g of vanillin, 5 mL of concentrated H_2SO_4 , 250 mL of 95% ethanol) for a few seconds and the spots were visualized by gentle heating over a hot plate. Liquid media were prepared using BactoTM malt extract broth (DIFCO Laboratories) and HP-20 Diaion resin (Mitsubishi Chemical Industries Ltd., supplied by TCI America - 9211 N. Horbagate St - Portland, OR 97203). Feeding experiments were performed with benzoic acid- α - ^{13}C , $[1\text{-}^{13}\text{C}]$ -sodium acetate, $[2\text{-}^{13}\text{C}]$ -sodium acetate, and $[1,2\text{-}^{13}\text{C}_2]$ -sodium acetate purchased from ICON Isotopes, ICON Services. The hydrogen bonding IR study on tremulenediol B (27) was performed in Prof. John E. Bertie's

to light petroleum (bp 60-68°C) All solvents were distilled prior to use. Molecular formulas of title compounds were established by HREIMS unless otherwise noted.

4.1. Growth of *Phellinus tremulae*

Cultures of *P. tremulae* (strain NOF 1464) were obtained from Dr. Y. Hiratsuka, Forestry Canada, Northern Forestry Centre, Edmonton, and are deposited at the University of Alberta Microfungus Herbarium (UAMH 7005). Plate cultures of *P. tremulae* were blended in a Waring blender with sterile water and ca. 30 mL aliquots were inoculated into 4-liter erlenmeyer flasks charged with 2 L of sterile malt extract medium with the following composition:

- **Medium A (with resin):** 40 g of malt extract broth DIFCO, 40 g of DIAION HP 20[®] resin^{24a} and 2 L of redistilled water;
- **Medium B (without resin):** 40 g of malt extract broth DIFCO and 2 L of redistilled water.

The final pH of the medium was 4.7. The cultures were shaken at room temperature for 16 days.

4.2. Isolation of the metabolites

Liquid cultures with added resin (medium **A**) - The culture broth was separated from the resin and mycelium by vacuum filtration. Resin and wet mycelium were transferred to a sintered-glass funnel and extracted with dichloromethane (3 x 100 ml. for each 2-L. culture). The organic extracts were combined and dried over anhydrous MgSO_4 or Na_2SO_4 . Evaporation of the solvent under reduced pressure afforded 0.5 g/L of a crude organic extract (dark yellow oil).

Liquid cultures without resin (medium **B**) - The culture broth was separated from the mycelium by vacuum filtration and extracted with dichloromethane (3 x 200 ml. for each 2-L. culture). After this extraction the broth was concentrated to *ca.* 20% of its original volume, under reduced pressure, and reextracted with dichloromethane. The organic extract was dried over anhydrous MgSO_4 or Na_2SO_4 and the solvent evaporated under reduced pressure to afford 77 mg/L of non-concentrated broth extract and 20 mg/L of concentrated broth extract (dark yellow oil). The composition of both extracts (media **A** and **B**) are identical according to TLC analysis.

Flash chromatography of the crude organic extract was carried out using a stepwise gradient of 0.5 to 5% (v/v) MeOH in CH_2Cl_2 . Fractions of similar composition, as determined by TLC and ^1H NMR, were pooled (Figure 3). Further purification is described for the individual components.

Methyl salicylate (7)

Methyl salicylate was eluted as a colorless liquid which exuded the characteristic smell of wintergreen. TLC $R_f = 0.5$ in $\text{CH}_2\text{Cl}_2/\text{hexanes}/\text{MeOH}$ (50:50:1); ^1H NMR (360 MHz, CDCl_3) δ 10.77 (1H, s, OH), 7.83 (1H, bd, $J = 8$ Hz, H-6), 7.45 (1H, bt, $J = 8$ Hz, H-4), 6.98 (1H, bd, $J = 8$ Hz, H-3), 6.87 (1H, bt, $J = 8$ Hz, H-5), 3.94 (3H, s, OMe); **homonuclear decoupling** (irradiation effect): δ 7.83 \rightarrow δ 7.45 (bt to t, $J = 8$ Hz), 6.87 (bt to bd, $J = 8$ Hz); δ 7.50 \rightarrow δ 7.83 (bd to d, $J = 8$ Hz), 6.98 (bd to d, $J = 1$ Hz), 6.87 (bt, to bd, $J = 8$ Hz)

Methyl benzoate (5)

Methyl benzoate was eluted right after methyl salicylate as a colorless liquid; TLC: $R_f = 0.5$ in $\text{CH}_2\text{Cl}_2/\text{hexanes}/\text{MeOH}$ (50:50:1); ^1H NMR (400 MHz, CDCl_3): δ 8.05 (2H, dd, $J = 8, 1$ Hz, H-2, H-6), 7.56 (1H, td, $J = 8, 1$ Hz, H-4), 7.45 (2H, td, $J = 8, 1$ Hz, H-3, H-5), 3.92 (3H, s, OMe).

2-Carbomethoxyezepin (22)

Compound 22 was eluted as a yellow liquid; TLC: $R_f = 0.4$ in $\text{CH}_2\text{Cl}_2/\text{hexanes}/\text{MeOH}$ (50:50:1). UV (MeOH) 253 nm (ϵ 2130), 313 (ϵ 1860); FTIR (CHCl_3 cast): 2952, 2929 (C-H), 1728 (C=O, ester), 1615 (C=C) cm^{-1} ; ^1H NMR (360 MHz, CDCl_3): δ 6.86 (1H, d, $J = 6$ Hz, H-3), 6.47 (1H, dd, $J = 10, 6$ Hz, H-5), 6.35 (1H, dd, $J = 10, 6$ Hz, H-4), 5.94 (1H, d, $J = 5$ Hz, H-7), 5.78 (1H, dd, $J = 6, 5$ Hz, H-6), 3.82 (3H, s, OMe); **homonuclear decoupling** (irradiation \rightarrow effect): δ 6.86 \rightarrow δ 6.35 (dd to d, 10 Hz); δ 6.47 \rightarrow δ 6.35 (dd to d, $J = 6$ Hz), 5.78 (dd to d, $J = 5$ Hz); δ 6.35 \rightarrow δ 6.86 (d to s), 6.47 (dd to d, $J = 6$ Hz); δ 5.94 \rightarrow δ 5.78 (dd to d, $J = 6$ Hz); δ 5.78 \rightarrow δ 6.47 (dd to d, $J = 10$), 5.94

(d to s), ^{13}C NMR (75 MHz, CDCl_3): δ 163.3 (s, C=O), 137.0 (d, C-7), 133.6 (d, C-5), 132.9 (s, C-2), 128.6 (d, C-4), 123.9 (d, C-3), 118.1 (d, C-5), 52.4 (q, OMe). INAPT (300 MHz): δ 6.86 \rightarrow δ 163.3, 132.9, δ 5.94 \rightarrow δ 133.6, 132.9, 128.5, HMQC (125, 500 MHz): δ 6.86 \rightarrow δ 123.9, δ 6.47 \rightarrow δ 133.6, δ 6.35 \rightarrow δ 128.6, δ 5.94 \rightarrow δ 137.0, δ 5.78 \rightarrow δ 118.1; δ 3.82 \rightarrow δ 52.4, HREIMS m/z 152.0474 (M^+ , 100%), calc for $\text{C}_8\text{H}_8\text{O}_3$: 152.0474), 121 (M^+ - OMe, 8%), 93 (M^+ - CO_2Me , 19%), 77 (C_6H_5^+ , 21%), 65 (C_5H_5^+ , 82%). The ^1H NMR spectrum was identical with that of an authentic sample kindly supplied by Prof. G. Berchtold.

Tremulenolide A (23)

Compound 23 was eluted as a colorless oil and was recrystallized from hexanes to give colorless crystals; mp 110-112°C; TLC: R_f 0.4 (CH_2Cl_2); UV (MeOH) 236 nm (ϵ 8270); $[\alpha]_D^{25} +110.7^\circ$ (c 0.14, MeOH); CD (0.0012 M, MeOH) $[\theta]_{252} +17820$, FTIR (CHCl_3 cast): 2953, 2924, 2866, 2858 (C-H), 1753 (C=O), 1673 (C=C) cm^{-1} ; ^1H NMR (400 MHz, CDCl_3) data are listed in Table 5, homonuclear decoupling (irradiation effect): δ 3.21 \rightarrow δ 3.09 (m to m), 2.46 (ddd to dd, $J = 19, 4.5$ Hz); 2.13 (pd to p, $J = 7.5$ Hz), 1.50 (d to s); δ 3.09 \rightarrow δ 3.21 (tm to bt, $J = 10$ Hz), 4.35 (dd to d, $J = 8.5$ Hz), 3.63 (dd to d, $J = 8.5$ Hz), 2.88 (dd to d, $J = 19$ Hz), 2.46 (ddd to bd, $J = 19$ Hz), 1.84 (m to m), 1.73 (dddd to ddd, $J = 13, 6.5, 1.5$ Hz); δ 2.88 \rightarrow δ 3.09 (m to m), 2.46 (ddd to m); δ 2.46 \rightarrow δ 3.21 (m to m), 3.09 (m to m), 2.88 (dd to bs), δ 2.13 \rightarrow δ 3.21 (tm to tt, $J = 10, 3.5$ Hz), 2.05 (m to m), 1.46 (m to m), 0.95 (d to s); δ 1.84 \rightarrow δ 3.09 (m to m), 2.05 (m to m), 1.73 (m to m), 1.46 (m to m); δ 1.73 \rightarrow δ 3.09 (m to m), 2.05 (m to m), 1.84 (m to m), 1.46 (m to m); δ 0.95 \rightarrow δ 2.13 (pd to dd, $J = 9, 2$ Hz); differential NOE: 14-Me to H-10 α 8.7%, H-7 to H-6 4.5%, H-12 α to H-3 5.6%, 13-Me to H-3 10%; ^{13}C NMR (75 MHz, CDCl_3) data are listed in Table 4; HMQC (125, 500 MHz): δ 70.9 \rightarrow δ 4.35, 3.63;

δ 48.4, δ 2.88, 2.46, δ 45.5, δ 3.21, δ 44.9, δ 1.50, δ 41.0, δ 3.09, δ 32.9, δ 1.46, 2.05, δ 32.7, δ 2.13, δ 29.0, δ 1.13, δ 28.1, δ 1.84, 1.73, δ 27.3, δ 0.99, δ 17.7, δ 0.95, **HMBC** (125, 500 MHz): δ 4.35, δ 171.5, 120.7, 41.0, δ 3.63, δ 171.5, 41.0, 28.1, δ 3.21, δ 161.5, 120.7, 44.9, 32.9, 17.7, δ 2.88, δ 161.5, 120.7, 45.5, 27.2, 29.0, δ 2.46, δ 161.5, 120.7, 29.0, δ 2.13, δ 161.5, 32.9, 28.1, 17.7, δ 2.05, δ 41.0, 32.7, 28.1, 17.7, δ 1.84, δ 120.7, 41.0, 32.9, δ 1.50, δ 161.5, 48.4, 45.5, 37.2, 32.7, 29.0, 27.3, δ 1.13, δ 48.4, 44.9, 37.2, 27.3, δ 0.99, δ 48.4, 44.9, 37.2, 29.0, δ 0.95, δ 45.5, 32.7, **HREIMS** m/z 234.1616 (M^+ , 18%, calcd for $C_{15}H_{22}O_2$ 234.1613), base peak at m/z 219.1377 [$M - CH_3$] $^+$.

Ozonolysis of tremulenolide A

Compound **23** (~6 mg) was dissolved in a mixture of dichloromethane-methanol (1:1, 4 mL) and cooled in an acetone-dry ice bath. Ozone was bubbled into the reaction mixture until a light blue color remained. A few drops of dimethyl sulfide were added and the reaction mixture was allowed to warm to room temperature. PTLC of the concentrated mixture (benzene/acetone/AcOH, 75:25:1) afforded an UV active compound (**23a**); FTIR (CH_2Cl_2 cast): 3200 (O-H), 2958, 2933, 2872 (C-H), 1780-1730 (C=O) cm^{-1} ; 1H and ^{13}C NMR (400 MHz, $CDCl_3$) data are listed in Table 6, **HREIMS** obsd 266.1515 (14%, calcd for $C_{15}H_{22}O_4$ 266.1518, m/z 182.0925 (13%, $C_{10}H_{14}O_3$), 167.1066 (13%, $C_{10}H_{15}O_2$), 165.1272 (13%, $C_{11}H_{17}O$), 152.1197 (15%, $C_{10}H_{16}O$), 143.0698 (18%, $C_7H_{11}O_3$), 139.1118 (62%, $C_9H_{15}O$), 112.0883 (100%, $C_7H_{12}O$).

Tremulenolide B (24)

Compound 24 was eluted as a colorless oil and was recrystallized from hexanes to give colorless needles. TLC: R_f 0.4 (CH_2Cl_2). FTIR (CHCl_3 , cast) 2953, 2922, 2853 (C-H), 1775 (C=O, ester) cm^{-1} ; ^1H NMR (400 MHz, CDCl_3) data are listed in Table 5, **homonuclear decoupling** (irradiation effect): δ 5.50 \rightarrow δ 3.16 (m to m), δ 4.36 \rightarrow δ 4.09 (dd to d, $J = 3.2$ Hz), 2.71 (m to m), δ 4.09 \rightarrow δ 4.36 (d, $J = 7$ Hz), 2.71 (m to m), δ 3.16 \rightarrow δ 5.50 (d to s), 1.81 (m to m), 1.72 (dd to d, $J = 12.5$), 1.37 (dd to d, $J = 12.5$ Hz); δ 2.71 \rightarrow δ 4.36 (dd to d, $J = 9.5$ Hz), 4.09 (dd to d, $J = 9.5$ Hz), δ 0.85 \rightarrow δ 1.81 (m to m), ^{13}C NMR (125 MHz, CDCl_3) data are listed in Table 4; HMQC (125, 500 MHz): δ 143.5 \rightarrow δ 5.50; δ 71.9 \rightarrow δ 4.36, 4.09; δ 48.0 \rightarrow δ 3.16; δ 45.8 \rightarrow δ 3.63, δ 42.2 \rightarrow δ 1.72, 1.37; δ 38.7 \rightarrow δ 2.71; δ 33.0 \rightarrow δ 1.81; δ 29.4 \rightarrow δ 1.10; δ 28.8 \rightarrow δ 1.92, 1.50; δ 28.4 \rightarrow δ 1.43; δ 27.1 \rightarrow δ 1.06; δ 19.3 \rightarrow δ 0.85; HREIMS obsd 234.1619, calcd for $\text{C}_{15}\text{H}_{22}\text{O}_2$ 234.1618, base peak at m/z 219.1387 [$\text{M} - \text{CH}_3$] $^+$.

Tremulenolial dibenzyl acetal (25)

The fractions eluted with 1.5% MeOH in CH_2Cl_2 exhibited an aldehydic signal at δ 9.72 twice as intense as the alkenic proton signal (δ 5.56). The unstable dialdehyde (25, 63 mg dissolved in 8 mL of CHCl_3) was isolated in the form of the diacetal by treatment with BnOH (78 mg dissolved in 2 mL of CHCl_3) and traces of TsOH, at room temperature. Flash chromatography of the crude reaction mixture (hexanes: CH_2Cl_2 , 3:1) afforded 25a as a colorless oil. TLC: R_f 0.6 (hexanes: CH_2Cl_2 , 1:1), FTIR (CH_2Cl_2 , cast): 2950, 2925, 2862 (C-H), 1454 (C=C), 1094, 1075 (C-O) cm^{-1} ; ^1H NMR (400 MHz, CDCl_3) data are listed in Table 5; **homonuclear decoupling** (irradiation effect): δ 5.47 \rightarrow δ 2.93 (m to m); δ 5.20 \rightarrow δ 3.52 (dd to d, $J = 8$ Hz); δ 4.98 \rightarrow δ 2.48 (m to m); δ 3.52 \rightarrow δ 5.20 (d to s), 2.48 (m to m); δ 2.93 \rightarrow 5.47 (d to s), 1.83 (m to m), 1.73 (dd to d, $J =$

13 Hz), 1.37 (dd to d, $J = 13$ Hz); δ 2.48 – δ 4.98 (d to s), 3.52 (dd to d, $J = 5.2$ Hz), 1.84 (m to m), 1.52 (m to m), δ 1.84/1.83 – δ 2.93 (m to bt, $J = 7$ Hz), 2.48 (m to bt, $J = 7.5$ Hz), 1.52 (m to m), 1.44 (m to m), 0.83 (d to s); δ 1.73 – δ 2.93 (m to m), 1.37 (dd to d, $J = 9$ Hz); δ 1.37 – δ 2.93 (m to m), 1.73 (dd to d, $J = 7.5$ Hz); δ 0.83 – δ 1.83 (m to m), **differential NOE**: H-2 to H-3 11.4%, H-2 to H-10 14.3%, H-2 to H-11 3.4%, H-3 to H-12 4.1%, **^{13}C NMR** (75 MHz, CDCl_3) data are listed in Table 4; **HMQC** (125, 500 MHz): δ 142.0 – δ 5.47, δ 107.9 – δ 4.98; δ 107.5 – δ 5.20; δ 69.9 – δ 4.88, 4.63; δ 69.1 – δ 4.85, 4.53; δ 49.2 – δ 3.52; δ 48.4 – δ 2.93; δ 47.9 – δ 2.48; δ 43.2 – δ 1.73, 1.37; δ 34.0 – δ 1.83; δ 29.6 – δ 1.44; δ 29.3 – δ 1.09; δ 27.9 – δ 1.02; δ 27.5 – δ 1.84, 1.52; δ 18.5 – δ 0.83; **HMBC** (125, 500 MHz): δ 5.47 – δ 139.5, 49.2, 43.2, 42.1; δ 5.20 – δ 139.5, 107.9, 69.9, 49.2; δ 4.98 – δ 107.5, 69.1, 49.2; δ 4.88 – δ 107.5, δ 4.85 – δ 107.9; δ 4.63 – δ 107.5; δ 4.53 – δ 107.9; δ 3.52 – δ 142.0, 139.5, 107.5, 48.4, 47.9, 27.5; δ 1.84 – δ 107.9, 49.2, 47.9, 34.0, 29.6; δ 1.83 – δ 43.2, 29.6, 27.5, 18.5; δ 1.73 – δ 142.0, 139.5, 48.4, 42.1, 27.9; δ 1.44 – δ 48.4, 47.9, 34.0, 27.5, 18.5; δ 1.37 – δ 48.4, 42.1, 34.0, 29.3, 27.9; δ 1.09 – δ 142.0, 43.2, 42.1, 27.9; δ 1.02 – δ 142.0, 43.2, 42.1, 29.3; δ 0.83 – δ 48.4, 34.0, 29.6; **NOESY** (500 MHz) data summarized in Scheme 8; **HREIMS** m/z 325.2157 (1%, $\text{C}_{22}\text{H}_{29}\text{O}_2$, $[\text{M} - \text{OBn}]^+$), 205.1569 (69%, $\text{C}_{14}\text{H}_{21}\text{O}$); **CIMS** (NH_3) m/z 450 (14%, $[\text{M} + 18]^+$, $\text{C}_{29}\text{H}_{36}\text{O}_3$), 325 (100%).

Tremulenolol A (26)

Compound 26 was eluted as a colorless oil and recrystallized from hexanes to give colorless crystals; mp 95-97°C; TLC: R_f 0.4 (benzene: acetone:AcOH, 75:25:1); $[\alpha]_D^{25} +41.7^\circ$ (c 0.24, MeOH); UV (MeOH) 212 nm (ϵ 4350); CD (0.002 M, MeOH) $[\theta]_{210} +4620$; FTIR (KBr): 3310 (O-H), 2952, 2927, 2899, 2865 (C-H), 1461 (C=C), 1030, 1024 (C-O) cm^{-1} ; **^1H NMR** (400 MHz, CDCl_3) data are listed in Table 5; **homonuclear**

decoupling (irradiation → effect): δ 4.24 → δ 3.83 (d to s), δ 4.01 → δ 3.61 (dd to d, $J = 5$ Hz); δ 3.83 → δ 4.24 (d to s), 3.10 (tm to tm), δ 3.61 → δ 4.01 (dd to d, $J = 10$ Hz), 2.53 (m to m); δ 3.10 → δ 1.93 (bd to bd, $J = 15.5$), 1.52 (ddd to bd, $J = 12.5$ Hz), 1.38 (dd to d, $J = 12.5$ Hz); δ 2.53 → δ 4.01 (dd to d, $J = 9$ Hz), 3.61 (dd to d, $J = 9$ Hz), 1.83 (dd to d, $J = 12$ Hz), 1.59 (dd to d, $J = 11.5$ Hz); δ 2.29 → δ 1.93 (bd to bs), 1.52 (ddd to dd, $J = 12.5, 8$ Hz); δ 0.82 → δ 1.76 (m to m); **^{13}C NMR** (75 MHz, CDCl_3) data are listed in Table 4; **HMQC** (125, 500 MHz): δ 65.6 → δ 4.24, 3.83; δ 63.2 → δ 4.01, 3.61, δ 48.0 → δ 2.29, 1.93; δ 46.0 → δ 3.10; δ 45.5 → δ 1.52, 1.38, δ 45.4 → δ 2.53, δ 32.6 → δ 1.83, 1.60; δ 31.6 → δ 1.76; δ 28.5 → δ 1.07; δ 26.9 → δ 0.87; δ 22.5 → δ 1.80, 1.59; δ 11.6 → δ 0.82; **HMBC** (125, 500 MHz): δ 4.24 → δ 145.6, 132.3, 45.4; δ 4.01 → δ 132.3, 45.4, 22.5; δ 3.83 → δ 145.6, 132.3, 45.4; δ 3.61 → δ 132.3, 45.4, 22.5; δ 2.53 → δ 32.6, 22.5; δ 2.29 → δ 145.6, 132.3, 46.0, 45.5, 37.0, 26.9; δ 1.93 → δ 145.6, 132.3; δ 1.76 → δ 22.5; δ 1.61 → δ 22.5; δ 1.59 → δ 32.6; δ 1.52 → δ 145.6, 48.0, 37.0, 26.9; δ 1.38 → δ 46.0, 37.0, 31.6, 28.5, 26.9; δ 1.07 → δ 48.0, 45.5, 37.0, 26.9; δ 0.87 → δ 48.0, 45.5, 37.0, 28.5; δ 0.82 → δ 46.0, 31.6; **NOESY** (500 MHz) data are listed in Table 7; **HREIMS** m/z obsd 238.1932 (0.2%, M^+ , calcd for $\text{C}_{15}\text{H}_{26}\text{O}_2$ 238.1931), 220.1827 (27%, $\text{C}_{15}\text{H}_{24}\text{O}$, [$\text{M}^+ - \text{H}_2\text{O}$]), 189.1641 (100, $\text{C}_{14}\text{H}_{21}$);

Tremulenediol B (27)

Compound 27 was eluted as a colorless oil containing ca. 15% of 26; **TLC**: R_f 0.4 (benzene:acetone:AcOH, 75:25:1); **FTIR** (CDCl_3 , cast): 3300 (O-H), 2951, 2916, 2871, 2862 (C-H), 1461, 1450 (C=C), 1044, 1027 (C-O) cm^{-1} ; **^1H NMR** (400 and 500 MHz, CDCl_3) data are listed in Table 5; **homonuclear decoupling** (irradiation → effect): δ 5.32 → δ 2.94 (dddd to ddd, $J = 11.5, 10, 6.5$ Hz); δ 3.90 → δ 3.64 (dd to d, $J = 5$ Hz), 2.85 (ddd to dd, $J = 5, 4$ Hz); δ 2.94 → δ 5.32 (d to s), 1.88 (ddq to dq, $J = 7.5, 7.5$ Hz), 1.61 (dd to d, $J = 11.5$ Hz), 1.32 (dd to d, $J = 11.5$ Hz); δ 2.85 → δ 3.90 (dd to d, $J = 11$ Hz),

3.64 (dd to d, $J = 11$ Hz), 1.70 (m to m); δ 1.88 \leftrightarrow δ 2.94 (dddd to ddd, $J = 11.5, 6.5, 2.5$ Hz), 1.34 (m to m), 0.84 (d to s); δ 1.76 \leftrightarrow δ 3.62 (dd to d, $J = 11$ Hz), 3.58 (dd to d, $J = 11$ Hz), 2.85 (ddd to dd, $J = 8.5, 5$ Hz), 1.52 (m to m); δ 0.84 \leftrightarrow δ 1.88 (ddq to dq, $J = 10, 7.5$ Hz); ^{13}C NMR (75 MHz, CDCl_3) data are listed in Table 4; HMQC (125, 500 MHz): δ 138.6 \leftrightarrow δ 5.32; δ 66.7 \leftrightarrow δ 3.62, 3.58; δ 60.8 \leftrightarrow δ 3.90, 3.64; δ 48.5 \leftrightarrow δ 2.94; δ 48.2 \leftrightarrow δ 1.70; δ 47.4 \leftrightarrow δ 2.85; δ 42.8 \leftrightarrow δ 1.61, 1.32; δ 35.7 \leftrightarrow δ 1.88; δ 30.8 \leftrightarrow δ 1.34; δ 29.5 \leftrightarrow δ 1.60, 1.52; δ 29.4 \leftrightarrow δ 1.04; δ 26.8 \leftrightarrow δ 0.98; δ 19.4 \leftrightarrow δ 0.84; HREIMS m/z 220.1824 (24%, $\text{C}_{15}\text{H}_{24}\text{O}$, $[\text{M} - \text{H}_2\text{O}]^+$), 189.1643 (100%); CIMS (NH_3) m/z 256 (1%, $[\text{M} + 18]^+$), 238 (1%, $\text{C}_{15}\text{H}_{26}\text{O}_2$), 221 (100%).

***p*-Bromobenzoylation of 26 and 27**

The di-*p*-bromobenzoates of 26 (26a, 35 mg) and 27 (27a, 16 mg) were prepared by stirring a mixture of 26 and 27 (88 mg) dissolved in CH_2Cl_2 (2 mL) with a suspension of *p*-Br-BzCl (178 mg) in CH_2Cl_2 (2 mL) and pyridine (0.8 mL) for 1 hour at room temperature. The residue was filtered off and the filtrate was evaporated to dryness. Most of the remaining *p*-Br-BzOH was removed by crystallization from hexanes. Separation of 26a and 27a was achieved by PTLC (hexanes: CH_2Cl_2 , 1:1, developed several times).

di-*p*-Bromobenzoyl derivative of 26 (26a)

TLC: R_f 0.4 (CH_2Cl_2 :hexanes, 1:1); UV (MeOH) 243 nm (ϵ 11400); $[\alpha]_D^{+6}$ (c 0.84, MeOH); FTIR (CH_2Cl_2 , cast): 2951, 2930, 2866 (C-H), 1718 (C=O), 1590 (C=C), 1268 (C-O) cm^{-1} ; ^1H NMR, (400 MHz, CDCl_3) data are listed in Table 8; homonuclear decoupling (irradiation \rightarrow effect): δ 4.82 \rightarrow δ 3.16 (bdd to ddt, $J = 11, 8, 2$ Hz); δ 4.55 \rightarrow δ 2.93 (m to bs); δ 3.16 \rightarrow δ 2.04 (bd to d, $J = 15.5$ Hz), 1.83 (m to m), 1.57 (ddd to dd, $J = 12, 2$ Hz), 1.44 (dd, bd, $J = 12$ Hz); δ 2.93 \rightarrow δ 4.55 (ABX to AB), 1.89 (dt to dd, $J = 15,$

2.5 Hz), 1.75 (ddd to dm); δ 2.35 \leftrightarrow δ 3.16 (bdd to dd, $J = 11, 8$ Hz), 2.04 (bd to bs), 1.57 (ddd to dd, $J = 12, 8$ Hz); δ 2.04 \leftrightarrow δ 3.16 (bdd to dd, $J = 11, 8$ Hz), 2.35 (dd to bs), δ 1.66 \leftrightarrow δ 1.98 (dt to t, $J = 2.5$ Hz), 1.89 (dt to dd, $J = 15, 2.5$ Hz), 1.83 (m to m); δ 1.57 \leftrightarrow δ 3.16 (bdd to bd, $J = 11$ Hz); 2.35 (dd to d, $J = 15.5$ Hz), 1.44 (dd to d, $J = 11$ Hz), δ 1.44 \leftrightarrow δ 3.16 (bdd to m), 1.57 (ddd to dd, $J = 8, 2$ Hz); δ 0.86 \leftrightarrow δ 1.83 (m to m). **^1H - ^1H -COSY (400 MHz):** δ 4.55 \leftrightarrow δ 2.93; δ 3.16 \leftrightarrow δ 2.04, 1.57, 1.44; δ 2.93 \leftrightarrow δ 1.89, 1.75; δ 2.35 \leftrightarrow δ 2.04, 1.57; δ 2.04 \leftrightarrow δ 3.16, 2.35, 0.88; δ 1.98 \leftrightarrow δ 1.89, 1.66, δ 1.89 \leftrightarrow δ 2.93, 1.98, 1.75, 1.66; δ 1.83 \leftrightarrow δ 0.86; δ 1.75 \leftrightarrow δ 2.93, 1.89, 1.66; δ 1.66 \leftrightarrow δ 1.98, 1.75, 1.89; δ 1.57 \leftrightarrow δ 3.16, 2.35, 1.44; δ 1.44 \leftrightarrow δ 3.16, 1.57; δ 0.86 \leftrightarrow δ 1.83. **^{13}C NMR (75 MHz, CDCl_3) data are listed in Table 4; HMQC (125, 500 MHz):** δ 131.7 \leftrightarrow δ 7.55; δ 131.0 \leftrightarrow δ 7.88; δ 69.0 \leftrightarrow δ 4.82; δ 63.2 \leftrightarrow δ 4.55; δ 48.3 \leftrightarrow δ 2.35, 2.04; δ 46.6 \leftrightarrow δ 3.16; δ 45.3 \leftrightarrow δ 1.57, 1.44; δ 41.3 \leftrightarrow δ 2.93; δ 31.7 \leftrightarrow δ 1.98, 1.75; δ 31.4 \leftrightarrow δ 1.83; δ 28.4 \leftrightarrow δ 1.09; δ 26.8 \leftrightarrow δ 0.88; δ 21.2 \leftrightarrow δ 1.89, 1.66; δ 11.7 \leftrightarrow δ 0.86. **HREIMS m/z** 404.1167 (0.13%), 402.1200 (0.14%, $\text{C}_{22}\text{H}_{27}\text{O}_2\text{Br}$ [M^+ -O-*p*-BrBz]), 202.1713 (100%, $\text{C}_{15}\text{H}_{22}$), 187.1485 (24%, $\text{C}_{14}\text{H}_{19}$); **CIMS (NH_3) m/z** 624 (17.4%), 622 (35.0%), 620 (17.9%, [$\text{M} + 18$] $^+$, $\text{C}_{29}\text{H}_{32}\text{O}_4\text{Br}_2$).

***di-p*-Bromobenzoyl derivative of 27 (27a)**

TLC: R_f 0.38 (CH_2Cl_2 :hexanes, 1:1); **FTIR (CH_2Cl_2 , cast):** 2952, 2925 (C-H), 1720 (C=O), 1590 (C=C), 1270 (C-O) cm^{-1} ; **^1H NMR, (400 MHz, CDCl_3) data are listed in Table 9; homonuclear decoupling (irradiation \leftrightarrow effect):** δ 3.26 \leftrightarrow δ 4.53 (d to s), 2.11 (m to m); δ 3.08 \leftrightarrow δ 5.41 (d to s), 2.04 (bq to m), 1.66 (dd to d, $J = 11$ Hz), 1.66 (dd to d, $J = 11$ Hz); δ 2.11 \leftrightarrow δ 4.30 (d to s), 3.26 (td to t, $J = 7.8$ Hz), 1.83 (m to m), 1.39 (m to m); δ 2.04 \leftrightarrow δ 3.08 (m to m), 0.89 (d to s); δ 1.66 \leftrightarrow δ 3.08 (m to m), 1.37 (dd to d, $J = 11$ Hz); δ 0.89 \leftrightarrow δ 2.04 (bq to m); **^{13}C NMR (75 MHz, CDCl_3) data are listed in Table 4; CIMS (NH_3) m/z** 624 (23.4%), 622 (46.4%), 620 (26.1%, [$\text{M} + 18$] $^+$, $\text{C}_{29}\text{H}_{32}\text{O}_4\text{Br}_2$).

Oxidation of tremulenediol A (26): preparation of tremulenolide A (23)

A solution of 26a (10 mg) in CH_2Cl_2 (0.5 mL) was added to a solution of 1% NaOH in MeOH (2 mL) and stirred for 1 h at rt⁵³. The solvent was evaporated under reduced pressure and the residue was suspended in water and extracted with CH_2Cl_2 . MnO_2 (35 mg) was added to the dry solution and the mixture was refluxed for 3 days⁵⁴. The resulting suspension was filtered through anhydrous MgSO_4 and the solvent evaporated. The ^1H NMR spectrum of the crude product indicated a mixture of 23 and methyl *p*-bromobenzoate. PTLC (hexanes: CH_2Cl_2 /MeOH, 50:50:1) of this mixture provided tremulenolide A (23) which showed the same R_f and ^1H NMR spectrum as the natural product.

Reduction of tremulenediol (25): preparation of tremulenediol B (27)

Crude dialdehyde 25 (71.6 mg) was dissolved in CH_2Cl_2 (2 mL, containing 0.2 mL of MeOH) and NaBH_4 or NaBD_4 (~60 mg) was added. The reaction mixture was stirred for 30 min, filtered, and evaporated to dryness. The residue was redissolved in dichloromethane and acidified with acetic acid (3 drops). The white solid which formed was filtered off and the resultant diol solution submitted to *p*-bromobenzoylation. Treatment of the solution with *p*-bromobenzoyl chloride (160 mg) as above and purification by PTLC (hexanes/ CH_2Cl_2 , 1:1) provided 27a, identical (R_f and ^1H NMR) with that previously described. The data for the deuterated diol (33a) are similar to those of 27a, except for the signals at δ 4.53 (1H, t, $J = 7.5$ Hz), δ 4.30 (1H, t, $J = 7.5$ Hz), and δ 3.26 (1H, dd, $J = 7.5, 3$ Hz) in the ^1H NMR and the resonances for C-11 and C-12 in the ^{13}C NMR (APT). These are shifted upfield by 0.3 ppm, appear as triplets, and have the phase reversed because of the presence of deuterium.

Tremulenediol C (28)

Compound **28** was eluted as a colorless oil; TLC: R_f 0.3 (benzene/acetone/AcOH, 75:25:1); FTIR (CH_2Cl_2 , cast): 3340 (O-H), 1459 (C=C), 1383 (C-O) cm^{-1} ; ^1H NMR, (400 MHz, CDCl_3) data are listed in Table 9; **homonuclear decoupling** (irradiation effect): δ 4.03 \leftrightarrow δ 1.94 (dd to d, $J = 2$ Hz), 2.97 (m to m); δ 3.79 \leftrightarrow δ 3.64 (dd to d, $J = 7$ Hz), 2.24 (m to m); δ 3.64 \leftrightarrow δ 3.79 (dd to d, $J = 8$ Hz), 2.24 (m to m); δ 2.97 \leftrightarrow δ 4.03 (dd to d, $J = 2$ Hz), 1.94 (dd to d, $J = 2$ Hz), 1.69 (m to m), 1.46 (dd to d, $J = 12$ Hz), 1.22 (dd to d, $J = 12$ Hz); δ 2.24 \leftrightarrow δ 3.79 (dd to d, $J = 10$ Hz), δ 3.64 (dd to d, $J = 10$ Hz), 1.78 (dm to bd, $J = 11$ Hz), 1.58 (m to m); δ 1.94 \leftrightarrow δ 4.03 (dd to d, $J = 2$ Hz), 2.97 (m to m); δ 1.69 \leftrightarrow δ 1.78 (dm to bs), 0.78 (d to s); δ 1.46 \leftrightarrow δ 1.22 (dd to d, $J = 8.5$ Hz), 2.97 (m to m); δ 1.22 \leftrightarrow δ 1.46 (dd to d, $J = 8.5$ Hz), 2.97 (m to m); δ 0.78 \leftrightarrow δ 1.69 (m to m); ^{13}C NMR (75 MHz, CDCl_3) data are listed in Table 4; HMQC (125, 500 MHz) δ 83.5 \leftrightarrow δ 4.03; δ 62.8 \leftrightarrow δ 3.79, 3.64; δ 50.4 \leftrightarrow δ 2.24; δ 43.7 \leftrightarrow δ 2.97; δ 41.2 \leftrightarrow δ 1.22, 1.46; δ 32.4 \leftrightarrow δ 1.69; δ 32.0 \leftrightarrow δ 1.78, 1.54; δ 26.5 \leftrightarrow δ 1.02; δ 22.8 \leftrightarrow δ 1.94; δ 21.0 \leftrightarrow δ 0.82; δ 20.8 \leftrightarrow δ 1.78, 1.58; δ 12.4 \leftrightarrow δ 0.78; HMBC (125, 500 MHz) δ 3.63 \leftrightarrow δ 134.5; δ 1.94 \leftrightarrow δ 140.1, 134.5, 50.4; δ 1.46 \leftrightarrow δ 140.1, 83.5, 21.0; δ 1.22 \leftrightarrow δ 43.7, 40.7; 32.4, 26.5, 21.0; δ 1.02 \leftrightarrow δ 83.5, 41.2, 40.7, 21.0; δ 0.82 \leftrightarrow δ 83.5, 41.2, 40.7, 26.5; δ 0.78 \leftrightarrow δ 43.7, 32.0, 32.4;

Tremulenediol (29)

Compound **29** was eluted as pale yellow oil; this compound is also obtained when tremulenediol C (**28**) is kept in CDCl_3 solution for several days; TLC: R_f 0.3 (CH_2Cl_2), UV (MeOH) 244 nm ($\epsilon \sim 5000$); FTIR (CH_2Cl_2 , cast): 3410 (O-H), 1458 (C=C) cm^{-1} ; ^1H NMR, (400 MHz, CDCl_3) data are listed in Table 5; **homonuclear decoupling** (irradiation \rightarrow effect): δ 3.13 \rightarrow δ 5.71 (d to s), 1.71 (dd to d, $J = 12$ Hz), 1.50 (dd to d, $J = 12$ Hz); δ 0.79 \rightarrow δ 1.80 (m to m); HREIMS m/z 220.1830 (25%, M^+ , calcd for $\text{C}_{15}\text{H}_{24}\text{O}$ 220.1833), 205.1590 (15%, $\text{C}_{14}\text{H}_{21}\text{O}$), 189.1642 (100%, $\text{C}_{14}\text{H}_{21}$).

4.3. Labelling experiments

4.3.1. Administration of benzoic acid- α - ^{13}C

Benzoic acid- α - ^{13}C (123 mg) was suspended in redistilled water (40 mL) and solubilized by adding NaOH aqueous solution (1 M) dropwise with heating. The pH was kept slightly acidic. This sterile solution was periodically added to *P. tremulae* culture (2 L) grown in medium A by injecting 10 mL after days 1, 3, 5, and 7 of growth. The culture was harvested at day 16 using the same procedure described in section 2 for the normal culture (Figure 3)

Labelled methyl salicylate (7)

Methyl salicylate (7), ^{13}C NMR (CDCl_3 , 100 MHz) enriched signal: δ 170.6 (C=O, 37% incorporation), natural abundance signals: δ 161.6 (C-2), 135.6 (C-4), 129.8 (C-6), 119.0 (C-5), 117.5 (C-3), 112.3 (C-1), 52.1 (OMe).

Labelled methyl benzoate (5)

Methyl benzoate (5), ^{13}C NMR (CDCl_3 , 100 MHz) enriched signal: δ 167.0 (C=O, 38% incorporation), natural abundance signals: δ 132.8 (C-4), 130.1 (C-1), 129.5 (C-2, C-6), 128.2 (C-3, C-5), 51.9 (OMe).

Labelled 2-carbomethoxyopinin (22)

2-Carbomethoxyopinin (22), ^{13}C NMR (CDCl_3 , 100 MHz) enriched signal: δ 163.2 (C=O, 94% incorporation), natural abundance signals: δ 137.0 (C-7), 133.6 (C-5), 132.9 (C-2), 128.6 (C-4), 123.9 (C-3), 118.1 (C-6), 52.4 (OMe).

4.3.2. Administration of labelled acetate

A sterile solution of labelled sodium acetate (0.75 g) in redistilled water (45 mL) was periodically supplemented to a *P. tremulae* culture (2 L.) grown in medium A by injecting 15 mL after day 1 and 10 mL after days 3, 5, and 7 of growth. The culture was harvested at day 16 using the same procedure described in section 2 for the normal culture (Figure 3). The fractions containing tremulenediols A and B were combined and converted into the corresponding di-*p*-bromobenzoyl derivatives (26a and 27a).

[1,2-¹³C₂] acetate labelled metabolites

Tremulenediol A di-*p*-bromobenzoate (26a), ¹³C NMR (CDCl₃, 125 MHz) spin-coupled carbons: δ 150.3 (C-1, $J_{1,10} = 40$ Hz), 126.5 (C-2, $J_{2,11} = 48$ Hz), 69.0 (C-11, $J_{2,11} = 48$ Hz), 48.3 (C-10, $J_{1,10} = 40$ Hz), 46.6 (C-7, $J_{7,8} = 35$ Hz), 45.3 (C-8, $J_{7,8} = 35$ Hz), 41.3 (C-3, $J_{3,4} = 34$ Hz), 37.2 (C-9, $J_{9,15} = 36$ Hz), 31.4 (C-6, $J_{6,13} = 36$ Hz), 26.8 (C-15, $J_{9,15} = 36$ Hz), 21.2 (C-4, $J_{3,4} = 34$ Hz), 11.7 (C-13, $J_{6,13} = 36$ Hz), enriched singlets: δ 63.2 (C-12), 31.7 (C-5), 28.4 (C-14); INADEQUATE (CDCl₃, 125 MHz) cross peaks (two double quantum): δ 150.3 (C-1) - 48.3 (C-10), 126.5 (C-2) - 69.0 (C-11), 41.3 (C-3) - 21.2 (C-4), 31.4 (C-6) - 11.7 (C-13), 46.6 (C-7) - 45.3 (C-8), 37.2 (C-9) - 26.8 (C-15); singlet carbons: δ 63.2 (C-12), 31.7 (C-5), 28.4 (C-14)

Tremulenediol B di-*p*-bromobenzoate (27a), ¹³C NMR (CDCl₃, 125 MHz) spin-coupled carbons: δ 144.2 (C-1, $J_{1,10} = 70$ Hz), 139.9 (C-10, $J_{1,10} = 70$ Hz), 63.4 (C-11, $J_{2,11} = 39$ Hz), 48.2 (C-7, $J_{7,8} = 34$ Hz), 44.7 (C-3, $J_{3,4} = 33$ Hz), 42.7 (C-8, $J_{7,8} = 34$ Hz), 42.4 ($J_{2,11} = 39$ Hz), 41.6 (C-9, $J_{9,15} = 35$ Hz), 35.7 (C-6, $J_{6,13} = 35$ Hz), 29.7 (C-4, $J_{3,4} = 33$ Hz), 26.4 (C-15, $J_{9,15} = 35$ Hz), 19.6 (C-13, $J_{6,13} = 35$ Hz); enriched singlets: δ 68.1 (C-12), 30.4 (C-5), 29.2 (C-14).

[1-¹³C] acetate labelled metabolites

[1-¹³C]-Tremulenediol A di-*p*-bromobenzoate (26a), ¹³C NMR (CDCl₃, 100 MHz) enriched signals: δ 150.3 (C-1), 126.5 (C-2), 45.3 (C-8), 37.2 (C-9), 31.4 (C-6), 21.2 (C-4), natural abundance signals: δ 69.0 (C-11), 63.2 (C-12), 48.3 (C-10,), 46.6 (C-7), 41.3 (C-3), 31.7 (C-5), 28.4 (C-14), 26.8 (C-15), 11.7 (C-13).

[1-¹³C]-Tremulenediol B di-*p*-bromobenzoate (27a), ¹³C NMR (CDCl₃, 100 MHz) enriched signals: δ 139.9 (C-10), 68.1 (C-12), 63.4 (C-11), 48.2 (C-7), 44.7 (C-3), 30.4 (C-5), 29.2 (C-14), 26.4 (C-15), 19.6 (C-13), natural abundance signals: δ 144.2 (C-1), 42.7 (C-8), 42.4 (C-2), 41.6 (C-9), 35.7 (C-6), 29.7 (C-4).

[2-¹³C] acetate labelled metabolites

[2-¹³C]-Tremulenediol A di-*p*-bromobenzoate (26a), ¹³C NMR (CDCl₃, 100 MHz) enriched signals: δ 69.0 (C-11), 63.2 (C-12), 48.3 (C-10,), 46.6 (C-7), 41.3 (C-3), 31.7 (C-5), 28.4 (C-14), 26.8 (C-15), 11.7 (C-13); natural abundance signals: δ 150.3 (C-1), 126.5 (C-2), 45.3 (C-8), 37.2 (C-9), 31.4 (C-6), 21.2 (C-4).

[2-¹³C]-Tremulenediol B di-*p*-bromobenzoate (27a), ¹³C NMR (CDCl₃, 100 MHz) enriched signals: δ 144.2 (C-1), 42.7 (C-8), 42.4 (C-2), 41.6 (C-9), 35.7 (C-6), 29.7 (C-4), natural abundance signals: δ 139.9 (C-10), 68.1 (C-12), 63.4 (C-11), 48.2 (C-7), 44.7 (C-3), 30.4 (C-5), 29.2 (C-14), 26.4 (C-15), 19.6 (C-13).

4.4. Oxidase activity

4.4.1. Preparation of methyl *o*-toluate

o-Toluic acid was dissolved in dichloromethane and an excess of an ethereal solution of diazomethane was added until a light yellow color persisted. The solution was kept until it became colorless. The ¹H NMR spectrum confirms the obtention of the methyl ester derivative and GC analysis provided the retention time (*t_R*) for the oxidase assay

Methyl *o*-toluate: TLC: 0.4 (Hexanes/CH₂Cl₂, 2:1); GC (2 min at 60°C to 260°C at 10°C/min): *t_R* 13.8 min; ¹H NMR (400 MHz, CDCl₃): δ 7.91 (1H, dd, *J* = 8, 1.8 Hz), 7.40 (1H, td, *J* = 8, 1.8 Hz), 3.90 (3H, s, OMe), 2.60 (3H, s, Ar-Me), additional signals masked by the chloroform peak.

4.4.2. Administration of *o*-toluic acid directly into the medium (exp-1)

P. tremulae was grown for 16 days in liquid shake culture on a sterile medium A (2 L), to which *o*-toluic acid (0.5 mM) was added. The extraction procedure was the same as described in section 2. A portion of the resin organic extract was applied to a PTLC and developed in a 2:1 mixture of hexanes and dichloromethane. The UV active material of higher *R_f* was separated, extracted with chloroform, and analyzed by GC, and ¹H NMR.

GC (2 min at 60°C to 260°C at 10°C/min): *t_R* 11.7 and 12.2 min; ¹H NMR (400 MHz, CDCl₃): δ 10.27 (aldehyde), δ 8.1-7.2 (aromatic protons), δ 3.94 (OMe), and δ 2.68 (Ar-Me).

4.4.3. Citrate-phosphate buffer pH 4 assay (exp-2)

P. tremulae was grown for 16 days in liquid shake culture on sterile medium B (2 L). The culture was filtered through cheese cloth and the mycelium was washed 3 times with distilled water. Half of the mycelium was transferred into a 2L-erlenmeyer flask charged with 1 L of citrate-phosphate buffer pH 4 and ~0.5 mM *o*-toluic acid. The other half of the mycelium was used to inoculate the control (buffer). The buffer was prepared as follows:

Buffer pH 4: 307 mL of citric acid solution (0.2 M) + 307 mL of distilled water + 386 mL of disodium phosphate solution (0.2 M).

- 0.2 M citric acid solution: 45 g made up to 1 L with distilled water.
- 0.2 M disodium phosphate solution: 72.5 g made up to 1 L with distilled water.

The harvesting of the buffer medium was performed after 4, 6, and 26 hours of growth. Approximately 100 mL aliquots were taken each time, filtered, and extracted with dichloromethane. After drying over anhydrous Na₂SO₄, the extract was concentrated and analyzed by GC under the same conditions used for the standards. Due to the appearance of a broad signal at $t_R = 14.7$, the crude extract was applied to a PTLC (developed in a 2:1 mixture of hexanes and dichloromethane) and the UV active material of higher R_f was separated, extracted with chloroform, and analyzed by GC, GC-IR, and ¹H NMR.

GC (2 min at 60°C, 10°C/min): t_R 11.7, 12.2, and 13.7 min; GC-IR (2 min at 60°C to 260°C at 10°C/min): t_R 14.0 (*o*-tolualdehyde), 14.4 (methyl benzoate), and 16.0 (methyl *o*-toluate) min; ¹H NMR (400 MHz, CDCl₃): δ 10.27 (aldehyde), δ 8.1-7.2 (aromatic protons), 3.94 (OMe), 3.90 (OMe), 2.68 (Ar-Me) and 2.60 (Ar-Me).

4.4.4. Extraction of rotted aspen and *Phellinus* conks

Freshly rotted aspen and *Phellinus* conks were separately cut into small pieces and each was shaken with dichloromethane for 1 day. The organic extract was separated, concentrated, and chromatographed as before (Figure 3). The fractions were analyzed by ¹H NMR which did not show characteristic peaks of the sesquiterpenes.

Rotted aspen extract: GC-MS (2 min at 50°C to 280°C at 5°C/min) 2-methyl phenol, methyl benzoate, methyl salicylate, diethyl phthalate, hexadecanoic acid, octadecanoic acid, eicosanoic acid, docosanoic acid, methyl docosanoate, methyl tricosanoate, 9-hexacosene, lupeol, sigmastadienone, sigmastadienol acetate (Figure 51).

Conk extract: three components were isolated and analyzed by ¹H NMR and HREIMS. The data suggest that these compounds correspond to ergosterol peroxide, some di or triglyceride, and long chain fatty acid.

V. BIBLIOGRAPHY

- 1 Peterson, E. B.; Peterson, N. M. *Ecology, Management, and Use of Aspen and Balsam Poplar in the Prairie Provinces, Canada*. For. Can., Edmonton, 1992.
- 2 (a) Chakravarty, P.; Hiratsuka, Y. *Eur. J. For. Pathol.* 1992, 22, 354-361.
(b) Hunt, K.; Bosham, J. T.; Kemperman, J. A. *Can. J. For. Res.* 1978, 8, 181-187.
- 3 Hiratsuka, Y.; Gibbard, D. A.; Bakowsky, O. *Classification and Measurement of Aspen Decay and Stain in Alberta*. For. Can., Edmonton, 1990.
- 4 Breitenbach, J.; Kränzlin, F. *Fungi of Switzerland*. v. 2. Verlag Mykologia, Lucerne, Switzerland, 1986. p 264.
- 5 Niemelä, T. *Ann. Bot. Fenn.* 1974, 11, 202-215.
- 6 Hutchison, L. J.; Hiratsuka, Y. *Abstracts*, Joint Meeting of the American Phytopathological Society and the Mycological Society of America, Portland, Oregon, 1992.
- 7 Hutchison, L. J.; Hiratsuka, Y. Personal communication.
- 8 Ayer, W. A.; Jimenez, L. D. *Abstracts*, 76th CSC Conference; Sherbrooke, Québec, Canada, 1993. p 693.
- 9 Trifonov, L. S.; Chakravarty, P.; Hiratsuka, Y.; Ayer, W. A. *Eur. J. For. Pathol.* 1992, 22, 441-448.
- 10 Tien, M.; Kirk, T. K. *Science* 1983, 221, 660-663.
- 11 Cain, R. B.; Bilton, R. F.; Darrah, J. A. *Biochem. J.* 1968, 108, 797-827.
- 12 Mann, J. *Secondary Metabolism*, 2nd ed; Clarendon: Oxford, 1987; pp 1-21.
- 13 Collins, R. P.; Halim, A. F. *Can. J. Microbiol.* 1972, 18, 65-66
- 14 Serck-Hansen, K.; Wikström. *Phytochemistry* 1978, 17, 1678-1679.
- 15 Nelson, G. J.; Matthea, D.; Lewis, D. E. *J. Nat. Prod.* 1993, 56, 1182-1183.
- 16 Harper, D. B.; Hamiton, J. T. G.; Kennedy, J. T.; McNally, K. J. *Appl. Environ. Microbiol.* 1989, 55, 1981-1989.
- 17 Harper, D. B.; Hamiton, J. T. G. *J. Gen. Microbiol.* 1988, 134, 2831-2839.
- 18 Coulter, C.; Kennedy, J. T.; McRoberts, W. C.; Harper, D. B. *Appl. Environ. Microbiol.* 1993, 59, 706-711.
- 19 McNally, K. J.; Hamiton, J. T. G.; Harper, D. B. *J. Gen. Microbiol.* 1990, 136, 1509-1515.
- 20 Jerina, D. M.; Dely, J. W. *Science* 1974, 185, 573-582.
- 21 Jerina, D. M.; Dely, J. W.; Witkop, B.; Zeltzman-Nirenberg, P.; Undenfriend, S. *J. Am. Chem. Soc.* 1968, 90, 6525.

22. (a) Vogel, E.; Günther, H. *Angew. Chem. Int. Ed. Engl.* **1967**, *6*, 385-476.
(b) Shirwaiker, G. S.; Bhatt, M. V. *Adv. Heterocycl. Chem.* **1985**, *37*, 67-165.
(c) Boyd, D. R. *Chem. Heterocycl. Compd.* **1985**, *42*, 197-282.
23. Manitto, P. *Biosynthesis of Natural Products*. J. Wiley, New York, 1981, pp 9-10
24. (a) Mitsubishi Chemical Industries Ltd., Tokyo, Japan.
(b) Tokiwa, Y.; Miyoshi-saitoh, M.; Kobayashi, H.; Sunaga, R.; Korushi, M.; Oki, T.; Iwasaki, S. *J. Am. Chem. Soc.* **1992**, *114*, 4107-4110.
(c) Ando, K.; Ito, T.; Kusano, H. In Streat, M. *Ion Exchange for Industry*. Ellis Horwood, England, 1988. pp 232-238.
25. (a) COSY: Bax, A.; Freeman, R.; Morris, G. *J. Magn. Reson.* **1981**, *42*, 164; Bax, A.; Freeman, R. *J. Magn. Reson.* **1981**, *44*, 542.
(b) APT: Rabenstein, D.; Nakashima, T. *Anal. Chem.* **1979**, *51*, 1465; Patt, S.; Shoolery, J. *J. Mag. Res.* **1982**, *46*, 535.
(c) HMQC: Bax, A.; Subramanian, S. *J. Magn. Reson.* **1986**, *67*, 565.
(d) INAPT: Bax, A. *J. Magn. Reson.* **1984**, *57*, 314; Bax, A.; Ferretti, J. A.; Nashed, N.; Jerina, D. M. *J. Org. Chem.* **1985**, *50*, 3029.
26. (a) IR and NMR spectra kindly provided by Dr. Berchtold, Department of Chemistry Massachusetts Institute of Technology.
(b) Gilchrist, T. L. *Heterocyclic Chemistry*. Wiley, New York, 1985. pp 342-344.
27. Vogel, E.; Alienbach, H.-J.; Drossard, J.-M.; Schmickler, H.; Stegelmeier, H. *Angew. Chem. Int. Ed. Engl.* **1980**, *19*, 1016-1018.
28. Silverstein, R. M.; Bassler, G. C.; Morrill, T. C. *Spectrometric Identification of Organic Compounds*, 5th ed. Wiley, New York, 1991. pp 302-305.
29. Boyd, D. R.; Berchtold, G. A. *J. Am. Chem. Soc.* **1979**, *101*, 2470-2474.
30. Marshall, B. J.; Ratledge, C. *Biochim. Biophys. Acta* **1972**, *264*, 106-116.
31. Yalpani, N.; Raskin, I. *Trends Microbiol.* **1993**, *1*, 88-92 and references therein.
32. Haslam, E. *The shikimate pathway*. Wiley, New York, 1974. pp 220-221.
33. Selander, H. G.; Jerina, D. M.; Piccolo, D. E.; Berchtold, G. A. *J. Am. Chem. Soc.* **1975**, *97*, 4428-4430.
34. (a) Ayer, W. A.; Pausler, M. G. *Abstracts, 76th CSC Conference*, Sherbrooke, Québec, Canada, 1993. p 476.
(b) NOE/NOESY: Schraml, J.; Bellama, J. M. *Two-Dimensional NMR Spectroscopy*, Wiley: New York. pp 132-143.
35. (a) Daniewski, W.; Kocór, M.; Thoren, S. *Polish J. Chem.*, **1978**, *52*, 561;
(b) Steiner, O.; Anke, T.; Sheldrick, W. S.; Steglich, W. *Tetrahedron* **1990**, *46*, 2389-2400.

- 36 Herz, W.; Grisebach, H.; Kirby G. W. *Progress in the Chemistry of Organic Natural Products*; Springer-Verlag: New York, 1979; Vol. 36, pp 36-63.
- 37 Ayer, W. A.; Trifonov, L. S. *J. Nat. Prod.* **1992**, *55*, 1454-1461.
- 38 (a) Tori, M.; Nakashima, K.; Toyota, M.; Asakawa, Y. *Tetrahedron Letters* **1993**, *34*, 3751-3752.
(b) *ibid.*, 3753-3754.
(c) HMBC: Bax, A.; Summers, M. F. *J. Am. Chem. Soc.* **1986**, *108*, 2093.
- 39 Anet, F. A. L. In *Conformational Analysis of Medium-Sized Heterocycles*; Glass, R. S., Ed.; VCH: Weinheim, 1988; p 50.
- 40 Lambert, J. B.; Shurvell, H. F.; Verbit, L.; Cooks, R. G.; Stout, G. H. *Organic Structural Analysis*. Macmillan: New York, 1976; p 39.
- 41 Jackman, L. M.; Sternhell, S. *Applications of Nuclear Magnetic Resonance Spectroscopy in Organic Chemistry*, 2nd ed.; Pergamon: Oxford, 1969; p 333-338.
- 42 Ref. 41; pp 72-73, 316-328.
- 43 Gaudemer, A. In *Stereochemistry: Fundamentals and Methods*; Kagan, H. B., Ed.; Georg Thieme: Stuttgart, 1977; Vol 1, p 90.
- 44 Ref. 41, pp 283-284.
- 45 Noggle, J. H.; Schirmer, R. E. *The Nuclear Overhauser Effect Chemical Applications*; Academic Press: New York, 1971; pp 59-62.
- 46 Rabideau, P. W. *Acc. Chem. Res.* **1978**, *11*, 141-147.
- 47 Ref. 43, pp 29-43.
- 48 Legrand, M.; Rougier, M. J. In *Stereochemistry: Fundamentals and Methods*; Kagan, H. B., Ed.; Georg Thieme: Stuttgart, 1977; Vol. 2, pp 140-141.
- 49 Daniewski, W. M.; Kocór, M.; Thoren, S. *Polish J. Chem.* **1978**, *52*, 561.
- 50 Ref. 48, pp 54-57.
- 51 Scott, A. I.; Wrixon, A. D. *Tetrahedron* **1971**, *27*, 4787.
- 52 Burden, R. S.; Crombie, L.; Whiting, D. A. *J. Chem. Soc. (C)* **1969**, 693.
- 53 Mashimo, K.; Sato, Y. *Tetrahedron* **1970**, *26*, 803.
- 54 Carlson, R. M.; White, L. L. *Synth. Commun.* **1983**, *13*, 237.
- 55 Haslam, E. *Metabolites and metabolism*; Clarendon: Oxford, 1985; pp 21-28.
- 56 (a) Ref. 55, pp 16-18.
(b) INADEQUATE: Bax, A.; Freeman, R. Kempell, S. P. *J. Am. Chem. Soc.* **1980**, *102*, 4849; Marci, T. H.; Freeman, R. *J. Magn. Reson.* **1982**, *48*, 158; Turner, D. L. *J. Mag. Reson.* **1982**, *49*, 175.
- 57 Mann, J. *Secondary Metabolites*, 2nd ed.; Clarendon: Oxford, 1987; pp 95-131.

58. Ayer, W. A.; Browne, L. M. *Tetrahedron* 1981, 37, 2199—2248 and references cited therein.
59. Jonassohn, M.; Anke, H.; Sterner, O. *Abstracts, 10th IUPAC Symposium on the Chemistry of Natural Products, Strasbourg, France, 1992* p 408.
60. Cane, D. E.; Nachbar, R. B. *J. Am. Chem. Soc.* 1978, 100, 3208-3212.
61. Geissman, T. A.; Crout, D. H. G. *Organic Chemistry of Secondary Plant Metabolism*; Freeman: San Francisco, 1969; pp 409-419.

END

2 7-0 8-9 6

FIN